

# NOTE TO USERS

This reproduction is the best copy available.

**UMI**<sup>®</sup>



**University of Alberta**

Molecular Characterization of UNC-119 in *Caenorhabditis elegans*

by

Wayne Paul Materi



A thesis submitted to the Faculty of Graduate Studies and Research in partial fulfillment

of the requirements for the degree of Doctor of Philosophy

in

Molecular Biology and Genetics

Department of Biological Sciences

Edmonton, Alberta

Fall 2004



Library and  
Archives Canada

Bibliothèque et  
Archives Canada

Published Heritage  
Branch

Direction du  
Patrimoine de l'édition

395 Wellington Street  
Ottawa ON K1A 0N4  
Canada

395, rue Wellington  
Ottawa ON K1A 0N4  
Canada

*Your file* *Votre référence*  
*ISBN: 0-612-95979-1*  
*Our file* *Notre référence*  
*ISBN: 0-612-95979-1*

The author has granted a non-exclusive license allowing the Library and Archives Canada to reproduce, loan, distribute or sell copies of this thesis in microform, paper or electronic formats.

L'auteur a accordé une licence non exclusive permettant à la Bibliothèque et Archives Canada de reproduire, prêter, distribuer ou vendre des copies de cette thèse sous la forme de microfiche/film, de reproduction sur papier ou sur format électronique.

The author retains ownership of the copyright in this thesis. Neither the thesis nor substantial extracts from it may be printed or otherwise reproduced without the author's permission.

L'auteur conserve la propriété du droit d'auteur qui protège cette thèse. Ni la thèse ni des extraits substantiels de celle-ci ne doivent être imprimés ou autrement reproduits sans son autorisation.

---

In compliance with the Canadian Privacy Act some supporting forms may have been removed from this thesis.

Conformément à la loi canadienne sur la protection de la vie privée, quelques formulaires secondaires ont été enlevés de cette thèse.

While these forms may be included in the document page count, their removal does not represent any loss of content from the thesis.

Bien que ces formulaires aient inclus dans la pagination, il n'y aura aucun contenu manquant.

# Canada

I would like to dedicate this work to

my wife, Sandra

## Acknowledgements

I would like to thank all of the members of the Pilgrim lab past and present for a welcoming, helpful, productive and fun working culture. Thanks to Jessica Smith and Paul Stothard for invaluable help in making published protocols actually work. I am grateful to Kathy Bueble, Angela Manning, Carlos Egydio de Carvalho and Bryan Crawford for many lively scientific discussions. I would also like to thank Morris Maduro for his pioneering work and for discussions over the years. Thanks also to Leanne Sayles and Karyn Berry for their enthusiasm and hard work as undergraduate project students. I would especially like to thank Dave Pilgrim for accepting me into the lab on short notice, for ongoing support, for encouraging me to participate in many conferences and for his scientific mentorship. I would also like to extend my appreciation to my committee members Ross Hodgetts and Jeff Goldberg as well as my candidacy examining committee members, Shelagh Campbell, Teresa Krukoff and Frank Nargang and defense committee members, Robert Campenot, Erik Jorgensen and Susan Jensen.

I would like to thank Rakesh Bhatnagar, Pat Murray and Lisa Ostafichuk for their technical support. A debt of gratitude also goes out to a number of labs for sharing worms, reagents and ideas. I would particularly like to thank Andy Fire, Brian Ackley, Theresa Stiernagle and Bob Barstead. I am grateful, as well, for many stimulating discussions at numerous conferences and meetings and would like to extend my appreciation to members of the worm and developmental biology communities for their interest. I would like to extend my thanks to several people in the Biological Sciences Department who have provided kind and competent administrative support. In particular, I would like to recognize the efforts of Bill Samuels, Gwen Jewett, Grant Tricker and Maggie Haag.

My deepest gratitude goes to my wife, Sandra, who followed me to Edmonton from Vancouver and has provided unflagging love, companionship and moral support throughout.

## Table of Contents

<b>Chapter 1 - Introduction .....</b>	<b>1</b>
1.1 <i>C. elegans</i> as a model for mammalian nervous system development.....	1
1.2 Advantages and disadvantages of <i>C. elegans</i> as a model system .....	2
1.3 <i>unc-119</i> mutants have neural defects .....	4
1.4 Analysis of the UNC-119 protein .....	6
1.5 Homologs of UNC-119 in other organisms .....	8
1.6 Axonogenesis .....	9
1.6.1 The growth cone.....	10
1.6.2 Elongation, collapse and turning.....	12
1.6.3 Axon branching.....	14
1.7 Molecular mechanisms of axonogenesis.....	15
1.7.1 Actin polymerization cycle .....	15
1.7.2 Rho family members (small GTPases).....	19
1.8 Axon guidance .....	21
1.8.1 Guidance signals .....	22
1.8.1.1 Netrins .....	23
1.8.1.2 Semaphorins .....	24
1.8.1.3 Ephrins.....	25
1.8.1.4 Slits.....	27
1.8.1.5 Neurotrophins .....	29
1.9 Adhesion .....	30
1.10 Axon maintenance and synaptic stability.....	34

1.11 Specific objectives of this work .....	35
1.12 References .....	53
<b>Chapter 2 - Expression of <i>C. elegans</i> UNC-119 outside the nervous system rescues movement and dauer formation defects .....</b>	<b>62</b>
2.1 Introduction .....	62
2.2 Materials and Methods .....	65
2.2.1 GFP nervous system reporters .....	65
2.2.2 Cell autonomy constructs .....	65
2.2.3 Transgenic strain construction .....	68
2.2.4 Genetic testing .....	68
2.2.5 Movement and dauer formation assays .....	69
2.2.6 Microscopy .....	70
2.3 Results .....	71
2.3.1 <i>unc-119</i> mutants exhibit fasciculation and branching defects .....	71
2.3.2 Cell placement defects along the VNC are common .....	72
2.3.3 Commissures make choice point errors .....	72
2.3.4 Axon elongation defects in mechanosensory and chemosensory neurons .....	73
2.3.5 ASI axon defects are distinct in <i>unc-119</i> mutants .....	75
2.3.6 UNC-119 rescues some axonal defects cell-autonomously .....	76
2.3.7 UNC-119 in neural subset does not rescue gross phenotypic defects .....	77
2.3.8 Intronic elements expand expression of gDNA-based constructs .....	78
2.3.9 Muscle-specific UNC-119 rescues gross phenotypic defects .....	78
2.4 Discussion .....	80

2.5 References.....	97
<b>Chapter 3 - Src, Arl, and Basement Membrane Collagen Interactions with <i>C. elegans</i> UNC-119 .....</b>	<b>101</b>
3.1 Introduction.....	101
3.2 Materials and Methods.....	104
3.2.1 PCR-based site-directed mutagenesis .....	104
3.2.2 Single strand site-directed mutagenesis .....	104
3.2.3 Unc-119 domain deletion analysis .....	105
3.2.4 Transgenic strain construction .....	106
3.2.5 Genetic testing.....	107
3.2.6 Microscopy.....	107
3.2.7 Yeast two-hybrid screen.....	108
3.2.8 Directed 2-hybrid assay.....	110
3.3 Results.....	111
3.3.1 Src-interacting motifs not required for UNC-119 function in worms.....	111
3.3.2 ARL-2 interaction with UNC-119.....	112
3.3.3 Interaction with LET-2.....	114
3.3.4 Other highly conserved residues are required .....	116
3.4 Discussion .....	117
3.5 References.....	129
<b>Chapter 4 - UNC-119 Protein and Antibody.....</b>	<b>133</b>
4.1 Introduction.....	133
4.2 Materials and Methods.....	134

4.2.1 Oligopeptide-based antibodies .....	134
4.2.2 Expressing UNC-119 in bacteria.....	134
4.2.3 Purification of antisera .....	136
4.2.4 Construction of Multi-epitope tag .....	137
4.2.5 Construction of tagged UNC-119 in insect cells.....	138
4.2.6 Construction of tagged UNC-119 in worms .....	140
4.2.7 Worm lysates.....	141
4.2.8 SDS-PAGE and Western Analysis.....	141
4.2.9 Tandem Affinity Purification and pull-down.....	142
4.2.10 Co-immunoprecipitation .....	143
4.3 Results.....	144
4.3.1 UNC-119 Antibodies.....	144
4.3.2 Epitope-tagged UNC-119 proteins.....	145
4.3.3 Pull-down and co-immunoprecipitation assays.....	146
4.4 Discussion .....	148
4.5 References .....	164
<b>Chapter 5 - General Discussion .....</b>	<b>165</b>
5.1 Future Directions.....	168

## List of Tables

Table 2.1 Transgenic strains used to test cell-autonomy .....	87
Table 2.2 Quantification of supernumerary branches in DA/DB class motor neurons. ...	88
Table 3.1 Primers used for Site-directed Mutagenesis .....	122
Table 3.2 Site-directed mutagenesis of motifs in HsUnc119 and Unc-119.....	123
Table 3.3 Primers used for domain deletion .....	124
Table 3.4 Strains used.....	125
Table 3.5 Directed yeast 2-hybrid $\beta$ -galactosidase staining results.....	126
Table 4.1 Primers used to construct multi-epitope tag .....	152

## List of Figures

Figure 1.1 The nervous system of <i>C. elegans</i> .....	40
Figure 1.2 <i>unc-119</i> mutant worms.....	41
Figure 1.3 UNC-119 protein family alignment.....	42
Figure 1.4 SH2 and SH3 binding and tyrosine phosphorylation motifs in UNC-119 .....	43
Figure 1.5 Src activation.....	44
Figure 1.6 Nerve fibers in <i>C. elegans</i> .....	45
Figure 1.7 The growth cone.....	46
Figure 1.8 Actomyosin contraction drives retrograde flow.....	47
Figure 1.9 Generation of forward force in filopodia.....	48
Figure 1.10 Actin polymerization is a dynamic, regulated process.....	49
Figure 1.11 Rho cycles between active and inactive states .....	50
Figure 1.12 Commissures elongate through a complex environment.....	51
Figure 1.13 Pioneering and following axons in the <i>C. elegans</i> VNC.....	52
Figure 2.1 <i>unc-119</i> mutants have VNC defasciculation and cell placement defect. ....	89
Figure 2.2 Axons of mechanosensory neurons terminate prematurely in the nerve ring.	90
Figure 2.3 Neurites of ASI amphid neurons are aberrant in <i>unc-119(ed3)</i> mutants.....	91
Figure 2.4 Comparison of ASI axon defects in several mutants.....	92
Figure 2.5 Neural-specific expression of UNC-119 rescues defects cell-autonomously.	93
Figure 2.6 Rescue of <i>unc-119</i> movement and dauer defects by tissue-specific UNC-119. .....	94
Figure 2.7 Phenotypic rescue of transgenic <i>unc-119</i> mutants is due to UNC-119 in muscles.....	95

Figure 2.8 UNC-119 expressed under muscle promoters.....	96
Figure 3.1 Domain deletion analysis of UNC-119 .....	127
Figure 3.2 Nervous system of transgenic worms with mutagenized SH2 or SH3 binding motifs .....	128
Figure 4.1 Oligopeptides used to raise UNC-119 antibodies .....	151
Figure 4.2 NOGFP + MycF1 .....	153
Figure 4.3 NOGFP + MycF2 .....	154
Figure 4.4 NOGFP + MycF3 .....	155
Figure 4.5 Epitopes common to STF1, STF2, STF3 .....	156
Figure 4.6 Dot blot of antibodies versus oligopeptides .....	157
Figure 4.7 GI698 expresses recombinant Thioredoxin::UNC-119 better than GI724....	158
Figure 4.8 Purified 9M5 antisera show improved specificity.....	159
Figure 4.9 Insect cells express soluble recombinant tagged UNC-119 .....	160
Figure 4.10 Multi-epitope tagged UNC-119 is detected in worm lysate.....	161
Figure 4.11 TAP purification of pDP#WM025e lysate.....	162
Figure 4.12 Soluble tagged-UNC-119 extracted by grinding method.....	163

## List of Symbols, Nomenclature, & Abbreviations

Ab	antibody
A/P	anterior/posterior
ABP	actin binding protein
ADF	actin depolymerization factor
ARF	adenosine ribosylation factor
Arl	adenosine ribosylation factor like
BDNF	brain derived neurotrophic factor
CAM	cell adhesion molecule
CBP	calmodulin binding protein
cGMP	cyclic guanine nucleotide monophosphate
CNS	central nervous system
DNC	dorsal nerve cord
ECM	extra-cellular matrix
EST	expressed sequence tag
evl	everted vulva
FAK	focal adhesion kinase
FNIII	fibronectin III
Gal4AD	Gal4 activation domain
Gal4BD	Gal4 DNA binding domain
GAP	GTPase activator
GDF	guanine dissociation factor

GDI	guanine dissociation inhibitor
GEF	guanine nucleotide exchange factor
GFP	green fluorescent protein
GPI	glycosyl phosphatidylinositol
GRP	guanyl releasing protein
HRP	horseradish peroxidase
hs	<i>Homo sapiens</i>
Ig	immunoglobulin
IgG	immunoglobulin G
IL5R $\alpha$	interleukin 5 receptor alpha subunit
LIMK	LIN-11, islet-1, MEC-3 domain kinase
MAP	microtubule associated protein
MAPK	mitogen activated protein kinase
MLCP	myosin light chain phosphatase
NC1	non-collagenous domain 1
NCAM	neural cell adhesion molecule
NGF	nerve growth factor
NT	neurotrophin
PAK	p21 associated kinase
PCR	polymerase chain reaction
PDE $\delta$	delta subunit of rod cGMP phosphodiesterase
PDL	phosphodiesterase delta like

PI3	phosphatidylinositol triphosphate
PIP <sub>2</sub>	phosphatidylinositol-4,5-diphosphate
Rho	Ras homolog
RNAi	RNA mediated interference
ROCK	rho-associated kinase
RPTP	receptor phosphotyrosine phosphatase
RT	room temperature
RT-PCR	reverse transcriptase-PCR
SDS-PAGE	sodium dodecyl sulfate polyacrylamide gel electrophoresis
SH	Src homology
Src	sarcoma virus oncogene
TAP	tandem affinity protocol
unc	uncoordinated
UTR	untranslated region
VNC	ventral nerve cord

## **Chapter 1 - Introduction**

The human brain is a marvel of organization. Over 10 billion neurons make hundreds of interconnections each to produce an organ that has unmatched cognitive ability. The brain is what makes humans capable of producing symphonies, understanding quantum physics or catching a high fly ball over the shoulder (although these distinct talents are rarely found together in a single brain). The most remarkable thing is not that the brain exists at all, but rather that it, along with rest of the body, develops from a single fertilized egg. This single cell carries within it all the instructions necessary for the trillions of synaptic connections found in the adult nervous system to organize themselves as the organism develops. One of the most ambitious goals of modern biological science is to understand the processes that permit this self organization.

Due to the complexity of this problem and the huge number of genes involved, research necessarily focuses on a small number of critical genes and their mechanisms of action. This thesis describes my work in determining the molecular and cellular mechanisms by which UNC-119 affects axon elongation and guidance in the nematode *Caenorhabditis elegans*.

### **1.1 *C. elegans* as a model for mammalian nervous system development**

The complexity of the mammalian brain is so daunting that we must employ simpler models to help us gain an understanding of molecular and cellular processes that are basic to all neural development. *C. elegans* is an excellent model for this purpose. Exactly 302 of the 959 somatic cells of the adult hermaphrodite worm are neurons. The lineage of all cells in the worm is known and is repeated in a completely stereotypical

manner from individual to individual. The location of all neural cell bodies, their axonal and dendritic projections and their synaptic connections are also highly stereotypical and have been mapped by serial electron-microscopy (White et al., 1986).

Neural cell bodies are found mainly in anterior and posterior ganglia and along the ventral midline (Figure 1.1). They send out axons and dendrites (collectively known as neurites) that fasciculate to form major nerve bundles such as the Ventral or Dorsal Nerve Cords (VNC or DNC, respectively). The major bundle, or neuropile, surrounds the pharynx between the anterior and posterior bulbs and is known as the Nerve Ring; the largest ganglion is found immediately adjacent to this structure. Motor neurons that innervate dorsal muscles are found along the VNC and they extend unbranched commissural axons circumferentially to the dorsal midline where they fasciculate to form the smaller DNC. Unlike vertebrates, axons of *C. elegans* motor neurons do not extend from the VNC or DNC to the muscles they innervate. Rather, body wall muscles extend neurite-like projections called muscle arms to their pre-synaptic targets in the VNC or DNC. Although morphologically similar to neurites, little is known about the composition or behaviour of muscle arms.

## **1.2 Advantages and disadvantages of *C. elegans* as a model system**

In addition to a simpler nervous system, the worm has other advantages compared to mammalian model systems, such as the mouse. *C. elegans* is small and transparent, allowing easy observation of nervous system structures, especially with the assistance of Green Fluorescent Protein (GFP) reporter constructs. Worms are amenable to genetic manipulation allowing for the discovery of new genes involved in developmental processes. *C. elegans* is particularly useful for studying genes which cause paralysis

when mutated because the hermaphroditic worm does not need to move to find a mate or to reproduce. *C. elegans* was the first metazoan to have its genome completely sequenced and a vast array of genetic tools have been developed, including chromosomal deletions, duplications, and tissue-specific GFP reporters. Transgenic animals are readily constructed, allowing for easy experimental manipulation of molecular mechanisms and *in vivo* testing of molecular hypotheses.

However, the worm is not without its challenges for studying cellular and molecular mechanisms in nervous system development. Its neurons and especially their processes are very tiny by comparison to the large structures studied in other organisms (e.g. the giant axons of the snail, *Helisoma*). This makes it difficult to study sub-cellular localization of proteins using light microscopy. Primary culture systems have only been possible in the last few years and require the dissolution of embryos, after which individual cells cease dividing and may adopt the correct post embryonic fate (Christensen et al., 2002).

Although powerful transgenic techniques are available, the lack of an efficient method for producing integrated single-copy, transgenes by homologous recombination means that GFP reporters are often expressed at higher levels than the endogenous cognate. While this may increase the GFP signal strength, it increases the difficulty in determining whether the sub-cellular expression pattern and subsequent phenotype precisely reflects the distribution and expression of the endogenous gene. For example, if a protein is normally found in stoichiometric balance with an interacting partner, over expression of that protein (as may be found with transgenic extra-chromosomal arrays) may change the normal localization or function of the molecule.

Protein biochemistry *in vivo* in the worm is more challenging than in some other systems. Immunohistochemistry for visible light detection is difficult due to the extensive chemical cross-linking of cuticular collagens in the worm hypodermis, which results in low permeability to antibodies. Extracting protein for use in Western blotting or co-immunoprecipitation is also somewhat difficult for the same reason though raising gram quantities of worms in liquid media is routine.

In partnership with other model systems, however, *C. elegans* provides a powerful tool for new gene discovery and for *in vivo* assays by genetic manipulation. In work toward this thesis, I have combined the power of other systems, such as yeast and insect cells, with studies in the worm to help understand the role of UNC-119 in axonogenesis.

### **1.3 *unc-119* mutants have neural defects**

The first *unc-119* mutant allele was isolated fortuitously by Dave Pilgrim. Further alleles were isolated and characterized and the gene cloned by Morris Maduro (Maduro and Pilgrim, 1995). Adults mutant for null alleles in *unc-119* are almost completely paralyzed (Figure 1.2) but muscle ultrastructure is normal. Further, mutant worms hyper contract when exposed to an acetylcholine agonist, levamisole, suggesting that paralysis is the result of a neural, rather than muscular, defect. Worms mutant for *unc-119* exhibit amphid dye-filling defects, constitutive feeding and an inability to form dauer larvae, suggesting a defect in structure or function of chemosensory neurons. The dauer larva is an alternative developmental state that worms can enter following the first larval stage (L1) upon sensing local overcrowding and lack of food (Riddle, 1988). Dauer larvae form a plug over their mouth and anus as well as a thickened cuticle and become resistant to environmental insults. Both entry into and exit from the dauer state

require sensing signals provided by the external environment.

An UNC-119::GFP reporter transgene is expressed throughout the nervous system in adults and in presumptive neuroblasts beginning at about the 80-cell stage of embryogenesis (Maduro, 1998). Using this reporter, a variety of neural structural defects are readily observed in adult mutants including defasciculation of the VNC, commissural guidance defects and supernumerary branches (Maduro, 1998). *unc-119* mutants exhibit normal growth cone morphology in DD and VD commissures with a reduced rate of migration (Knobel et al., 1999; Knobel et al., 2001). However, following initial elongation, these axons subsequently fail to stabilize and retract from the DNC, then subsequently generate supernumerary branches. These branches can be suppressed by the cell autonomous expression of UNC-119 in affected neurons; other neurons without wild-type UNC-119 are not rescued. AIY head interneurons also have shortened axons with supernumerary branches in *unc-119* mutants (Altun-Gultekin et al., 2001).

Several mechanisms have been proposed to explain the post-differentiation generation of supernumerary axon branches in *unc-119* mutants (Knobel et al., 2001). For example, functional synapses may fail to form in mutant animals leading to the activity-dependent formation of extra branches as seen in *ttx-2* and *ttx-4* mutants (Coburn et al., 1998). Alternatively, *unc-119* mutants may fail to correctly process target-dependent differentiation signals, fail to properly stabilize microtubule arrays in axons, or fail to maintain the neuronal polarity that differentiates axons from dendrites. A comparison of axon branching between *unc-119* mutants and strains without functional synapses, such as *unc-13* (Richmond et al., 1999) or *unc-104* (Antebi et al., 1997) suggests that the additional branches do not likely result from defects in neural activity.

Rather, guidance, stability or polarity defects are likely to be more important in determination of the mutant phenotype.

#### **1.4 Analysis of the UNC-119 protein**

UNC-119 was the first member of this protein family to be discovered (Maduro and Pilgrim, 1995) but many other homologues have been found since in diverse species such as the fly, zebrafish, mouse, cow and in humans (Higashide et al., 1998, Maduro et al., 2000). An amino acid alignment of some representative homologues is shown in Figure 1.3. In addition to structural conservation these genes are functionally homologous; both *Drosophila* and human Unc119 are capable of rescuing the mutant worm when provided as transgenes behind the worm promoter (Maduro et al., 2000).

No domains (regions of 60 amino acids or more having sequence similarity to functional regions in other proteins) have been identified from this primary sequence though several motifs (shorter amino acid sequences of 6 to 12 residues with known function) have been proposed. Computer analysis of the human homolog, HsUnc119, identified putative SH3 and SH2 binding motifs along with conserved tyrosine phosphorylation signals (Figure 1.4) (Cen et al., 2003). In human eosinophils, following HsUnc119 activation by the cytoplasmic domain of the interleukin 5 receptor alpha sub chain (IL5R $\alpha$ ), these motifs activate both Lyn and Hck Src-type non-receptor tyrosine kinases. Similarly, HsUnc119 activation of the Src kinases Fyn and Lck is essential for T-cell activation (Gorska et al., 2004).

Members of the Src family play crucial roles in cytoskeleton dynamics (Frame et al., 2002). Src contains internal low-affinity SH3 and SH2 binding motifs that interact with its SH3 and SH2 domains, respectively (Figure 1.5). Displacement of these motifs

by higher-affinity motifs from an interacting protein leads to a conformational change. This permits an essential tyrosine in the kinase domain to become phosphorylated and thus Src becomes activated. Inactive Src allows actin stress fibers to form resulting in surface adhesion while activating Src signaling leads to a loss of both stress fibers and adherence. Src kinase activity is required for strengthening the F-actin linkage to NCAM during growth cone steering in *Aplysia* (Suter and Forscher, 2001) highlighting its role in axon elongation and guidance.

A weakly-similar *C. elegans* paralog, PDL-1 (phosphodiesterase delta like) having 26% amino acid identity and 51% similarity over a 92 residue domain, has been identified but no nervous system structural defects have yet been found in a *pdl-1* deletion mutant (Maduro, 1998; Smith, 2003). The closest human homolog to PDL-1 is the delta subunit of rod phosphodiesterase (PDE $\delta$ ). Directed two-hybrid assays with human PDE $\delta$  indicated an interaction with the constitutively activated forms of ARL1, ARL2 and ARL3 (Van Valkenburgh et al., 2001). HsUnc119 is somewhat more promiscuous, interacting with both active and inactive forms of ARL1-3. An independent yeast two-hybrid screen of a human retinal cDNA library with HsUnc119 also detected this interaction with ARL2 and subsequent co-immunoprecipitation and immunofluorescence studies of rat retinas demonstrated *in vitro* and *in vivo* interactions between the rat homologs of UNC-119 and ARL2 (Kobayashi et al., 2003).

The function of Arl (ADP ribosylation factor-like) proteins is not well understood. They have been implicated in regulation of the golgi apparatus (Lu et al., 2001), tubulin stabilization (Bhamidipati, Lewis and Cowan, 2000), male fertility (Schurmann et al., 2002), and hypodermal enclosure of the worm embryo (Antoshechkin and Han, 2002).

EVL-20 is the nematode homolog most similar to Arl2. Mutants in *evl-20* have defects in vulva and gonad formation as well as in hypodermal enclosure and elongation (Anotshechkin and Han, 200). *evl-20* mutant worms have been rescued by transgenic expression of human Arl2, suggesting that *evl-20* and Arl2 are functionally conserved. Based on the co-crystallization structure of PDE $\delta$  and Arl2 it has been suggested that HsUnc119 may also be an effector of retinal Arl2 which solubilizes membrane-bound prenylated proteins (Kobayashi et al., 2003 and Hanzal-Bayer et al., 2002).

### **1.5 Homologs of UNC-119 in other organisms**

Mammalian homologs (HsUnc119/HRG4 in humans) of UNC-119 have been reported (Higashide et al., 1996; Swanson et al., 1998). These are enriched in retinal rods and cones (Higashide et al., 1996; Higashide et al., 1998) but expression can also be detected in adrenal glands, cerebellum, cultured fibroblasts and kidney (Swanson et al., 1998). A patient with late-onset cone-rod dystrophy has been shown to be heterozygous for a premature stop codon in HsUnc119 and a heterozygous transgenic mouse with the identical respective mutation also showed age-dependent retinal degeneration (Kobayashi et al., 2000). HsUnc119 cDNA homologs can be found in EST libraries derived from human fetal brain, a human neuronal cell line and mouse embryo. The *Drosophila* homolog (DmUNC-119) is expressed throughout the embryonic nervous system and both the human and *Drosophila* homologs are functional in *C. elegans* (Maduro et al., 2000). Several zebrafish homologs have been reported, one of which is expressed in neural tissue (A. Manning et al., submitted). This expression begins as early as 4 hours post-fertilization and lasts into adulthood. Reducing the level of expression of the neural homolog disrupts embryonic neural organization.

## 1.6 Axonogenesis

Mutations in *unc-119* lead to a wide variety of neuronal defects including a reduced rate of axon elongation, defasciculation of nerve cords, pathfinding defects and maintenance defects leading to supernumerary branches (Maduro, 1998; Knobel et al., 2001). Understanding how UNC-119 might affect so many different processes in the development of the *C. elegans* nervous system requires placing it into the context of known cellular and molecular mechanisms. While nematode neurons may be structurally simpler than those of vertebrates (White et al., 1986), the underlying processes that drive axonogenesis are likely conserved. Below, I outline some of these processes with an emphasis on the underlying cell biology and molecular mechanisms.

Neurons are polarized cells with specialized cellular protrusions known as neurites. In many organisms a single neuron initially sprouts a large number of neurites but one neurite soon develops a predominant morphology, generally becoming longer than the others. This special neurite becomes the axon while the remaining processes develop as dendrites. Most neurons in *C. elegans* are either unipolar or bipolar (one or two processes, respectively) and axons in the worm are typically simple, unbranched extensions (Figure 1.6) (White et al., 1986). While bipolar neurons such as the DA and DB class of motoneurons may separate dendritic (post-synaptic) inputs and axonal (pre-synaptic) outputs onto their two different processes, unipolar neurons such as the AVA, AVB, AVD and AVE interneurons have post- and pre-synaptic regions along their single process. Thus the distinction between axon and dendrite is not always clear in the *C. elegans* nervous system.

### 1.6.1 The growth cone

Growth cones are specialized structures at the distal ends of axons which drive elongation in a precisely-guided manner to specific targets. Growth cones are highly-organized structures rich in actin and microtubules (Dent and Gertler, 2003; Zhou and Cohan, 2003; Gordon-Weeks, 2004). They can be subdivided into central, transitional and peripheral domains (Figure 1.7). The central domain consists primarily of stable microtubules with a small amount of filamentous actin while the peripheral domain contains large amounts of actin and few microtubules. The transitional domain contains both stable and dynamic microtubules as well as an actin mesh. This actin mesh extends into the periphery where it forms lamellipodia which are flattened, veil-like extensions of the cell. In addition, individual actin fibers form bundles that originate in the transitional zone and penetrate through the peripheral zone to form cylindrical extensions, called filopodia, that may project several tens of microns past the periphery of the growth cone.

Growth cones are highly dynamic structures, extending and retracting filopodia and lamellipodia into their surrounding environment in response to attractive and repulsive cues. Such a dynamic structure requires continuous regulated polymerization and depolymerization of both actin and tubulin. Polymerization of both these components occurs rapidly at fiber plus ends in the periphery of the growth cone and more slowly at the minus ends near the center. Depolymerization also occurs at both the plus and minus ends at different rates resulting in net growth or shrinkage of the fibers. Constitutive actin turnover is dependent on myosin driven contraction of actin fibers (Gallo et al., 2002; Brown and Bridgman, 2003). Actin fibers in the lamellipodial actin mesh are thought to be linked orthogonally by myosin II (Figure 1.8). Contraction of this

actomyosin network pulls the peripheral regions towards the center. Actin bundles in filopodia are crosslinked by accessory proteins and linked to the actin mesh by myosin. Likewise, actomyosin contraction of this network pulls the filopodial actin bundle in toward the center where both it and the mesh are depolymerized. This movement of polymerized actin from the periphery to the center, where it is depolymerized, is known as retrograde flow. Actin monomers can then be recycled to the periphery and take place in further polymerization, resulting in dynamic actin flow.

Microtubules may penetrate from the central domain through the actin mesh into the peripheral region and even into filopodia, following actin bundles. Microtubules that extend along actin bundles may be linked to fibrillar actin by protein complexes that could include plakins (Leung et al., 2002), the tumor-suppressor adenomatous polyposis protein (APC) or formin-homology proteins such as mDia (Zhou and Cohan, 2003). Actin retrograde flow causes attached microtubules to be pulled back towards the center by actomyosin contraction; unattached microtubules are also swept back by the actin flow and prevented from crossing the periphery (Figure 1.7). Under this buckling stress, microtubules may actually break, generating new plus and minus ends where polymerization and depolymerization may be initiated (Gordon-Weeks, 2004).

Actin fibers in the filopodial actin bundle may be linked to the extracellular matrix by transmembrane integrins (Figure 1.9) in which case actomyosin contraction causes the bundle to move distally relative to the central domain, exerting a forward force on the filopodia. This force is required for axon elongation. As actin bundles push against the interior of the plasma membrane extra lipid is added to the membrane at the growth cone (Dai and Sheetz, 1995). This membrane is delivered in the form of small

vesicles produced by the golgi and transported along axon microtubules to the growth cone. An octameric protein complex known as the exocyst complex (or the Sec6/8 complex in mammals) targets these vesicles to the growth cone where they fuse to the plasma membrane through typical SNARE-mediated exocytosis (Hazuka et al., 1999; Vega and Shu, 2001). Besides adding membrane to the growth cone, this exocytosis releases vesicular contents, including neurotransmitters into the extra-cellular environment (Young and Poo, 1983; Taylor et al., 1990).

In addition, as filopodia collapse and retract, excess plasma membrane is taken back into the cell by endocytosis at the growth cone (Dai and Sheez, 1995b; Deifenbach et al., 1999; Fournier et al., 2000). Vesicles produced by endocytosis may bring activated ligand-receptor complexes into the cytoplasm for retrograde transport to the cell body where they fulfill their signaling role (Howe et al., 2001). Endocytosis is required for neurite outgrowth; RNA interference of dynamin (a component that is critical for endocytosis) inhibits neuritogenesis in cultured rat hippocampal neurons (Torre et al., 1994). This requirement may be due to transcytosis (endocytosis followed by translocation within the growth cone followed by exocytosis) of the L1 CAM (cell adhesion molecule) from the central domain to the periphery of the growth cone (Kamiguchi and Yoshihira, 2001). Coupled endocytosis and exocytosis may be used by the cell to rapidly change receptor and adhesive properties of specific growth cone plasma membrane domains (Sabo and McAllister, 2003).

### **1.6.2 Elongation, collapse and turning**

The dynamic nature of the growth cone can lead to three distinct behaviours of the entire neurite that are dependent on microtubule stabilization. The neurite can elongate,

it can collapse and stop or it can change direction. Microtubules elongate by relatively slow, steady addition of  $\alpha\beta$  dimers at both the plus and minus ends of the fiber and contract by occasional catastrophic collapse and depolymerization, most rapidly at the plus end. This switching between growth and collapse is known as dynamic instability and is thought to be regulated by a GTP-bound  $\beta$  subunit cap at the plus end. Dynamic instability of microtubules is required for axon elongation and growth cone turning as it allows the microtubules to probe the ever-changing actin filament network. Treating growth cones with agents that either destabilize (e.g. nocodazole) or hyper-stabilize (e.g. taxol) microtubules makes growth cones resistant to turning in response to signaling cues (Jordan and Wilson, 1998).

Net elongation of the neurite requires stabilization of microtubules in the same direction as the current shaft. This seems to occur in a multi-step process. Following protrusion of a filopodium, microtubules and organelles from the central domain advance into the peripheral domain in the region of the protrusion. This is referred to as engorgement and is followed by consolidation, the collapse of the growth cone around the base of the central domain, forming new axon shaft.

Although this process is not well understood, it may involve microtubule associated proteins (MAPs) such as MAP2c or tau which have been shown to decorate the length of individual microtubules *in vitro* (Al-Bassam et al., 2002). Microtubules in the neurite shaft are more stable than microtubules in the more distal growth cone, possibly because they are bundled in the shaft by these cross-linking proteins but defasciculated in the growth cone (Gordon-Weeks, 2004). In addition a complex of proteins known as the plus-end complex, which binds and stabilizes the dynamic

microtubule plus end, are important. The vertebrate EB1 MAP has been shown to bind elongating plus ends and to recruit the adenomatous polyposis coli (APC) microtubule stabilizing protein as well. Another pair of proteins known as CLIP-170 and CLASP may stabilize the microtubule plus end by causing it to associate with the actin cortex (reviewed in Gordon-Weeks, 2004).

Growth cone collapse is the process whereby a growth cone loses its filopodia and lamellipodia and discontinues elongation. The loss of filopodia, in particular, does not permit microtubules to probe the peripheral region of the growth cone and so elongation is abruptly halted. Growth cone turning is the result of localized collapse at one side of the growth cone and associated stabilization at a different side and is dependent on both filopodial actin bundles and microtubule dynamic instability. Drug-induced focal loss of actin bundles causes growth cones to turn away from the source of the disruptive drug (Zhou et al., 2002). Inducing microtubule instability in only a part of the growth cone by focal application of nocodazole also induces growth cone turning away from the drug whereas focal application of the microtubule-stabilizing drug taxol induces growth cones to turn towards the drug (Buck and Zheng, 2002).

### **1.6.3 Axon branching**

Axons can form branches in two ways. Growth cones may split, forming two elongating neurites, or collateral branches may sprout from the sides of the axon shaft behind the growth cone. Drug-induced focal loss of actin bundles near the middle of the growth cone is thought to recapitulate the normal splitting process and results in two separate growth cones at the distal end of two elongating neurites (Zhou et al., 2002). However, many branches do not arise directly from the growth cone but rather they

extend from an interstitial region of the axon shaft (Kalil et al., 2000). Repeated cycles of growth cone collapse, retraction and elongation (collectively called growth cone pausing) have been observed in dissociated cortical neurons using time-lapse microscopy (Kalil et al., 2000). This growth cone pausing results in a region of the axon shaft which has a large lamellar expansion and seems to determine future regions of the axon shaft from which collateral branches will arise. The microtubules in this region are often organized in large loops and the lamellar zone exhibits actin dynamics similar to the growth cone (Dent and Kalil, 2001). A single actin-based filopodium arises and the microtubule loop structure frays, producing new plus ends that elongate and invade the filopodium. This structure subsequently stabilizes and a new growth cone emerges at the tip of the new branch. Branching in worm axons is less well understood, though it is intriguing to note that commissural growth cones similarly pause at obstructions to elongation (Knobel et al., 1999) and supernumerary branches in *unc-119* mutants seem to arise from these pausing regions (Knobel et al., 2001).

## **1.7 Molecular mechanisms of axonogenesis**

Understanding the regulation of growth cone dynamics (and, thus, of axonogenesis) requires a knowledge of underlying molecular mechanisms. Over the last decade many of the major molecular players have been identified and their interactions elucidated. In this section I will describe some of these molecules and the ways in which they interact to regulate axonogenesis.

### **1.7.1 Actin polymerization cycle**

Globular actin (G-actin) monomers circulate freely in the cytoplasm where they may bind either ADP or ATP (dos Remedios et al., 2003). The ABP (actin binding

protein) profilin is concentrated in the peripheral region of the growth cone where it stoichiometrically binds to actin molecules and mediates the exchange by actin of ADP for ATP (Suetsugu et al., 1998). Actin-ATP (or, preferably, profilin-bound actin-ATP) is capable of spontaneous self-assembly to form filamentous actin (F-actin) polymers known as actin fibers or filaments (Figure 1.10). ATP hydrolysis provides the energy required for this polymerization process which occurs primarily at what is known as the barbed or plus end of the elongating filament. Members of the formin family of ABPs likely nucleate actin fibers *in vivo* and “walk” with the barbed end as it elongates (Zigmond, 2004). Capping proteins, such as CapZ, bind to the plus end and limit elongation of F-actin while members of the ena/VASP (enabled/vasodilator-stimulated phosphoprotein) family of ABPs compete with CapZ and promote F-actin elongation in combination with formins.

Actin “treadmilling” (the process whereby actin filaments seem to move in an anterograde fashion without changing length) is characterized by spontaneous association of G-actin-ATP monomers into an elongating F-actin polymer at the plus end and associated depolymerization of F-actin-ADP driven by ADF(Actin Depolymerization Factor)/cofilin at the minus end. The non-receptor tyrosine kinase Abl (Abelson) promotes actin polymerization possibly by activating ena/VASP or RhoGAP or directly through its F-actin bundling activity (Moresco and Koleske, 2003). The RPTP (Receptor Phosphotyrosine Phosphatase) LAR antagonizes Abl phosphorylation of ena/VASP. Members of the Rho family of small GTPases (including Rho, Rac and Cdc42) control the depolymerization activity of ADF/cofilin by activating LIMK (LIM kinase). Regulating the relative rates of polymerization and depolymerization determines the net

length of the actin filament but also affects actin dynamics, which may have an overall stronger influence on the growth cone. For example, overactive LIMK reduces cofilin-dependent depolymerization but, seemingly paradoxically, suppresses growth cone extension. On the other hand activating cofilin-dependent depolymerization through the cofilin phosphatase, Slingshot, activates growth cones (Endo et al., 2003). These effects are likely due to changes in the rate of actin turnover which affect the available pool of monomeric actin.

Actin filaments are organized into larger structures, bundles in filopodia and meshes in lamellipodia. Actin bundles in growth cones typically consist of 15 to 20 individual actin fibers cross-linked so that they are parallel to each other (Ishikawa et al., 2003). A number of proteins have been implicated in cross-linking these individual F-actin filaments including espin (Loomis et al., 2003) and fimbrin (Volkman et al., 2001) in microvilli and fascin in growth cones (Cohan et al., 2001). Fascin colocalizes with actin bundles in *Helisoma* growth cones, especially with bundles in new growth cones formed following axon severing, suggesting that it is an integral component of bundle formation (Cohan et al., 2001). Purified fascin cross-links actin *in vitro* with an inter-fiber spacing comparable to the spacing found in *in vivo* bundles and actin/fascin bundles slide as fast on myosin II as individual actin fibers, suggesting fascin is not inhibitory to retrograde flow (Ishikawa et al., 2003).

The actin mesh in lamellipodia consists of shorter individual actin fibers with many branches at an angle of about 70° to each other. The heptameric Arp2/3 complex nucleates new actin filaments off the side of existing filaments through a synergistic action with capping protein and profilin (Meyer and Feldman, 2002). N-WASP (neural

Wiscott-Aldrich syndrome protein) binds directly to Arp2/3 resulting in an increase in Arp2/3 nucleation activity. N-WASP contains binding sites for the small GTPase Rho family member Cdc42 and for phosphatidylinositol-4,5-diphosphate (PIP<sub>2</sub>) which, together, regulate N-WASP activation of Arp2/3. Hydrolysis of actin-ATP to actin-ADP at the branch initiation site leads to pruning and disassembly of the branch.

Homologues of most of the molecules involved in actin polymerization/depolymerization have been characterized in *C. elegans*. Three putative profilin homologues have been identified and RNAi knockdown against one of them (PFN-1) results in embryonic lethality due to early cytokinesis failure (Severson et al., 2002); the other two have no RNAi phenotype. (RNAi does not always work efficiently in the worm nervous system.) PFN-1 binds to the worm formin homolog, CYK-1 and RNAi knockdown of CYK-1 gives a phenotype similar to RNAi knockdown of PFN-1. Disruption of any of the worm homologues of the Arp2/3 complex (ARX-1, 2, 4, 5, 6,7) or N-WASP (WSP-1), by contrast, causes gastrulation, elongation and epidermal enclosure defects though cell division occurs normally (Sawa et al., 2003). Mutants of the worm ena/VASP homolog, UNC-34, have also been isolated and shown to have a variety of axon guidance defects. *unc-34* mutants also suppress excessive axon elongation resulting from stimulation by ectopic axon guidance factors (Gitai et al., 2003). Two isoforms of the actin depolymerizing protein, ADF/cofilin have been identified in the worm (UNC-60A, UNC60-B). Null mutations in UNC-60B have disorganized muscle actin filaments while RNAi of UNC-60A causes a failure in cytokinesis early in embryogenesis, highlighting the critical role of actin turnover in many processes (Ono et al., 2003). The functions of worm homologues of ROCK and PAK have also been

investigated. ROCK (LET-502) is believed to play a role in embryo elongation (Wissmann et al., 1997) while PAK (PAK-1) localization suggests a role in hypodermal enclosure (Chen et al., 1996).

### **1.7.2 Rho family members (small GTPases)**

It is clear from Figure 1.10 and the above discussion that members of the Rho family of small GTPases are involved in regulating actin polymerization/depolymerization at several key points in the process. Rho family members involved in cytoskeletal reorganization include Rho, Rac and Cdc42 (Kaibuchi et al., 1999). The Rho family is part of the Ras GTPase superfamily and Rhos are similarly activated when bound to GTP and inactivated when that GTP is hydrolyzed to GDP. Rho proteins cycle between GTP-bound active and GDP-bound inactive states under the control of other proteins (Figure 1.11). RhoGEFs (Rho Guanyl Exchange Factors also sometimes called RhoGRPs or Rho Guanyl Releasing Proteins) replace GDP with GTP to activate Rho while RhoGAPs (Rho GTPase Activation Proteins) inactivate Rho by inducing the hydrolysis of GTP to GDP. Inactive Rho-GDP may be sustained in that state by binding to RhoGDI (Rho Guanyl Dissociation Inhibitor) until RhoGDF (Rho Guanyl Dissociation Factor) displaces RhoGDI exposing the GDP to substitution for GTP by RhoGEF. Upstream signaling cascades regulate Rho family member activity by phosphorylating (activating) or dephosphorylating (deactivating) these regulatory proteins, RhoGEF, RhoGAP, RhoGDI and RhoGDF.

The specific roles of Rho, Rac and Cdc42 in actin cytoskeletal remodelling have been elucidated by microinjection of these proteins into cultured fibroblasts or by expression of constitutively-active or dominant-negative forms of the protein in cultured

neurons (reviewed in Meyer and Feldman, 2002). Activated Rho results in the formation of actin stress fibers and focal adhesions. Rac activation leads to the formation of lamellipodia. Cdc42 activation results in the formation of filopodia. Although the complete mechanisms for the formation of filopodia, lamellipodia and focal adhesions have not yet been elucidated much is known about some of the sub-components (Figure 1.10).

Cdc42 binds N-WASP and together with PIP<sub>2</sub> activates the Arp2/3 complex to promote the formation of actin fiber branches. In addition both Cdc42 and Rac can activate the p21-associated serine/threonine kinase, PAK, which, in turn, phosphorylates and activates LIMK. Activated LIMK phosphorylates ADF/cofilin resulting in an inactive form of this protein which is unable to depolymerize actin fibers at the pointed (minus) end. Similarly, Rho also inactivates ADF/cofilin depolymerization of the actin filament by phosphorylating LIMK via the Rho-associated kinase, ROCK. Thus activated forms of all three Rho family members suppress actin depolymerization through LIMK. This may result in growth cone extension by shifting actin dynamics towards increased polymerization or it may lead to stalling or collapse by inhibiting actin turnover. Unfortunately, it is not yet clear how generally deactivating actin fiber depolymerization results in increased filopodial or lamellipodial extension when Cdc42 or Rac is activated but results in decreased motility when Rho is activated.

As noted previously, activated Cdc42 has other effects on actin polymerization via N-WASP and it is likely that Rho and Rac, similarly, have other partners that mediate their specific effects. For example, in addition to causing the formation of actin stress-fibers, activated Rho induces growth cone collapse. Rho-GTP activates ROCK which

phosphorylates and inactivates MLCP (myosin light chain phosphatase) leading to an increase in active myosin II (Kimura et al., 1996). This stimulates actomyosin activity in both filopodia and lamellipodia leading to an increase in retrograde flow and a retraction of these protrusions. In addition, it is likely that Rho, Rac and Cdc42 cross-regulate each other's activity to some extent, though the precise mechanisms are unknown.

### **1.8 Axon guidance**

In order for axons to reach their eventual targets elongation at the growth cone must be steered through a complex environment consisting of other neurons, glia and extra-cellular matrix (ECM). For instance, DA/DB class motor neurons in the worm have cell bodies that lie along the VNC but extend commissures dorsolaterally to the DNC (Figure 1.12). These commissures first exit the cell body, travel some small distance along the VNC either anteriorly or posteriorly, turn (perhaps crossing the midline), project circumferentially along the inner surface of hypodermal cells until they reach the DNC where they again turn and fasciculate with the DNC.

Along the way these axons encounter several major barriers including body wall muscles and the lateral nerve cord made of CAN, ALA and PVD axons. The lateral nerve cord adheres to the overlying lateral hypodermal cells and a commissural axon needs to break this connection before extending its growth cone between the nerve and the hypodermis (Knobel et al., 1999). By contrast, worm muscle cells have a basement membrane layer sandwiched between themselves and the hypodermis; all three layers are connected by hemidesmosome struts. The distance between the hypodermis and basement membrane is too narrow for the growth cone to traverse in its normal form. Instead it sends filopodia through this region; the first one to reach the other side signals

the others to collapse and the growth cone is reassembled at the tip of this filopodium (Knobel et al., 1999).

### **1.8.1 Guidance signals**

Various guidance molecules in the extracellular environment signal to the growth cone as either attractant or repellent cues. Four major classes of guidance molecules have been identified: netrins, semaphorins, ephrins and slits (reviewed in Huber et al., 2003). In addition receptor phosphotyrosine phosphatases (RPTPs), neurotrophins, cell-adhesion molecules and metalloproteinases may either modulate signaling or act as guidance cues themselves.

Attraction towards and repulsion from localized guidance cues requires coordination of localized growth cone stabilization and collapse (Gallo and Letourneau, 2003). Attraction towards a cue requires growth cone stabilization in the direction of the cue or along a signaling gradient and growth cone collapse most distal from the signal. Repulsion away from a guidance cue requires the opposite process, stabilization of the growth cone most distal with concomitant collapse of the proximal growth cone. Because these are coordinated movements, Rho, Rac and Cdc42 may all be simultaneously involved in both attraction and repulsion though at different sites within the growth cone. While growth cone collapse is usually accompanied by F-actin depolymerization, it is possible to separate these two processes, indicating depolymerization is not a requirement of collapse (Journey et al., 2002).

As an axon moves up or down a guidance cue gradient it may need to adjust its sensitivity to the changing concentration of the guidance molecule so that the growth cone maintains a consistent response. The coordination of Rho family members to effect

complex movements associated with attraction or repulsion and putative mechanisms for adjusting growth cone sensitivity are not understood at all.

#### **1.8.1.1 Netrins**

Netrins are small, secreted proteins with sequence similarities to portions of basement membrane laminins. In worms, netrin (UNC-6) is expressed in early ventral neurons and is presumed to form a ventrolateral gradient with the highest concentration at the ventral midline (Wadsworth et al., 1996). Mutant worms show extensive axon guidance defects, primarily a failure of commissures to fully elongate from the VNC to the DNC or to extend to the VNC from lateral positions. Netrins can act as attractants or repellants depending on which receptors they engage.

Attraction results when netrin binds to DCC (deleted in colo-rectal cancer) receptors (UNC-40 in worms, Frazzled in *Drosophila*). These molecules have large extracellular domains containing multiple immunoglobulin (Ig) and fibronectin III (FNIII) repeats, and large cytoplasmic domains. Netrin binding causes DCC homodimerization through conserved cytoplasmic motifs and activation of Cdc42 and Rac, possibly through the Nck (DOCK - Dreadlocks - in flies) adaptor protein and Trio (UNC-73) RhoGEF.

Neurons which also express members of the UNC-5 family form DCC/UNC-5 heterodimers upon binding netrin and this results in repulsion of the growth cone. The mechanism is not known, though interaction of the ligand-receptor complex with the phosphotyrosine phosphatase Shp2 leading to down-regulation of Rho has been implicated (Tong et al., 2001).

### 1.8.1.2 Semaphorins

Semaphorins comprise a large number of guidance molecules containing a conserved 500 amino acid extracellular Sema domain (Mueller, 1999; Raper, 2000). Semaphorins may be secreted or cell-bound, the latter either by transmembrane domains or GPI (glycosylphosphatidylinositol) anchors. The *C. elegans* genome contains three semaphorins (Fuji et al., 2002), two transmembrane (*Ce-sema-1a/smp-1* and *Ce-sema-1b/smp-2*) and one secreted (*Ce-sema-2a/mab-20*). Mutations in any of the semaphorins in the worm result in variable epidermal migration and adhesion defects, as well as mechanosensory neuron axon guidance and branching defects (Ginzburg et al., 2002).

All classes of semaphorin bind to a heteromeric or multimeric receptor complex containing a plexin family member as a common component. Plexins are a large, conserved family of transmembrane proteins. Secreted class III semaphorins bind to a multimeric complex that includes plexin, neuropilin and the cell adhesion molecule, L1 (Huber et al., 2003). Neuropilins are short, transmembrane proteins that contain a small cytoplasmic domain which has no known signaling function and is not required for transducing the semaphorin signal. The L1 CAM likely plays a signal modulating role and is discussed below.

*C. elegans* has two plexin family members, PLX-1 and PLX-2 but no known neuropilin homolog, so other molecules likely act as co-receptors. PLX-1 is likely the receptor for SMP-1 as *plx-1* mutants largely recapitulate the *smp-1* mutant phenotype but not that of *mab-20* mutants and recombinant SMP-1 but not MAB-20 binds PLX-1 expressed on the surface of HEK293T cells (Fuji et al., 2002). PLX-2 is likely the receptor for MAB-20 as *plx-2* null mutants enhance weak *mab-20* alleles and *plx-2*

mutants exhibit similar epidermal defects to those found in *mab-20* mutants (Ikegami et al., 2004).

Although downstream transduction of semaphorin signals is not well-understood, it is clear that Rho GTPases play an important part. Rho family members may be sequestered away from LIMK at the plasma membrane through semaphorin-dependent binding to the cytoplasmic domain of plexin. This may induce growth cone collapse through blocking LIMK activity (and concomitant increase in ADF/cofilin actin depolymerization). Alternatively different Rho family members may compete for direct binding to paxilin, activate LIMK locally, decrease ADF/cofilin activity and reduce actin turnover required for elongation. It is not clear which of these opposed mechanisms may predominate and how they lead to growth cone collapse.

Other semaphorins bind to different plexin-co-receptor complexes and may have different downstream mechanisms. For instance, the *Drosophila* Class 1 semaphorin binds a complex containing a plexin and the Off-track (OTK) kinase-dead receptor tyrosine kinase (Winberg et al., 2001). Downstream signaling events are not known but likely involve recruiting an active kinase and activation of MCLP.

### **1.8.1.3 Ephrins**

Ephrins are membrane-bound signaling molecules and thus require cell-cell contact to initiate their guidance cues, which may be either repulsive or adherent. Ephrins fall into two classes based on their mechanism of attachment to the plasma membrane; Ephrin-As are tethered via GPI-linkages while Ephrin-Bs contain transmembrane and highly-conserved cytoplasmic domains (Mueller, 1999; Cutforth and Harrison, 2002). Ephrin receptors, called Ephs, make up the largest vertebrate family of

receptor tyrosine kinases. They are characterized by a weakly-conserved extra-cellular Ig-like domain, a highly-conserved cysteine-rich region and two FN III repeats.

Ephrins and their receptors are involved in a wide variety of contact-mediated tissue morphogenesis, including topographic mapping of neural projections, cell migration, vascularization and tissue-border formation (Huber et al., 2003). The worm genome contains four Ephrins (EFN-1 to EFN-4), all GPI-anchored, and a single Eph receptor (VAB-1) (Wang et al., 1999; Chin-Sang et al., 2002). Worms mutant in ephrin signaling exhibit embryonic hypodermal enclosure defects, head formation defects and other problems associated with epidermal cell fusion. Although ephrins are expressed in neuroblasts in the worm, the primary signaling is to overlying epidermal cells rather than between neurons.

Ephrins and their Eph receptors form a tetrameric complex consisting of two signaling molecules and two receptors (Himanen et al., 2001). Signaling can be in both the “forward” and “reverse” direction, that is from Ephrin to Eph receptor or vice-versa. Forward signaling is initiated when Ephrin ligand binding induces dimerization and autophosphorylation of the Eph receptors. A constitutively-bound RhoGEF, ephexin, is then activated and activates Rho while inhibiting Cdc42 and Rac. This leads to activation of ROCK and inhibition of PAK and, thus, F-actin depolymerization. At the same time the MAPK (mitogen-activating protein kinase) pathway is deactivated by Ras signaling and this also results in neurite retraction by unknown mechanisms. Lastly Eph receptor signaling leads to dephosphorylation of Abl tyrosine kinase, which inhibits actin polymerization through reduced Ena/VASP activity at F-actin barbed (plus) ends.

Ephrin-B cytoplasmic domains can also be autophosphorylated upon binding to the Eph receptors, leading to “reverse” signaling in the ligand-displaying cell. Although the mechanism of this reverse signaling is not as well understood as forward signaling, it is likely to involve a reduction in FAK (focal adhesion kinase) activity via an SH2/SH3 adaptor protein leading to the disassembly of F-actin stress fibers. This combination of repulsive forward and reverse signaling, causes a pair of axons to pull away from each other following contact. Though this kind of repulsion is unknown in worms, it is common in neurons containing highly-branched axons or dendrites and limits such branching networks to their own non-overlapping fields.

#### **1.8.1.4 Slits**

Slits are a small family of conserved, secreted molecules involved in a wide variety of axon development processes including pathfinding, branching and cell migration (reviewed in Wong et al., 2002). A typical Slit protein contains an N-terminal secretory signal, four leucine-rich repeats, seven or nine EGF repeats and a C-terminal cysteine knot. Slits may act as repellants or attractants or exhibit activity that is unrelated to axon guidance, such as promoting dendritic branching (Wang et al., 1999). Slit signaling is mediated by transmembrane Robo (Roundabout) receptors, Ig super-family proteins with multiple extra-cellular Ig and FNIII repeats and conserved cytoplasmic domains involved in protein-protein interactions. Slit binds Robo through an interaction between the Slit leucine-rich repeats and the Robo Ig repeats.

Slit-Robo signaling has been most intensely studied in commissure formation at the ventral midline of *Drosophila*. Slit initially acts as an attractant for commissural axons as they project from lateral nerve bundles to the ventral midline. However, once

axons cross the midline, Slit acts as a repellent to prevent the axons from re-crossing. Before crossing the midline, Robo receptor levels at the surface of the axon are kept low through the action of Comm (Commissureless) which causes Robo to be endocytosed and, possibly, degraded (Keleman et al., 2002). Robo down-regulation is also dependent on a secreted metalloproteinase (Kuzbanian in flies), indicating the importance of a possible cleavage signal in Robo (Schimmelpfeng et al., 2001). After crossing the midline Comm is down-regulated through an unknown mechanism and Robo localizes to the axon surface where it can mediate Slit repulsion.

Slit acts as a short range repellent to axons after they cross the midline and sensitivity to Slit is modulated by different Robo receptors. Three separate longitudinal bundles are found on each side of the ventral midline of the fly and their distance from the midline seems to be dictated by combinations of Robo receptors. Neurons in the most medial bundle express only Robo, the intermediate bundle contains Robo and Robo3 while the most lateral bundle expresses Robo, Robo3 and Robo2.

The worm genome contains only a single Slit homolog (SLT-1) and a single Robo homolog (SAX-3). Worms mutant for *sax-3* or *slt-1* exhibit VNC midline defects that are reminiscent of fly Robo mutants (Zallen et al., 1998; Hao et al., 2001). In addition amphid axons in the head of *sax-3* mutants have A/P placement defects so that they form an anteriorly displaced nerve ring structure (Zallen et al., 1999). *slt-1* mutants display no such defects.

Slit-Robo signaling is likely mediated through several independent pathways. Slit binding to Robo activates so-called srGAPs (Slit-Robo GAPs) through SH3-binding motifs in the Robo cytoplasmic domain. This leads to a decrease in Cdc42 and Rho, but

not Rac, activity. Robo activation also leads to activation of Ena/VASP which, as seen above, increases the rate of F-actin polymerization. It is not clear how these downstream effectors result in neurite elongation towards the midline prior to the growth cone crossing but elongation away from the midline after. It is possible that other unknown signaling molecules are responsible for modulating the response to Slit binding or that localized signaling at the leading or trailing edge of the growth cone could explain the different behaviours. Activated Robo has also recently been shown to inhibit cadherin-mediated adhesion by Abl-mediated phosphorylation of  $\beta$ -catenin (Rhee et al., 2002). This allows retracting filopodia to release their attachment to the underlying substrate and pull back towards the central domain of the growth cone.

#### **1.8.1.5 Neurotrophins**

The Neurotrophin family of secreted signaling molecules consist of neurotrophins (NT), nerve growth factor (NGF) and brain-derived neurotrophic factor (BDNF). They are best known for their role in neuronal survival, growth and plasticity (Huber et al., 2003) though they are also proposed to protect neurons from damage following injuries such as axotomy or ischemia (Sofroniew et al., 2001). In addition neurotrophins have recently been shown to modulate axon guidance signals and to act as attractants on their own. Neither neurotrophin homologs nor their receptors have been identified in the worm.

Neurotrophins signal by binding either of two receptors.  $p75^{\text{NTR}}$  is the first member of a family of transmembrane receptor proteins that includes tumor necrosis factor receptor (TNF-R). Trks are receptor tyrosine kinases with a glycosylated extracellular domain containing Ig repeats, a single transmembrane domain and a cytosolic

kinase domain. Each neurotrophin binds to a specific Trk receptor: NGF binds to TrkA, BDNF and NT-4/5 bind to TrkB and NT-3 binds to TrkC. Like other receptor tyrosine kinases, ligand binding leads to Trk dimerization and autophosphorylation of the kinase domain. By contrast p75<sup>NTR</sup> seems to bind its neurotrophin ligand as a monomer.

Activation of the Trk receptor leads to a large variety of downstream events including activation of the Ras/MAPK and PI3K/AKT pathways that are crucial for cell-survival. In addition, activation of Cdc42, Rho and Rac by PI3K is the likely mechanism by which Neurotrophins exert their attractive influence. Although signaling through p75<sup>NTR</sup> is less well-understood, it is hypothesized to involve Rho and ROCK activation leading to reduced actin depolymerization. Neurons grown in the presence of different Neurotrophins exhibit different levels of sensitivity to Semaphorin-induced growth cone collapse, highlighting this molecule's ability to fine-tune cellular processes.

## **1.9 Adhesion**

Axons may elongate over a variety of substrates but, in every case, adhesion to the underlying substrate is necessary to provide the force required for elongation as well as to provide neural survival signals. Pioneer axons extend over a substrate that may include glial cells, epidermal cells or extra-cellular matrix. Follower axons fasciculate with pioneer axons and so can be considered to acquire some of their adhesive forces via axon-axon interactions. In the worm the AVG neuron in the retrovesicular ganglion near the head pioneers the right side of the VNC (Figure 1.13). In the preanal ganglion in the posterior of the animal, the PVPL axon decussates (crosses the midline) and extends anteriorly, fasciculating with the pioneering AVG axon. PVPR (the partner of PVPL on the right side of the body) also extends an axon across the midline and then pioneers the

left VNC. Subsequently PVQ axons elongate and fasciculate with ipsilateral PVP axons in the VNC. Thus, pioneer axons elongate over ECM and hypodermis while follower axons elongate by fasciculating along the surface of pioneer axons.

Axon-axon and axon-epidermis adhesion is largely mediated by members of the Ig super-family, including neural cell-adhesion molecules (NCAMs), L1 and cadherins (Walsh and Doherty, 1997) while axon-ECM adhesion is mediated by integrins (Milner and Campbell, 2002). NCAMs and the closely-related L1 are characterized by multiple extra-cellular FNIII domains followed by several Ig domains, a single transmembrane domain and a short cytoplasmic domain. They interact by homophilic binding through their Ig domains to similar molecules on the surface of adjacent cells (or their axons) and, thus, are most likely involved in regulating axon fasciculation (Goodman, 1996). Flies mutant in FasII (the *Drosophila* homologue of NCAM) exhibit fasciculation defects in longitudinal nerve fibers and FasII overexpression causes axons to fail to defasciculate at their normal choice points. Worm homologues of NCAM have been tentatively identified but no mutants have yet been isolated (Teichmann and Chothia, 2000). LAD-1 has been identified as the only worm homolog of L1 and, though no mutants have been isolated, expression of a putative dominant-negative LAD-1 behind the native promoter causes variable morphological defects, gonad formation defects and uncoordinated movement (Chen et al., 2001).

NCAM on elongating axons is often post-translationally modified to contain variable-length chains of the carbohydrate polysialic acid (PSA). Increased levels of PSA associated with NCAM on axons reduces NCAM-mediated adhesion yet, paradoxically, complete enzymatic removal of PSA phenocopies NCAM loss-of-function

mutants. NCAMs (including L1) interact with the cytoskeleton and cluster in sub-cellular cell-surface microdomains through interaction with ankyrins (UNC-44) and spectrin in the cell cortex. NCAM clustering activates MAPK signaling that is likely required for continued neural survival and axon growth. L1 signaling is likely mediated through internalization into a signaling endosome and downstream Src activation of the MAPK cascade.

Cadherins are calcium-dependent transmembrane molecules that share a cadherin-repeat domain of about 100 amino acids and that bind by homophilic interactions between pairs of dimers located on opposing cell-surfaces (Juliano, 2002). The cytoplasmic domains of cadherins attach directly to  $\beta$ -catenins and these subsequently recruit  $\alpha$ -catenins which link to the actin cytoskeleton through actin-bundling proteins such as  $\alpha$ -actinin and vinculin. A worm homolog of the classic cadherin (HMR-1) has been identified and worms mutant for the neural-specific isoform have defasciculated VNCs as well as guidance defects and supernumerary branch formation in commissures (Broadbent and Pettitt, 2002). In vertebrates it is possible that a large number of splice variants of different cadherin family members may act as a sort of axon code, allowing for the fasciculation of similar axons and as a synapse code, allowing target recognition (Ranscht, 2000).

Integrins are transmembrane  $\alpha\beta$  heterodimeric glycoproteins that mediate cell-cell and cell-ECM adhesion (Milner and Campbell, 2002). Different integrin subunits interact with different ligands. Interactions with cell-surface CAMs or fibronectins and collagens in the ECM are mediated through so-called RGD (arginine-glycine-aspartate) binding integrins while a different class of integrins directly binds to ECM laminins.

Integrins activate MAPK signaling in a manner similar to NCAMs, through activation of FAK and Ras, and regulate the actin cytoskeleton through suppression of Rho and activation of Rac (Huber et al., 2002).

Both classes of integrins have worm homologues and mutations in all subunits have been identified (Brown, 2000). PAT-2 $\alpha$ /PAT-3 $\beta$  integrin complexes are likely to bind RGD motifs while INA-1 $\alpha$ /PAT-3 $\beta$  integrins are putative laminin binding proteins. Worm integrins are found at many cell-ECM attachment sites and are involved in cell migration, gut morphogenesis, epithelial attachment and in transmitting muscle contractions to the ECM. Thus *pat-2* and *pat-3* mutants arrest at the two-fold stage of embryogenesis and are paralyzed due to disruption of muscle sarcomere structure. By contrast, *ina-1* mutants form misshapen head and pharynx and exhibit defects in long-distance migration of neural cell bodies as well as in axon fasciculation.

Axon guidance signals may be modulated through interaction with adhesion molecules (Rougon and Hobert, 2003). For example, *Xenopus* retinal axons grown on fibrinogen are attracted to netrin but those grown on laminin are repelled by netrin in an integrin-dependent manner (Hopker et al., 1999). Semaphorin-mediated repulsion of cortical axons is similarly dependent on L1 and a soluble L1 fragment switches this repulsion to attraction. Although the mechanisms are not well understood, L1 associates with the semaphorin receptor, neuropilin, and they are co-endocytosed following semaphorin activation. *Trans* interaction between L1 on one cell surface and neuropilin on another blocks endocytosis of the receptor complex and switches the semaphorin response from repulsion to attraction (Castellani et al., 2004).

### 1.10 Axon maintenance and synaptic stability

As axons approach their ultimate targets their growth cones begin to form the structures required for synaptic specialization. This process of synaptogenesis is outside the scope of this work (but for a review, see Broadie and Richmond, 2002). However, synapses may degenerate over time allowing axons to retract and, in vertebrates, this process is inhibited by both electrical activity at the synapse and by neurotrophic signaling from the post-synaptic cell (reviewed in Lim et al., 2003).

In worms, lack of neural activity either during development (Zhao and Nonet, 2000) or following axonogenesis (Coburn et al., 1998) can cause neurons to sprout additional branches. However, aberrant synaptic structure (as in the kinesin transport mutant, UNC-104) or function does not always result in morphologically incorrect axons (Antebi et al., 1997). This suggests that, in the worm, synaptic and axonal stability is likely due to a chemical cue rather than synaptic activity.

Although the mechanism by which synapses may be stabilized is largely unknown, several proteins that may be involved have been recently identified. RPM-1, the worm homolog of *Drosophila* Highwire, is a large cytoplasmic protein of unknown function (Schaefer et al., 2000). *rpm-1* mutant worms exhibit a variety of neural defects including mild guidance defects, aberrant synapse formation, supernumerary branches and axon retraction. The pathway by which RPM-1 might signal axon retraction is completely unknown but studies in the fly have found that inhibiting p190 RhoGAP activity causes mature axons in the CNS to retract, suggesting a role for actin and tubulin stabilization (Billuart et al., 2001).

### 1.11 Specific objectives of this work

The *unc-119* mutant phenotype has been previously shown to be neural in origin and to be the result of a failure in axonogenesis rather than synaptic function (Maduro, 1998; Knobel et al., 2001). Still, the brief preceding review of the molecular mechanisms involved in axon elongation and guidance demonstrates that there are many possibilities for perturbation of this process. The primary purpose of this work was to elucidate the molecular mechanism by which UNC-119 regulates nervous system development in *C. elegans*. Many of the mechanisms described above have only been discovered in the past few years and could not help guide my research until recently. I outline below some of the most obvious roles UNC-119 could theoretically play within the various processes that comprise axonogenesis.

a) UNC-119 could be directly involved in actin or tubulin polymerization or depolymerization. Complete abrogation of actin or tubulin dynamics abruptly halts axon elongation of neurons in culture and it is generally thought that the *in vivo* axon response is similar. Thus, if UNC-119 were involved directly in this process, we might expect axons to elongate only a very short distance, if at all, before the lack of actin or tubulin dynamics led to complete growth cone collapse. This is certainly not what has been previously observed.

However, if UNC-119 were involved in regulation of actin or tubulin turnover (e.g. through regulation of Rho family members) the resulting phenotype would be much more difficult to predict. For example, in cultured neurons, suppression of actin turnover through activation of LIMK by a Rho family member can have different overall effects on growth cone morphology and axon behaviour depending on which specific molecule

(Rho, Rac, or Cdc42) is involved. The different behaviour is likely due to other pathways that are differently activated by the different Rhos. Further, while a reduced rate of axon elongation (Knobel et al., 2001) might be explained by a failure of mutant UNC-119 to correctly regulate actin or tubulin dynamics, it is considerably more difficult to explain UNC-119's role in stabilizing properly-elongated commissures by this mechanism.

b) Alternatively, UNC-119 might be involved in mediating axon guidance signals, such as netrins, semaphorins or ephrins. Compared to mutations in genes involved in netrin-mediated axon guidance, commissures in *unc-119* mutants initially elongate fully from the VNC to the DNC, suggesting the protein is not directly involved in this pathway. Similarly, epidermal migration or closure defects associated with mutations in worm homologues of the semaphorin or ephrin pathways are not found in *unc-119* mutants, though a neural-specific role for UNC-119 in these pathways can not be ruled out on this basis. There are no known neurotrophin homologues in the worm and *unc-119* mutants do not have an anteriorly-displaced nerve ring as seen in mutations in the slit pathway. Thus UNC-119 does not seem to fall strictly into any of these well-known axon guidance pathways.

c) UNC-119 may play a role in cell-cell adhesion. Axon adhesion in the worm has not been studied extensively so it is difficult to relate the neural structure of adhesion mutants to *unc-119* animals. Certainly mutations in some molecules known to be involved in adhesion (such as UNC-44/ankyrin or HMR-1/cadherin) are grossly similar to *unc-119* mutants. However, gross morphological defects in body shape, such as those associated with the L1 NCAM, or with mutations in the integrin complex are not found in *unc-119* mutants.

However, these observations come with the caveat that a single molecule may have multiple roles in different tissues in the worm. Thus, while some genes known to be involved in axon guidance in other organisms (e.g. semaphorins, ephrins and integrins), have non-neural phenotypes in the worm, UNC-119 could act in the same pathway but its effects could be limited to neurons. Further, some mutations result in embryonic lethality prior to, or concomitant with, nervous system development and the function of the affected molecules in worm neurons may not have been studied. In addition the molecular basis of a phenotype may be difficult to establish *a priori* because it is not always easy to distinguish between primary and secondary defects. For example, certain mutations in neural activity (e.g. *tax-2*, *tax-4*) lead to neurons that sprout supernumerary axons from near the cell body. It is generally accepted that these additional branches are a secondary effect resulting from the cell's response to a lack of activity and that TAX-2 and TAX-4 are not directly involved in suppressing axon branching *per se*.

In order to distinguish between these candidate mechanisms or to discover alternate explanations of the *unc-119* mutant phenotype, I identified the following intermediate objectives:

i) Characterize nervous system defects in *unc-119* mutants more thoroughly. The initial step in understanding UNC-119 at the molecular level is to determine its phenotype more precisely. Although the worm has only 302 neurons, characterizing specific axon defects in all neurons in *unc-119* mutants is still a nearly-impossible task. Thus, by using GFP reporters that are only expressed in some neurons, I selected several small neural subsets for closer investigation. In order to more precisely compare axon defects in *unc-119* mutants to other well-characterized mutants, I closely observed the

morphology of a single pair of axons in a variety of mutant strains.

ii) Determine the temporal and tissue-specific requirement for UNC-119. Other clues to the role of UNC-119 might come from an investigation of the spatial and temporal requirement for the functional protein. Constructs expressing UNC-119 in specific tissues at specific times were employed to address this question. If UNC-119 acts intracellularly, we would expect that expression in specific neurons only would rescue the mutant phenotype of those neurons and only those neurons. A role as a mediator of actin or tubulin dynamics (e.g., through Rho-type effectors) or in the signal transduction pathway for guidance cues would be supported by such cell-autonomous behaviour of UNC-119. On the other hand, if UNC-119 acted cell-nonautonomously (i.e. non-neural expression rescuing neural defects) that might suggest that it can serve as a secreted guidance cue itself or that its role might be to regulate some extra-cellular signal (e.g. adhesion) between cells.

UNC-119 is normally expressed from a stage that precedes axonogenesis right through adulthood and it is required post-embryonically for stability of axon structure. However, it is still not known if expression is required at the earliest stage a reporter construct is detectable. This study used some constructs whose expression begins at later stages to address this question.

iii) Determine putative molecular mediators of UNC-119 activity. Much of this work involved searching for potential partners of UNC-119 in the hope that this would permit me to place this gene into some existing pathway. Although UNC-119 homologues have been identified in a wide variety of organisms (Figure 1.3) no known domains, which might give clues to the protein's function, have yet been identified. If

UNC-119 acts in a complex with other proteins (e.g. as a signal mediator, response modulator or adaptor) then we might be able to identify that interaction using standard yeast two-hybrid or co-immunoprecipitation methods. Because the human homolog of UNC-119 is functional in worms (Maduro et al., 2000), it should also exert its effect through the same mechanisms as the worm protein and have the same interacting partners. I carried out yeast two-hybrid screens with both the worm and human UNC-119 proteins looking for potential partners and attempted to raise antibodies to verify these interactions *in vitro*.

iv) Verify candidate molecular interactions. Proteins generally interact through defined domains (or smaller motifs). In order to determine which segments of the UNC-119 protein were required for putative interactions with other proteins, I conducted domain-deletion and site-directed mutagenesis experiments. Domain-deletion experiments entail removing entire sections of the protein and assaying the remaining sections for functionality. Site-directed mutagenesis is a more focused version of this experiment where only a small number of residues (between 1 and 6 amino acids) are specifically mutated and the altered protein is assayed for functionality. These latter experiments were designed to directly address specific hypotheses about the function of UNC-119 in the worm based on findings from other researchers about functions of the mammalian homologues.

Because an amino acid primary sequence analysis of UNC-119 did not suggest any candidate molecular mechanisms underlying the role of UNC-119 in the worm, the approach used in this research was to generate hypotheses through phenotypic and molecular analysis and then to test these via molecular and transgenic experiments.

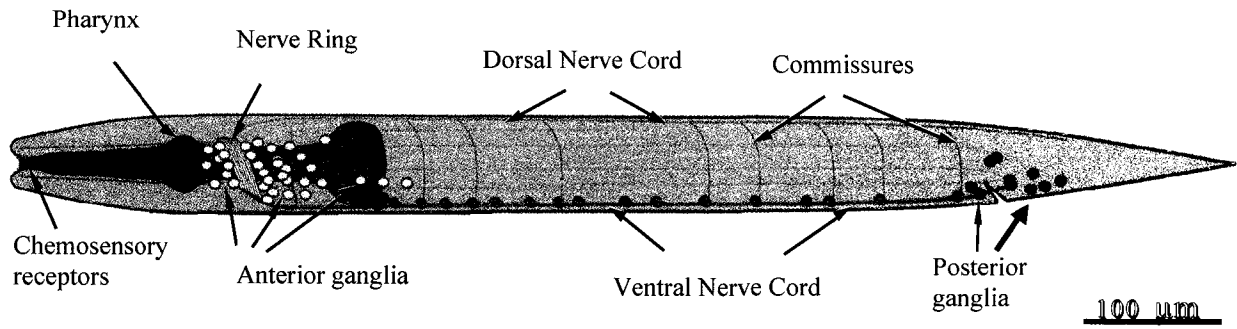


**Figure 1.1** The nervous system of *C. elegans*.

The 302 neurons of the adult hermaphrodite are organized into anterior and posterior ganglia and are found along the ventral midline. The nerve ring (yellow) and its associated cell bodies are found surrounding the pharynx (blue) between the primary and secondary pharyngeal bulbs. Axons extend from cell bodies and fasciculate to form the Ventral and Dorsal nerve cords as well as the circumferential commissures. Anterior is to left, posterior to right. Dorsal is up, ventral down. Adapted from Wadsworth and Hedgecock, 1996.

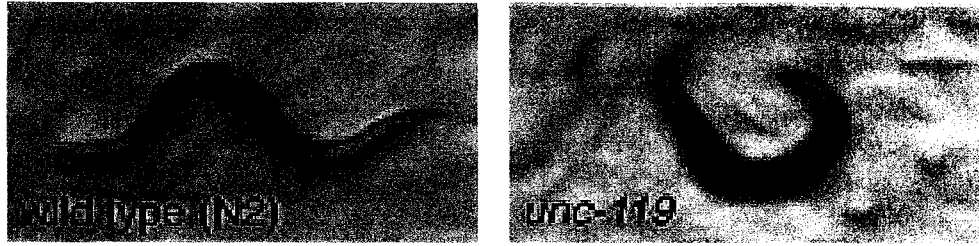


**Figure 1.2 *unc-119* mutant worms**

Mutant worms (right) are paralyzed relative to wild type (left). Images taken on a dissecting microscope show sinusoidal shape of a moving wild-type worm and ventrally-coiled shape typical of adult *unc-119* worms. Young mutant larvae generally move better than adults but not as well as wild type. Adapted from Maduro and Pilgrim, 1995.

```

Human          -----MKVK--KGGGAGTATESAPGPSQSVAPIQPPAESSESGSESEPDAGPGPRP
Zebrafish      -----MKVK--KG---CNT-TD-----LG---VPVT-----T--EEE-----
Xenopus        ---MNRLKARRVQGKE-SGT-SDQ---SS-----IT-----RFRREE-----
Drosophila     MSVVGKQLNPVQSSGAG-AVTTSSSAAGSSSSNSGVEANGGSGGSSGAAAAGAGASGDA
C. elegans     -----MKAEQQQS IAPGSATFP-----SQMPRPPPVTEQAITTEAE-----
C. briggsae   -----MKAEQQQ-SIPPGSATFP-----SQMPRPPPSTEQGITTESE-----
                ::      .      :      :      .

Human          -GPLQRKQPIGPEDEVLGLQRITGDYLCSPENIYKIDFVRFKIRDMSDGTVLFEIKKPPVS
Zebrafish      ---LLANKTISPEDVLGLQKI TENYLCSPEDNLYNIDFTRFKIRDMDTGTVLFEITKPPST
Xenopus        ---LLGLNELRPEHVLGLSRVTDNLYLCKPEDNIFGIDFTRFKIRDLETGTVLFEISKPCSE
Drosophila     MKRPAESSSVTPDEVLHLTKITDDYLCANANVFEIDFTRFKIRDLESGAVLFEIAKPPSE
C. elegans     ---LLAKNQITPNDVLAALPGITQGFLLCSPSANVYNI EFTKQIRDLDEHVLFEIAKPENE
C. briggsae   ---LAKKAQITPNDVLAALPGITQGFLLCSPSANIYNI EFTKQIRDLDEHVLFEIAKPEND
                : *:.** * :* .:**... *:: *:*:*:****::: ***** **

Human          -ERLPINRRD-----LDPNAGRFVRYQFTPAFLRLRQVGATVEFTVGDKPV
Zebrafish      -DRG--DKRD-----VDPNAGRFVRYQFTPAFLRLRQVGATVEFTVGDIP I
Xenopus        -QEEEEESTH-----LDASAGRFVRYQFTPAFLRLRQVGATVEFTVGDKPV
Drosophila     MQYPEGLSSDETMLAAAEKLSLDDTADPNAGRYVRYQFTPAFLNLKTVGATVEFTVGSQPL
C. elegans     -TEE---NLQ-----AQAESARYVRYRFAPNFKLKTVGATVEFKVGDVPI
C. briggsae   --QE---NDE-----SPQESARYVRYRFAPNFKLKTVGATVEFKVGDIP I
                ..*:*:*:*:* * *.*: *****.*. *

Human          -NNFRMIERHYFRNQLLKSFDHFGFCIPSSKNTCEHIYDFPPLSEELISEMIRHPYETQS
Zebrafish      -NNFRMIERHYFREQLLKSFDHFGFCIPSSKNTCEHIYDFPPLSEELIREMILHPYETQS
Xenopus        -KSFMIERHYFRDRI LKSFDHFGFCIPNSRNTCEHMYEFPQLSEELIRLMTENPYETRS
Drosophila     MNNFRMIERHFFRDRL LKTFDFEFGFCFPFSKNTVEHIYDFPNLPPDLVAEMISSPFETRS
C. elegans     -THFRMIERHFFKDRLLKCFDFEFGFCMPNSRNNCEHIYDFPQLSQQLMDDMINNPNETRS
C. briggsae   -HHFRMIERHFFKDRLLKCFDFEFGFCIPNSRNNCEHIYDFPQLSQQLMDDMINNPNETRS
                *****:*:~::~** **.*****:* * *.*.*:*:* * .:*: * * **:*

Human          -DSFYFVDDRLVMHKNKADYSYSGTP--
Zebrafish      -DSFYFVDNKLVMHKNKADYSYSGGP--
Xenopus        -DSFYFVDKKLIMHKNKADYAYNGRP--
Drosophila     MDSFYFVGNRLVMHKNKADYAYDGGNIV
C. elegans     -DSFYFVENKLVHKNKADYSYDA----
C. briggsae   -DSFYFVDNKLVMHKNKADYSYDA----
                ***** .:*:*****:..

```

**Figure 1.3 UNC-119 protein family alignment**

ClustalW alignment of primary amino acid sequence from representative members of the UNC-119 family. “\*” shows identity of amino acids across all proteins in the alignment; “:” shows high degree of similarity; “.” shows lower conservation. ClustalW parameters were modified to improve alignment in divergent regions (Opening and ending gap penalties changed from 10 to 5; extending gap and separation gap penalties changed from 0.05 to 0.5). The alignment was adjusted manually in some poorly-conserved regions. The carboxyl region is generally more conserved, while the amino region is more divergent. GenBank accession numbers: Human – NM005148; Zebrafish – AF387341 ; *Drosophila* – NM13216; *Xenopus* – BG513306; *C. elegans* – NM06698; *C. briggsae* – U45326.

	SH2	SH3 ligand		Tyrosine phosphorylation	
	ligand	#1	#2	#1	#2
Human	EHYDF	APIPQPP	RKQPIGPE	RMIERHY	KNTCEHIY
Zebrafish	EHYEF	VPVT---	ANKTISPE	RMIERHY	KNTCEHIY
Xenopus	EHMYEF	--IT---	GLNELRPE	RMIERHY	RNTCEHMY
Drosophila	EHYEF	SGVEANG	ESSSVTPD	RMIERHF	KNTVEHIY
C. elegans	EHYEF	SQMPRPP	AKNQITPN	RMIERHF	RNNCEHIY
C. briggsae	EHYEF	SQMPRPP	KKAQITPN	RMIERHF	RNNCEHIY
	**:*:*		:*:	*****:	:*..**:*

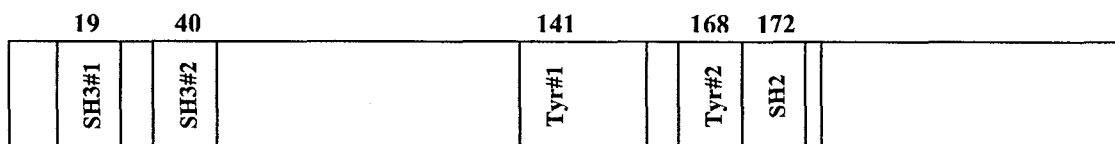


**Figure 1.4 SH2 and SH3 binding and tyrosine phosphorylation motifs in UNC-119**

SH2 binding motif ([DE]-X<sub>2,3</sub>-Y\*-[DE]-[FWP]) is highly-conserved including obligate phosphorylated tyrosine (bold). The first SH3 binding motif is very poorly conserved in other animals, although consensus motif (RX<sub>2</sub>PX<sub>2</sub>P) is present in worms. Residues of second SH3 binding motif in HsUnc119 are slightly conserved in other animals but consensus motif is not present in worm UNC-119. Two tyrosine phosphorylation motifs ([RK]-X<sub>2,3</sub>-[DE]-X<sub>2,3</sub>-Y\*) are well conserved, except the tyrosine in the first motif is a phenylalanine in worms and flies. Although the second motif is somewhat more divergent, the consensus sequence is found in all these animals. \* shows identity of amino acids across all proteins in the alignment; : shows high degree of similarity; . shows lower conservation. Lower figure shows relative location of motifs within entire protein. Numbers represent residue number where motif in figure below begins.

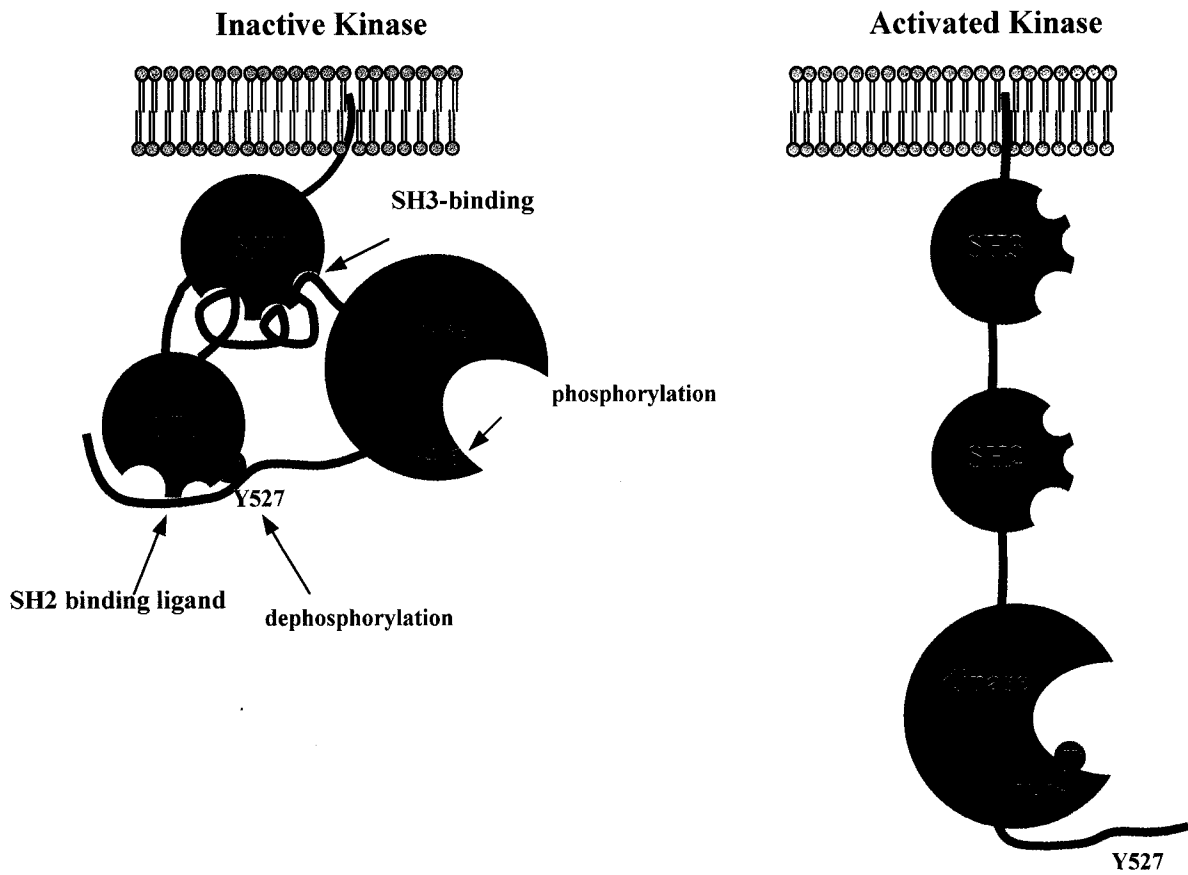


**Figure 1.5 Src activation.**

Src contains low-affinity internal SH2 and SH3 binding motifs that hold the kinase domain in an inactive confirmation. Activating proteins contain higher-affinity binding motifs that displace the internal Src ligands. This permits phosphorylation of tyrosine 416 and a conformational change to expose the activated kinase domain. Adapted from Martin, 2001.



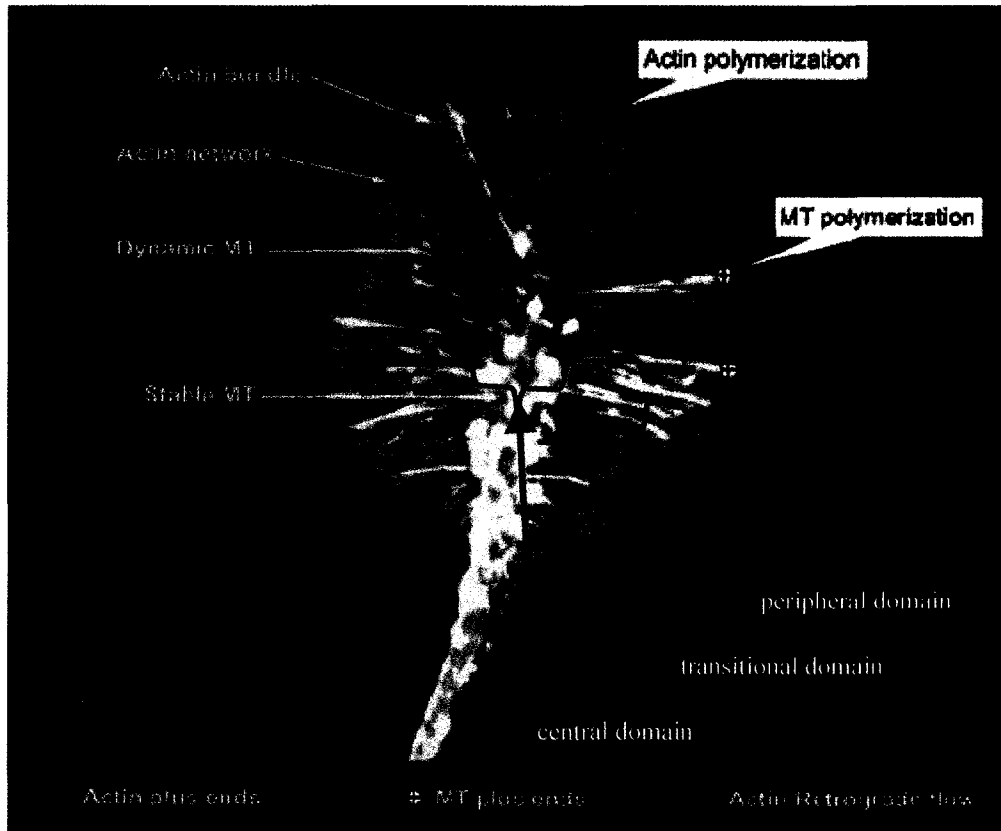


**Figure 1.7 The growth cone**

*Helisoma* growth cone with actin stained green and tubulin stained red (yellow shows overlap). The peripheral domain contains the lamellipodia and is composed primarily of short actin filaments organized in a meshwork. The central domain consists of both stable and dynamic microtubules. Actin bundles extend from the central domain through the peripheral domain and form filopodia. (a) Some microtubules also extend from the central domain into the peripheral domain by tracking along actin bundles. Actin and microtubule polymerization occurs at the plus end at the periphery. (b,c) Microtubules buckle and bend when they are carried rearward by actin retrograde flow. (e) Two microtubules may attach to a single actin bundle or (d) single microtubule may attach to more than one actin bundle. Adapted from Zhou and Cohan, 2003.

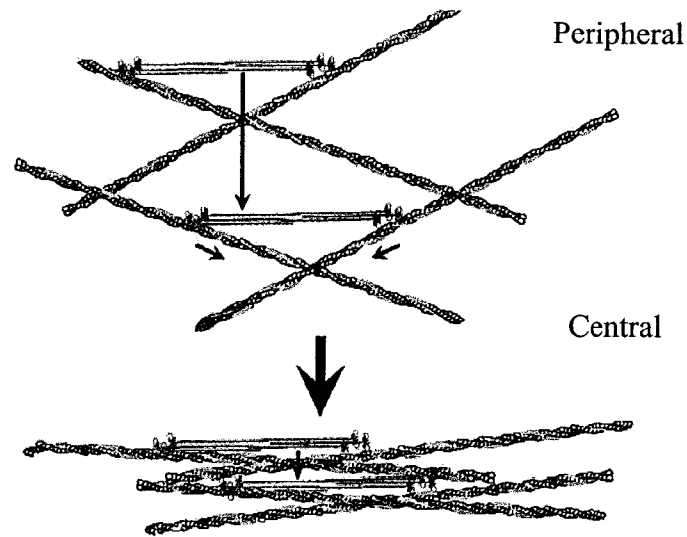


**Figure 1.8 Actomyosin contraction drives retrograde flow**

Actin mesh in lamellipodia (black and gray) is linked by myosin II fibers (gray). Activation of myosin causes head domains to “walk up” actin fibers and pulls the mesh inward towards central domain. Adapted from Brown and Bridgman, 2003.

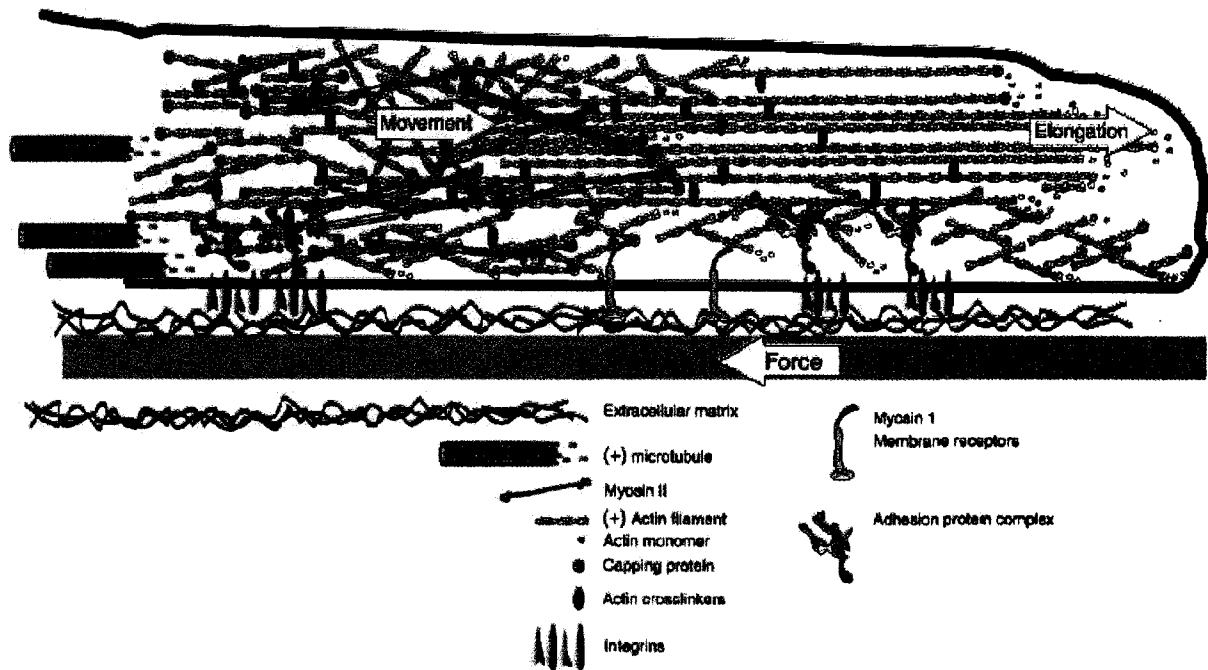


**Figure 1.9 Generation of forward force in filopodia**

Actin bundles are linked to the actin mesh by myosin and to the extracellular matrix (ECM) through integrins. Actomyosin contraction results in the filopodium exerting a backward force on the ECM which drives the bundle (and the plasma membrane that surrounds it) forward. Adapted from Brown and Bridgman, 2003.

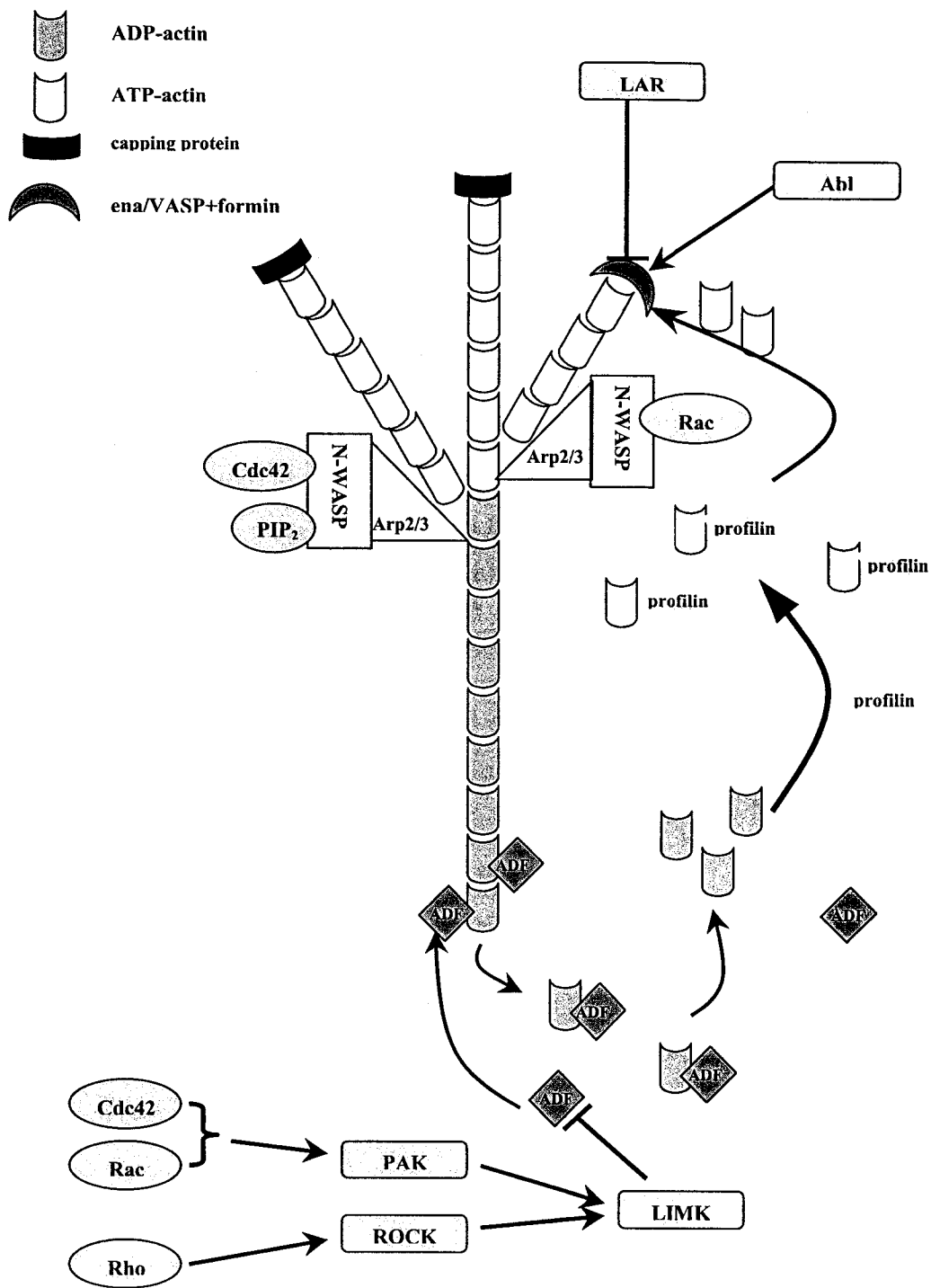


**Figure 1.10 Actin polymerization is a dynamic, regulated process**

Profilin activates G-actin by exchanging ADP for ATP. ena/VASP + formin at the barbed end of an elongating actin fiber competitively dissociates the inhibitory capping protein and allows for the addition of new actin-ATP monomers to the fiber. Individual actin monomers inside the F-actin eventually hydrolyze ATP to ADP nearer the central region. This allows ADF/cofilin to depolymerize the actin filament near the central region and for new G-actin monomers to be freed into the cytoplasm. ADF activity is regulated by LIM kinase which is in turn regulated by PAK and ROCK under the control of the small GTPases Rho, Rac and Cdc42. The N-WASP/Arp2/3 complex nucleates new branches at 70° to the original and this is also regulated by small GTPases. Adapted from Meyer and Feldman, 2002

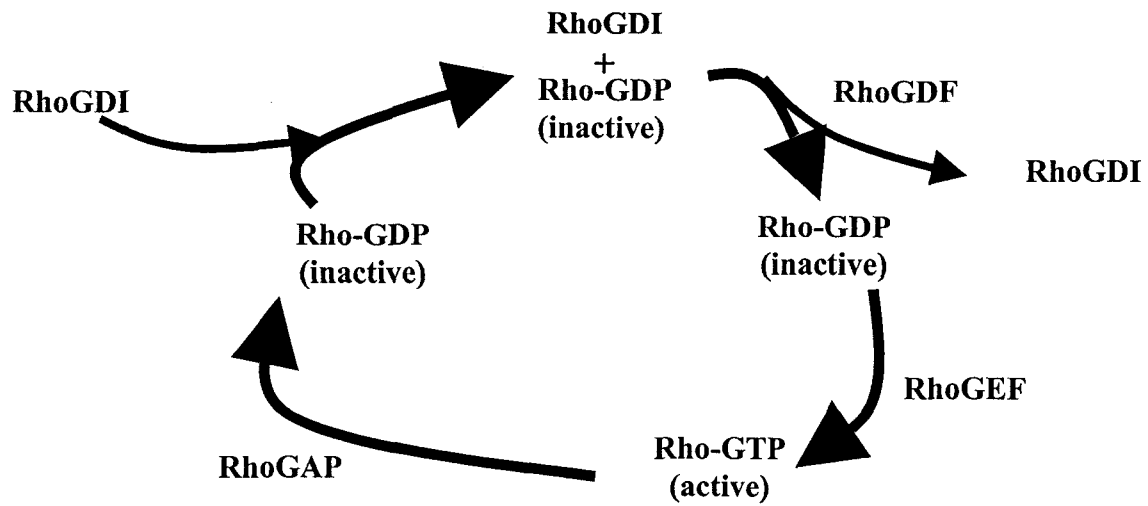


**Figure 1.11 Rho cycles between active and inactive states**

Rho-GDP is held in an inactive state by binding to RhoGDI. When RhoGDI is displaced by RhoGDF then RhoGEF exchanges GDP for GTP leading to activated Rho-GTP. Hydrolysis of the GTP to GDP by RhoGAP returns Rho to the inactive state. External control of the activity level of Rho can then be exercised by regulating the activities of RhoGEF, RhoGAP, RhoGDI or RhoGDF.

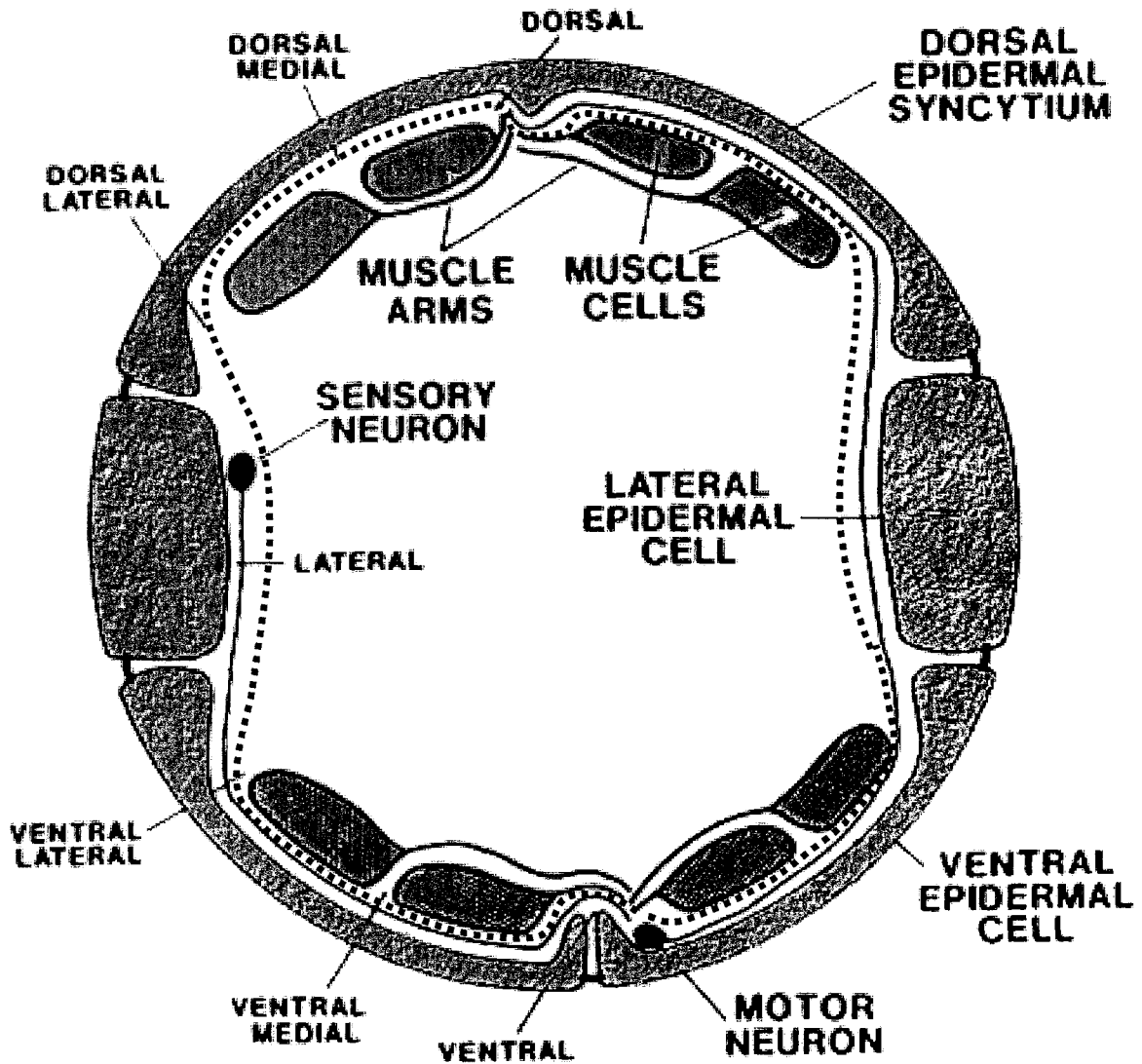


**Figure 1.12 Commissures elongate through a complex environment**

Cross-section through the mid-body shows body wall muscles (dark gray) and basement membranes (dotted line) underlying hypodermis (light gray). Commissures in body of worm extend from motor neuron cell body in VNC to DNC by elongating between the basement membrane and the hypodermis. Adapted from Antebi et al., 1997.

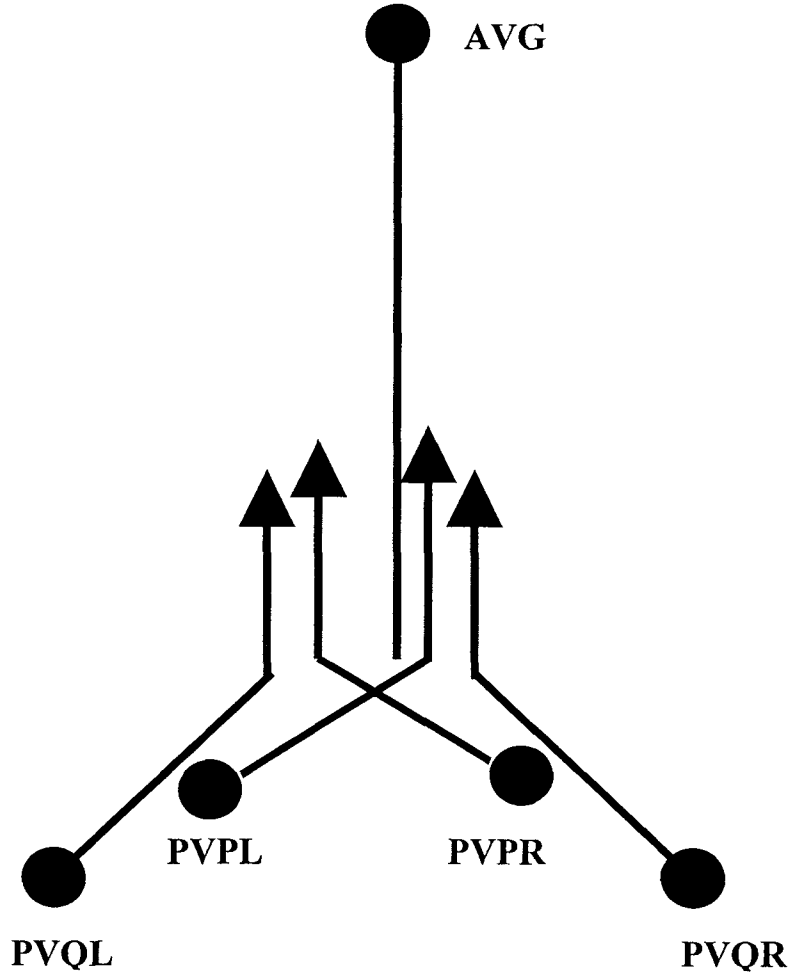


**Figure 1.13 Pioneering and following axons in the *C. elegans* VNC**

AVG pioneers the right VNC by extending an axon from the retrovesicular ganglion in the head to the preanal ganglion near the tail of the worm. PVPL fasciculates with AVG on the right side while its sister PVPR pioneers the left VNC. PVQL and PVQR then fasciculate with ipsilateral pioneer axons. Adapted from Antebi et al., 1997.

## 1.12 References

- Al-Bassam, J., Ozer, R.S., Safer, D., Halpain, S. and Milligan, R.A. (2002), MAP2 and tau bind longitudinally along the outer ridges of microtubule protofilaments, *Journal of Cell Biology*, **157**: 1187–1196
- Altun-Gultekin, Z., Andachi, Y., Tsalik, E.L., Pilgrim, D., Kohara, Y. and Hobert, O. (2001), A regulatory cascade of three homeobox genes, *ceh-10*, *ttx-3* and *ceh-23*, controls cell fate specification of a defined interneuron class in *C. elegans*, *Development*, **128**: 1951-69
- Antebi, A., Norris, C.R., Hedgecock, E.M. and Garriga, G. (1997) Cell and growth cone migrations, in *C. Elegans II*, Riddle, D.M., Blumenthal, T., Meyer, B.J. and Priess, J.R., eds., Cold Spring Harbor Laboratory Press, Plainview, New York, USA
- Antoshechkin, I. and Han, M. (2002), The *C. elegans evl-20* gene is a homolog of the small GTPase ARL2 and regulates cytoskeleton dynamics during cytokinesis and morphogenesis, *Developmental Cell*, **2**: 579-591
- Billuart, P., Winter, C.G., Maresh, A., Zhao, X. and Luo, L. (2001), Regulating axon branch stability: the role of p190 RhoGAP in repressing a retraction signaling pathway, *Cell*, **107**: 195-207
- Bhamidipati, A., Lewis, S.A. and Cowan, N.J. (2000), ADP ribosylation factor-like protein 2 (Arl2) regulates the interaction of tubulin-folding cofactor D with native tubulin. *Journal of Cell Biology*, **149**: 1087-96
- Broadbent, I.D. and Pettitt, J. (2002), The *C. elegans hmr-1* gene can encode a neuronal classic cadherin involved in the regulation of axon fasciculation, *Current Biology*, **12**: 59–63
- Broadie, K.S. and Richmond, J.E. (2002), Establishing and sculpting the synapse in *Drosophila* and *C. elegans*, *Current Opinion in Neurobiology*, **12**: 491-8
- Brown, J. and Bridgman, P.C. (2003), Role of myosin II in axon outgrowth, *Journal of Histochemistry and Cytochemistry*, **51**: 421-8
- Brown, N.H. (2000), Cell-cell adhesion via the ECM: integrin genetics in fly and worm, *Matrix Biology*, **19**: 191-201
- Buck, K.B. and Zheng, J.Q. (2000), Growth cone turning induced by direct local modification of microtubule dynamics, *Journal of Neuroscience*, **22**: 9358–9367
- Castellani, V., Falk, J. and Rougon, G. (2004), Semaphorin3A-induced receptor endocytosis during axon guidance responses is mediated by L1 CAM, *Molecular and Cellular Neuroscience*, **26**: 89-100

- Cen, O., Gorska, M.M., Stafford, S.J., Sur, S. and Alam, R. (2003), Identification of UNC119 as a novel activator of src-type tyrosine kinases, *Journal of Biological Chemistry*, **278**: 8837-8845
- Chen, L., Ong, B. and Bennett, V. (2001), LAD-1, the *Caenorhabditis elegans* L1CAM homolog, participates in embryonic and gonadal morphogenesis and is a substrate for fibroblast growth factor receptor pathway-dependent phosphotyrosine-based signaling, *Journal of Cell Biology*, **154**: 841–855
- Chen, W., Chen, S., Yap, S.F. and Lim, L. (1996), The *Caenorhabditis elegans* p21-activated kinase (CePAK) colocalizes with CeRac1 and CDC42Ce at hypodermal cell boundaries during embryo elongation, *Journal of Biological Chemistry*, **271**: 26362-8
- Chin-Sang, I.D., Moseley, S.L., Ding, M., Harrington, R.J., George, S.E. and Chisholm, A.D. (2002), The divergent *C. elegans* ephrin EFN-4 functions in embryonic morphogenesis in a pathway independent of the VAB-1 Eph receptor, *Development*, **129**: 5499-510
- Christensen, M., Estevez, A., Yin, X., Fox, R., Morrison, R., McDonnell, M., Gleason, C., Miller, D.M. 3<sup>rd</sup> and Strange, K. (2002), A primary culture system for functional analysis of *C. elegans* neurons and muscle cells, *Neuron*, **33**: 503-514
- Coburn, C.M., Mori, I., Ohshima, Y. and Bargmann, C.I. (1998), A cyclic nucleotide-gated channel inhibits sensory axon outgrowth in larval and adult *Caenorhabditis elegans*: a distinct pathway for maintenance of sensory axon structure, *Development*, **125**: 249-58
- Cohan, C.S., Welnhof, E.A., Zhao, L., Matsumura, F. and Yamashiro, S. (2001), Role of the actin bundling protein fascin in growth cone morphogenesis: localization in filopodia and lamellipodia, *Cell Motility and the Cytoskeleton*, **48**: 109 –120
- Cutforth, T. and Harrison, C.J. (2002), Ephs and ephrins close ranks, *Trends in Neuroscience*, **25**: 332-333
- Dai, J. and Sheetz, M.P. (1995), Axon membrane flows from the growth cone to the cell body, *Cell*, **83**: 693-701
- Dai, J. and Sheetz, M.P. (1995b). Regulation of endocytosis, exocytosis, and shape by membrane tension, *Cold Spring Harbor Symposium in Quantitative Biology*, **60**: 567-71
- Diefenbach, T.J., Guthrie, P.B., Stier, H., Billups, B. and Kater, S.B. (1999), Membrane recycling in the neuronal growth cone revealed by FM1–43 labeling, *Journal of Neuroscience*, **19**: 9436–9444

- Dent, E.W. and Gertler, F.B. (2003), Cytoskeletal dynamics and transport in growth cone motility and axon guidance, *Neuron*, **40**: 209–227
- Dent, E.W. and Kalil, K. (2001), Axon branching requires interactions between dynamic microtubules and actin filaments, *Journal of Neuroscience*, **21**: 9757–9769
- dos Remedios, C.G., Chhabra, D., Kekic, M., Dedova, I.V., Tsubakihara, M., Berry, D.A. and Nosworthy, N.J. (2003), Actin binding proteins: regulation of cytoskeletal microfilaments, *Physiological Reviews*, **83**: 433-73
- Fournier, A.E., Nakamura, F., Kawamoto, S., Goshima, Y., Kalb, R.G. and Strittmatter, S.M. (2000), Semaphorin3A enhances endocytosis at sites of receptor-F-actin colocalization during growth cone collapse, *Journal of Cell Biology*, **49**: 411-22
- Frame, M.C., Fincham, V.J., Carragher, N.O. and Wyke, J.A. (2002) V-Src's hold over actin and cell adhesions, *Nature Reviews. Molecular Cell Biology*, **3**: 233-245
- Fujii, T., Nakao, F., Shibata, Y., Shioi, G., Kodama, E., Fujisawa, H. and Takagi, S. (2002), *Caenorhabditis elegans* PlexinA, PLX-1, interacts with transmembrane semaphorins and regulates epidermal morphogenesis, *Development*, **129**: 2053-2063
- Gallo, G. and Letourneau, P.C. (2003), Regulation of growth cone actin filaments by guidance cues, *Journal of Neurobiology*, **58**: 92–102
- Gallo, G., Yee, H.F., Jr. and Letourneau, P.C. (2002), Actin turnover is required to prevent axon retraction driven by endogenous actomyosin contractility, *Journal of Cell Biology*, **158**: 1219-28
- Ginzburg, V.E., Roy, P.J. and Culotti, J.G. (2002), Semaphorin 1a and semaphorin 1b are required for correct epidermal cell positioning and adhesion during morphogenesis in *C. elegans*, *Development*, **129**: 2065-2078
- Gitai, Z., Yu, T.W., Lundquist, E.A., Tessier-Lavigne, M. and Bargmann, C.I. (2003), The netrin receptor UNC-40/DCC stimulates axon attraction and outgrowth through enabled and, in parallel, Rac and UNC-115/AbLIM, *Neuron*, **37**: 53-65
- Goodman, C.S. (1996), Mechanisms and molecules that control growth cone guidance, *Annual Review of Neuroscience*, **19**: 341-77
- Gordon-Weeks, P.R. (2004), Microtubules and growth cone function, *Journal of Neurobiology*, **58**: 70-83
- Grunwald, I.C. and Klein, R. (2002), Axon guidance: receptor complexes and signaling mechanisms, *Current Opinion in Neurobiology*, **12**: 250–259

- Hanzal-Bayer, M., Renault, L., Roversi, P., Wittinghofer, A. and Hillig, R.C. (2002), The complex of Arl2-GTP and PDE $\delta$ : from structure to function, *The EMBO Journal*, **21**: 2095-2106
- Hao, J.C., Yu, T.W., Fujisawa, K., Culotti, J.G., Gengyo-Ando, K., Mitani, S., Moulder, G., Barstead, R., Tessier-Lavigne, M. and Bargmann, C.I. (2001), *C. elegans* slit acts in midline, dorsal-ventral, and anterior-posterior guidance via the SAX-3/Robo receptor, *Neuron*, **32**: 25-38
- Hazuka, C.D., Foletti, D.L., Hsu, S-C., Kee, Y, Hopf, F.W. and Scheller, R.H. (1999), The sec6/8 complex is located at neurite outgrowth and axonal synapse-assembly domains, *Journal of Neuroscience*, **19**: 1324-1334
- Higashide, T., Murakami, A., McLaren, M.J. and Inana G. (1996) Cloning of the cDNA for a novel photoreceptor protein, *Journal of Biological Chemistry*, **271**: 1797-1804
- Higashide, T., McLaren, M.J. and Inana, G. (1998) Localization of HRG4, a photoreceptor protein homologous to *unc-119*, in ribbon synapse, *Investigative Ophthalmology & Visual Science*, **39**: 690-698
- Himanen, J.P., Rajashankar, K.R., Lackmann, M., Cowan, C.A., Henkemeyer, M. and Nikolov, D.B. (2001), Crystal structure of an Eph receptor-ephrin complex, *Nature*, **414**: 933-8
- Hopker, V.H., Shewan, D., Tessier-Lavigne, M., Poo, M., Holt, C. (1999), Growth-cone attraction to netrin-1 is converted to repulsion by laminin-1, *Nature*, **401**: 69-73
- Howe, C.L., Valletta, J.S., Rusnak, A.S. and Mobley, W.C. (2001), NGF signaling from clathrin-coated vesicles: evidence that signaling endosomes serve as a platform for the Ras-MAPK pathway, *Neuron*, **32**: 801-814
- Huber, A.B., Kolodkin, A.L., Ginty, D.D. and Cloutier, J-F. (2003), Signaling at the growth cone: ligand-receptor complexes and the control of axon growth and guidance, *Annual Review of Neuroscience*, **26**: 509-63
- Ikegami, R., Zheng, H., Ong, S-H. and Culotti, J. (2004), Integration of semaphorin-2A/MAB-20, ephrin-4, and UNC-129 TGF- $\beta$  signaling pathways regulates sorting of distinct sensory rays in *C. elegans*, *Developmental Cell*, **6**: 383-395
- Ishikawa, R., Sakamoto, T., Ando, T., Higashi-Fujime, S. and Kohama, K. (2003), Polarized actin bundles formed by human fascin-1: their sliding and disassembly on myosin II and myosin V *in vitro*, *Journal of Neurochemistry*, **87**: 676-685
- Jordan, M.A. and Wilson, L. (1998), Use of drugs to study role of microtubule assembly dynamics in living cells, *Methods in Enzymology*, **298**: 252-276

- Juliano, R.L. (2002), Signal transduction by cell adhesion receptors and the cytoskeleton: functions of integrins, cadherins, selectins and immunoglobulin-superfamily members, *Annual Review of Pharmacology and Toxicology*, **42**: 283–323
- Jurney, W.M., Gallo, G., Letourneau, P.C., McLoon, S.C. (2002), Rac1 mediated endocytosis during ephrin-A2 and semaphorin 3A induced growth cone collapse, *Journal of Neuroscience*, **22**: 6019–6028
- Kaibuchi, K., Kuroda, S., Amano, M. (1999), Regulation of the cytoskeleton and cell adhesion by the Rho family GTPases in mammalian cells, *Annual Review of Biochemistry*, **68**: 459–486
- Kalil, K., Szebenyi, G. and Dent, E.W. (2000), common mechanisms underlying growth cone guidance and axon branching, *Journal of Neurobiology*, **44**: 145–158
- Kamiguchi, H. and Yoshihara, F. (2001), The role of endocytic L1 trafficking in polarized adhesion and migration of nerve growth cones, *Journal of Neuroscience*, **21**: 9194–9203
- Keleman, K., Rajagopalan, S., Cleppien, D., Teis, D., Paiha, K., Huber, L., Technau, G. and Dickson, B.J. (2002). Comm sorts Robo to control axon guidance at the *Drosophila* midline, *Cell*, **110**: 415–427
- Kimura, K., Ito, M., Amano, M., Chihara, K., Fukata, Y., Nakafuku, M., Yamamori, B., Feng, J., Nakano, T., Okawa, K., Iwamatsu, A. and Kaibuchi K. (1996), Regulation of myosin phosphatase by Rho and Rho-associated kinase (Rho-kinase), *Science*, **273**: 245–48
- Knobel, K.M., Jorgensen, E.M. and Bastiani, M.J. (1999) Growth cones stall and collapse during axon outgrowth in *Caenorhabditis elegans*, *Development*, **126**: 4489–4498
- Knobel, K.M., Davis, W.S., Jorgensen, E.M. and Bastiani, M.J. (2001) UNC-119 suppresses axon branching in *C. elegans*, *Development*, **128**: 4079–4092
- Kobayashi, A., Higashide, T., Hamasaki, D., Kubota, S., Sakuma, H., An, W., Fujimaki, T., McLaren, M.J., Weleber, R.G. and Inana, G. (2000), HRG4 (UNC119) mutation found in cone-rod dystrophy causes retinal degeneration in a transgenic model, *Investigative Ophthalmology & Visual Science*, **41**: 3268–77
- Leung, C.L., Green, K.J. and Liem, R.K. (2002), Plakins: a family of versatile cytolinker proteins, *Trends in Cell Biology*, **12**: 37–45
- Lim, K-C., Lim, S.T. and Federoff, H.J. (2003), Neurotrophin secretory pathways and synaptic plasticity, *Neurobiology of Aging*, **24**: 1135–1145

- Loomis, P.A., Zheng, L., Sekerková, G., Changyaleket, B., Mugnaini, E. and Bartles, J.R. (2003), Espin cross-links cause the elongation microvillus-type parallel actin bundles in vivo, *Journal of Cell Biology*, **163**: 1045–1055
- Lu, L., Horstmann, H., Ng, C. and Hong W. (2001), Regulation of Golgi structure and function by ARF-like protein 1 (Arl1), *Journal of Cell Science*, **114**: 4543-55
- Maduro, M.F., Gordon, M., Jacobs R. and Pilgrim, D.B. (2000) The UNC-119 family of neural proteins is functionally conserved between humans, *Drosophila* and *C. elegans*, *Journal of Neurogenetics*, **13**: 191-212
- Maduro, M. (1998) Characterization of the *unc-119* gene of *Caenorhabditis elegans*, PhD. Thesis, University of Alberta, Canada
- Maduro, M. and Pilgrim, D. (1995) Identification and Cloning of *unc-119*, a Gene Expressed in the *Caenorhabditis elegans* Nervous System. *Genetics* **141**, 977-988.
- Martin, G.S. (2001), The hunting of the Src, *Nature Reviews. Molecular Cell Biology*, **2**: 467-75
- Meyer, G. and Feldman, E.L. (2002), Signaling mechanisms that regulate actin-based motility processes in the nervous system, *Journal of Neurochemistry*, **83**: 490–503
- Milner, R. and Campbell, I.L. (2002), The integrin family of cell adhesion molecules has multiple functions within the CNS, *Journal of Neuroscience Research*, **69**: 286–291
- Moresco, E.M.Y and Koleske, A.J. (2003), Regulation of neuronal morphogenesis and synaptic function by Abl family kinases, *Current Opinion in Neurobiology*, **13**: 535–544
- Mueller, B.K. (1999), Growth cone guidance: first steps towards a deeper understanding, *Annual Review of Neuroscience*, **22**: 351–88
- Ono, K., Parast, M., Alberico, C., Benian, G.M. and Ono, S. (2003), Specific requirement for two ADF/cofilin isoforms in distinct actin-dependent processes in *Caenorhabditis elegans*, *Journal of Cell Science*, **116**: 2073-85
- Ranscht, B. (2000), Cadherins: molecular codes for axon guidance and synapse formation, *International Journal of Developmental Neuroscience*, **18**: 643-651
- Raper, J. (2000), Semaphorins and their receptors in vertebrates and invertebrates, *Current Opinion in Neurobiology*, **10**: 88–94
- Rhee, J., Mahfooz, N.S., Arregui, C., Lilien, J., Balsamo, J. and VanBerkum, M.F.A. (2002), Activation of the repulsive receptor Roundabout inhibits N-cadherin mediated cell adhesion, *Nature Cell Biology*, **4**: 798-805

- Richmond, J.E., Davis, W.S. and Jorgensen, E.M. (1999) UNC-13 is required for synaptic vesicle fusion in *C. elegans*, *Nature Neuroscience*, **2**: 959-964
- Riddle, D.L. (1988), The dauer larva, in the nematode *Caenorhabditis elegans*, Wood, W.B. (ed.), Cold Spring Harbor Laboratory Press, Cold Spring Harbor, NY
- Rougon, G. and Hobert, O. (2003), New insights into the diversity and function of neuronal immunoglobulin superfamily molecules, *Annual Review of Neuroscience*, **26**: 207–38
- Sabo, S.L. and McAllister, A.K. (2003), Mobility and cycling of synaptic protein-containing vesicles in axonal growth cone filopodia, *Nature Neuroscience*, **6**: 1264-9
- Sawa, M., Suetsugu, S., Sugimoto, A., Miki, H., Yamamoto, M. and Takenawa, T. (2003), Essential role of the *C. elegans* Arp2/3 complex in cell migration during ventral enclosure, *The Journal of Cell Science*, **116**: 1505-18
- Schaefer, A.M., Hadwiger, G.D. and Nonet, M.L. (2000), *rpm-1*, a conserved neuronal gene that regulates targeting and synaptogenesis in *C. elegans*, *Neuron*, **26**: 345-56
- Schimmelpfeng, K., Gogel, S. and Klambt, C. (2001), The function of leak and kuzbanian during growth cone and cell migration, *Mechanisms of Development*, **106**: 25-36
- Schurmann, A., Koling, S., Jacobs, S., Saftig, P., Krauss, S., Wennemuth, G., Kluge, R. and Joost, H.G. (2002), Reduced sperm count and normal fertility in male mice with targeted disruption of the ADP-ribosylation factor-like 4 (Arl4) gene, *Molecular and Cellular Biology*, **22**: 2761-8
- Severson, A.F., Baillie, D.L. and Bowerman, B. (2002), A formin homology protein and a profilin are required for cytokinesis and Arp2/3-independent assembly of cortical microfilaments in *C. elegans*, *Current Biology*, **12**: 2066–2075
- Smith, J. (2003), Characterization of PDE $\delta$  in *Caenorhabditis elegans* and *Danio rerio*, PhD. Thesis, University of Alberta, Canada
- Sofroniew, M.V., Howe, C.L. and Mobley, W.C. (2001), Nerve growth factor signaling, neuroprotection, and neural repair, *Annual Review of Neuroscience*, **24**: 1217–281
- Suetsugu, S., Miki, H. and Takenawa, T. (1998), The essential role of profilin in the assembly of actin for microspike formation, *The EMBO Journal*, **17**: 6516–6526
- Suter, D.M. and Forscher, P. (2001) Transmission of growth cone traction force through apCAM–cytoskeletal linkages is regulated by Src family tyrosine kinase activity, *Journal of Cell Biology*, **155**: 427–438

- Swanson, D.A., Chang, J.T., Campochiaro, P.A., Zack, D.J. and Valle, D. (1998) Mammalian orthologs of *C. elegans unc-119* highly expressed in photoreceptors, *Investigative Ophthalmology & Visual Science*, **39**: 2085-2094
- Taylor, J., Docherty, M. and Gordon-Weeks, P.R. (1990), GABAergic growth cones: release of gamma-aminobutyric acid precedes the expression of synaptic vesicle antigens, *Journal of Neurochemistry*, **54**: 1689-1699
- Teichmann, S.A. and Chothia, C. (2000), Immunoglobulin Superfamily Proteins in *Caenorhabditis elegans*, *Journal of Molecular Biology*, **296**: 1367-1383
- Tong, J., Killeen, M., Steven, R., Binns, K.L., Culotti, J. and Pawson, T. (2001), Netrin stimulates tyrosine phosphorylation of the UNC-5 family of netrin receptors and induces Shp2 binding to the RCM cytodomain, *Journal of Biological Chemistry*, **276**: 40917-40925
- Torre, E., McNiven, M.A. and Urrutia, R. (1994), Dynamin 1 antisense oligonucleotide treatment prevents neurite formation in cultured hippocampal neurons, *Journal of Biological Chemistry*, **269**: 32411-7
- Vega, I.E. and Hsu, S-C. (2001), The exocyst complex associates with microtubules to mediate vesicle targeting and neurite outgrowth, *Journal of Neuroscience*, **21**: 3839-3848
- Volkman, N., DeRosier, D., Matsudaira, P. and Hanein, D. (2001), An atomic model of actin filaments cross-linked by fimbrin and its implications for bundle assembly and function, *Journal of Cell Biology*, **153**: 947-956
- Wadsworth, W.G., Bhatt, H. and Hedgecock, E.M. (1996), Neuroglia and pioneer neurons express UNC-6 to provide global and local netrin cues for guiding migrations in *C. elegans*, *Neuron*, **16**: 35-46
- Wadsworth, W.G. and Hedgecock, E.M. (1996), Hierarchical guidance cues in the developing nervous system of *C. elegans*, *BioEssays*, **18**: 355-362
- Walsh, F.S. and Doherty, P. (1997), Neural cell adhesion molecules of the immunoglobulin superfamily: Role in axon growth and guidance, *Annual Review of Cell and Developmental Biology*, **13**: 425-56
- Wang, K.H., Brose, K., Arnott, D., Kidd, T., Goodman, C.S., Henzel, W. and Tessier-Lavigne, M. (1999), Biochemical purification of a mammalian slit protein as a positive regulator of sensory axon elongation and branching, *Cell*, **96**: 771-84
- Wang, X., Roy, P.J., Holland, S.J., Zhang, L.W., Culotti, J.G. and Pawson, T. (1999), Multiple ephrins control cell organization in *C. elegans* using kinase-dependent and -independent functions of the VAB-1 Eph receptor, *Molecular Cell*, **4**: 903-13

White, J.G., Southgate, E., Thomson, J.N. and Brenner, S. (1986) The structure of the nervous system of *Caenorhabditis elegans*. *Philosophical Transactions of the Royal Society of London. Series B, Biological Sciences*, **314**: 1-340.

Winberg, M.L., Tamagnone, L., Bai, J., Comoglio, P.M., Montell, D. and Goodman, C.S. (2001), The transmembrane protein Off-track associates with Plexins and functions downstream of Semaphorin signaling during axon guidance, *Neuron*, **32**: 53-62

Wissmann, A., Ingles, J., McGhee, J.D. and Mains, P.E. (1997), *Caenorhabditis elegans* LET-502 is related to Rho-binding kinases and human myotonic dystrophy kinase and interacts genetically with a homolog of the regulatory subunit of smooth muscle myosin phosphatase to affect cell shape, *Genes and Development*, **11**: 409-22.

Wong, K., Park, H.T., Wu, J.Y. and Rao, Y. (2002), Slit proteins: molecular guidance cues for cells ranging from neurons to leukocytes, *Current Opinion in Genetics and Development*, **12**: 583-91

Young, S.H. and Poo, M.M., (1983), Spontaneous release of transmitter from growth cones of embryonic neurones, *Nature*, **305**: 634-637

Zallen, J.A., Yi, B.A. and Bargmann, C.I. (1998), The conserved immunoglobulin superfamily member Sax-3/Robo directs multiple aspects of axon guidance in *C. elegans*, *Cell*, **92**: 217-227

Zallen, J.A., Kirch, S.A. and Bargmann, C.I. (1999), Genes required for axon pathfinding and extension in the *C. elegans* nerve ring, *Development*, **126**: 3679-92.

Zhao, H. and Nonet, M.L. (2000), A retrograde signal is involved in activity-dependent remodeling at a *C. elegans* neuromuscular junction, *Development*, **127**: 1253-1266

Zhou, F-Q. and Cohan, C.S. (2003), How actin filaments and microtubules steer growth cones to their targets, *Journal of Neurobiology*, **58**: 84-91.

Zhou, F-Q., Waterman-Storer, C.M. and Cohan, C.S. (2002), Focal loss of actin bundles causes microtubule redistribution and growth cone turning, *Journal of Cell Biology*, **157**: 839-849

Zigmond, S.H. (2004), Formin-induced nucleation of actin filaments, *Current Opinion in Cell Biology*, **16**: 99-105

## **Chapter 2 - Expression of *C. elegans* UNC-119 outside the nervous system rescues movement and dauer formation defects**

### **2.1 Introduction**

A likely neural basis for the *C. elegans unc-119* mutant phenotype has been previously demonstrated (Maduro and Pilgrim, 1995). Mutant adults are nearly paralyzed except for moderate foraging head movement and they constitutively assume a ventrally-coiled position on the plate. Muscle ultrastructure is normal and animals exhibit a normal postsynaptic response to an acetylcholine agonist, levamisole, with hypercontraction of body wall muscles suggesting that the body paralysis is due to a neural defect (Lewis et al., 1980; Maduro and Pilgrim, 1995). Mutants also exhibit retention of eggs, constitutive pharyngeal pumping and an inability to form dauer larvae, the diapause state triggered by overcrowding and starvation (Maduro et al., 2000). The dauer defect is suppressible by a constitutively-expressed TGF $\beta$ /*daf-7* dauer formation signal, suggesting that UNC-119 acts upstream of synthesis and secretion of this ligand in ASI amphid neurons (Thomas, 1993; Maduro and Pilgrim, 1995; Ren et al., 1996).

A neural role for UNC-119 is supported by its observed pattern of expression. In the worm *unc-119* reporter transgenes are expressed throughout the nervous system and in presumptive neural precursors beginning at about the 80-cell stage of embryogenesis and expression is maintained throughout life, consistent with a role in both development and maintenance of neural organization or function (Maduro and Pilgrim, 1995). The *Drosophila* homolog (DmUNC-119) is similarly expressed throughout the fly embryonic nervous system (Maduro et al., 2000). Mammalian homologs of UNC-119 (HsUnc119/HRG4 in humans) show enriched mRNA expression in retinal rods and cones

(Higashide et al., 1996; Higashide et al., 1998) but expression has also been reported in the adrenal glands, cerebellum, cultured fibroblasts and kidney (Swanson et al., 1998). A zebrafish homolog is expressed in many neural tissues as early as 4 hours post-fertilization and into adulthood and anti-sense oligonucleotides disrupt embryonic neural organization (A. Manning et al., submitted). By contrast, a second zebrafish homolog is found exclusively in muscles, suggesting that UNC-119 may also play a non-neural role (A. Manning, personal communication).

*C. elegans unc-119* mutants exhibit normal growth cone morphology of the DD and VD neurons but axons elongate at a reduced rate (Knobel et al., 2001). Supernumerary branches in DD and VD commissures are generated after initial establishment of the axon scaffold and subsequent retraction from the dorsal nerve cord (DNC). These branches can be suppressed by expression of UNC-119 in affected neurons. AIY interneurons in *unc-119* mutants also exhibit truncated axons and sprout supernumerary neurites (Altun-Gultekin et al., 2001). However our preliminary observations clearly demonstrated that UNC-119 is important for many neural developmental processes beyond suppression of branches, indicating that a reasonable molecular mechanism requires a consideration of other neural defects.

Regulation of *unc-119* expression is clearly modulated by intronic enhancer elements, as a promoterless construct containing the full-length genomic *unc-119* DNA (coding sequence plus introns) rescues the mutant phenotype (Maduro et al., 2000). Similarly, a full-length genomic *unc-119::GFP* fusion construct expressed under the regulation of the DD/VD interneuron-specific *unc-47* promoter results in an expanded expression pattern and also rescues the mutant phenotype (Knobel et al., 2001). In

addition to the expression in DD and VD neurons, GFP in this earlier experiment was also observed in six unidentified head neurons, but it was not known how this expression might be sufficient to rescue the gross movement phenotype. Taken together, these results suggested to us a possible cell nonautonomous role for UNC-119. Examples of neurally-expressed proteins that act cell-autonomously on neurons but that can have cell nonautonomous effects on non-neural migration (i.e. distal tip cells in the gonad) have been observed (Ackley et al., 2001). It has been proposed that the apparent cell-autonomous behaviour of such a protein when it is only expressed neurally may be due to a limited concentration and range of action. We speculated that UNC-119 might behave in a similar manner.

Here we show that UNC-119 is required for correct formation of axons of chemosensory, mechanosensory and motor neurons. Neural specific expression of UNC-119 can rescue axon elongation defects in some neurons but not in others. Also, neural-specific constructs based on full-length genomic *unc-119* DNA expand their expression beyond that specified by their promoters as previously observed. Surprisingly, expression of such constructs spreads into all four pairs of head muscles rather than into other neurons. This expanded expression pattern results in rescue of gross movement and dauer formation defects. UNC-119 expressed only in neural subsets does not rescue gross movement or dauer formation defects, but expression in body wall muscle remarkably results in partial rescue of movement and restores dauer formation ability. This suggests that extra-cellular UNC-119 has a cell nonautonomous ability to rescue the structural defects in neurons that are the basis for the observed phenotypic defects.

## 2.2 Materials and Methods

### 2.2.1 GFP nervous system reporters

The NW1229 strain (a kind gift of J. Culotti, Samuel Lunenfeld Research Institute) contains an integrated pan neural *PF25B3.3::GFP* reporter, *evIs111* (Altun-Gultekin et al., 2001). DP248 is an *unc-119(ed3)* mutant strain into which this reporter has been crossed. ASI amphid neurons were marked using *Pdaf-7::GFP* reporter strains DP171 (*edIs24[Pdaf-7::GFP; pRF4]*) and DP172 (*unc-119(ed3); edIs24[Pdaf-7::GFP; pRF4]*) (Ren et al., 1996). Strains NW1099(*evIs82a[pAC12]*) (Colavita et al., 1998, also a gift of J. Culotti), and DP166(*unc-119(ed3);evIs82[pAC12]*) carrying an integrated *Punc-129::GFP* reporter were used to view DA and DB class motor neurons. ALM, AVM, PLM and PVM mechanosensory neurons were visualized using the *mec-4::GFP* reporter strain SK4005 (*zdIs5[Pmec-4::GFP;lin-15(+)]*) obtained from the *Caenorhabditis* Genetics Center, University of Minnesota (Lai et al., 1996). *unc-119(ed3)* was crossed into this strain to yield DP317 (*unc-119(ed3);zdIs5[Pmec-4::GFP;lin-15(+)]*). Correct expression of the reporters after crossing into an *unc-119(ed3)* background was verified using fluorescent microscopy.

### 2.2.2 Cell autonomy constructs

Full length genomic *unc-119* (including the entire coding region, plus the 5' UTR plus introns) was amplified by long PCR (Barnes, 1994) from pDP#MM016 (Maduro and Pilgrim, 1995) using primer pair WM004aU (5' CGCCAGGTACCATCTCTGTCAATC) and WM004aL (5' ATCGGCGGGAAGGTACCAATCATA). These primers added 5' and 3' KpnI restriction sites for subsequent insertion into GFP vectors and the resultant in-frame insertion into a GFP-containing vector added a VPVEK amino acid bridge

between the carboxyl UNC-119 residue and the amino terminal GFP residue; no amino acids were changed at the amino end of the UNC-119 protein. The PCR reaction was carried out in 200µl tubes containing the following: 5µl 10 X PCR Buffer (500 mM Tris-HCl pH9.2, 160 mM (NH<sub>4</sub>)<sub>2</sub>SO<sub>4</sub>, 20mM MgCl<sub>2</sub>), 2 µl 10 mM dNTPs, 5µl pDP#MM016 template DNA (approx. 50 ng/µl), 2 µl WM004aU (5pmol/µl), 2 µl WM004aL (5pmol/µl), 1 µl Taq+Pfu (50:1), 33 µl ddH<sub>2</sub>O. The reaction was carried out in an MJ Research PT-100 Thermo-cycler as follows: 94°C for 30" then 35 cycles of (94 °C for 15", 54 °C for 20", 68 °C for 1'30") then held at 4 °C. Following PCR, the product was electrophoresed on a 0.8% agarose gel and the 3.3 kbp band was cut out. DNA was isolated from the agarose slice using the Sephaglass BandPrep Kit (Amersham) per the manufacturer's instructions. This product was digested with KpnI and used in subsequent ligations.

Plasmids containing GFP under the control of various promoters were the kind gift of Andrew Fire, Stanford University ([ftp://ftp.wormbase.org/pub/elegans\\_vector/FireLabVectors/](ftp://ftp.wormbase.org/pub/elegans_vector/FireLabVectors/)). pPD118.20 contains the *myo-3* promoter and drives GFP expression in body wall muscle while pPD118.15 contains no worm promoter. Purified plasmid was digested with KpnI and dephosphorylated with Calf Intestinal Alkaline Phosphatase (New England BioLabs). The digested, dephosphorylated products (6.5 kbp for pPD118.20 and 3.8 kbp for pPD118.15) were purified from an agarose gel as above. The PCR product from pDP#MM016 was ligated into each of these to yield pDP#WM006 (*Pmyo-3:unc-119 gDNA::GFP*) and pDP#WM005(*Pnull:unc-119 gDNA::GFP*) and transformed into competent XL1-B *E. coli*. Plasmid DNA was isolated using standard alkaline lysis and silica binding techniques and confirmed by restriction analysis.

A plasmid containing the *mec-4* promoter was the kind gift of Monica Driscoll, Rutgers University. *Pmec-4* was isolated from this plasmid by HindIII, BamHI double digest and inserted into the corresponding sites in pDP#WM005 upstream from the *unc-119* CDS to make pDP#WM008 (*Pmec-4:unc-119 gDNA::GFP*). This plasmid expresses UNC-119::GFP in ALM, AVM, PLM and PVM mechanosensory neurons. Similarly the *daf-7* promoter was isolated from the pDP#SU007 plasmid by an XbaI, XmaI double digest and inserted into the corresponding sites in pDP#WM005 to make pDP#WM009 (*Pdaf-7:unc-119 gDNA::GFP*). Expression of GFP under the control of this promoter is seen in ASI chemosensory neurons. Correct formation of these constructs was confirmed by sequencing across the 5' join to the promoter and across the 3' join to GFP and by verifying expression in transgenic animals (described below). The ability of the genomic DNA-based construct to rescue the *unc-119* phenotype was confirmed by cloning the 1.2kb upstream *unc-119* promoter region from pDP#MM016 into pDP#WM005 to make pDP#WM014(*Punc-119:unc-119 gDNA::GFP*). Rescue of *unc-119(ed3)* mutant worms containing this transgene verified that no functional alterations to UNC-119 were introduced by the PCR reactions.

As has been previously noted (Knobel et al., 2001) expression of GFP reporters containing full-length genomic *unc-119* DNA (gDNA, including coding sequence plus introns) expands beyond that specified by the promoter within the construct. In order to avoid this complication, cDNA versions of the above constructs were subsequently made by amplifying *unc-119* cDNA from pDP#MM051 (Maduro and Pilgrim, 1995) with similar KpnI restriction sites as in the gDNA construct but replacing primer WM004aL with WM004bL (5' ATCGACGGGAGGTACCGCATCATA). The *unc-119* gDNA in

pDP#WM005, pDP#WM006, pDP#WM008 and pDP#WM009 was then replaced with PCR product containing the corresponding cDNA to give pDP#WM005b(*Pnull:unc-119 cDNA::GFP*), pDP#WM006b (*Pmyo-3: unc-119 cDNA::GFP*), pDP#WM008b (*Pmec-4: unc-119 cDNA::GFP*) and pDP#WM009 (*Pdaf-7:unc-119 gDNA::GFP*). The ability of the cDNA-based construct to rescue the *unc-119* phenotype was confirmed by cloning the 1.2kb upstream *unc-119* promoter region from pDP#MM051 (Maduro and Pilgrim, 1995) into pDP#WM005b to make pDP#WM014c(*Punc-119::unc-119 cDNA::GFP*). The ability of this cDNA-based construct as a transgene to fully rescue the *unc-119* mutant phenotype was also confirmed, verifying that no functional alterations to UNC-119 were introduced by PCR.

Also, in order to determine more precisely the temporal requirement for UNC-119 we replaced a small PstI, BamHI fragment upstream from the *unc-119* CDS in pDP#WM005b with the *F25B3.3* promoter from pDP#SU006 (Altun-Gultekin et al., 2001) to make pDP#WM075(*PF25B3.3:unc-119 cDNA::GFP*).

### **2.2.3 Transgenic strain construction**

Germline transformation was accomplished as described (Mello *et al.*, 1991) by coinjecting a desired construct from above with a *lin-15(+)* wild type rescuing construct into a *lin-15(n765ts)* mutant strain. F1 progeny with a wild type vulva were selected and assayed for GFP expression. Table 2.1 lists the transgenic strains used in this work.

### **2.2.4 Genetic testing**

Worms were maintained at room temperature on agar plates seeded with *E. coli* strain OP50 (Brenner, 1974) except for temperature sensitive (ts) strains which were maintained at 16°C . Upon verification of GFP expression in a transgenic strain (see

above), 12-15 *unc-119* worms were mated overnight to 15-20 *him-8* males on a spot-seeded plate. Male F1 progeny from this cross should all be heterozygous for *unc-119*. These males were then mated overnight to 12-15 transgenic hermaphrodites. The next day the hermaphrodites were singled on seeded plates and 20 F1 L4 hermaphrodite progeny were later selected from plates with many males and subsequently singled onto seeded plates. About one-half of these would be expected to be heterozygous for *unc-119*. After four days F2 progeny were examined for the presence of the GFP reporter in the transgene and for the Unc phenotype. If the *unc-119* construct in the transgenic array did not rescue, about one-quarter of the progeny of heterozygous worms could be expected to be Unc. If it did rescue, this number would be reduced as only those worms that have lost the array would be Unc. If Unc worms expressing GFP were observed some were singled and maintained and the construct was considered to be non-rescuing. If no GFP+ Unc worms were observed on a plate but non-GFP Unc worms were, then 40 GFP+ non-Unc hermaphrodites were singled from such plates. Approximately one-quarter of these should be homozygous for *unc-119*. The construct was considered to be rescuing if plates could be found on which all worms were either GFP+ non-Unc or non-GFP, Unc.

### **2.2.5 Movement and dauer formation assays**

Plates were flooded with M9 buffer and swirled gently to dislodge worms from their food. Under the dissecting UV microscope GFP+ and non-GFP worms of various stages were found and the number of complete sinusoidal motions were counted over a one minute period. For each strain ten individuals from among the best-moving worms were selected for counting.

To assay dauer larva formation, mixed stage worms were washed off two or three plates four days after clearing (more than 2,000 worms for each strain in total) with M9 bath and into 15ml Falcon tubes then 10% SDS was added a final concentration of 2%. Worms were then incubated at 26 °C for two hours with rocking every thirty minutes. At the end of this period worms were allowed to settle and were washed three times with M9 before being deposited onto seeded plates. Moving dauers were scored after one hour and recovered adults were counted two days later. No non-dauers survived the SDS treatment and plates with dauers had at least 40 such animals, almost all of which subsequently grew to adulthood.

### **2.2.6 Microscopy**

Worms were screened and maintained with the assistance of a Zeiss Stemi SV 11 dissecting microscope equipped with a 100W UV bulb, 6.6 X zoom and a high-power (10X) objective. For higher-powered imaging, animals were mounted in 10-15 µL of 15mM sodium azide (Sigma) in M9 buffer (Wood, 1988) directly on a microscope slide under a coverslip which was then sealed with nail polish. Confocal images were taken on a Molecular Dynamics 2001 microscope using 40X non-immersion or 100X or 60X oil immersion objectives under 485-565 nm excitation and detected by photomultiplier following filtering to exclude light outside the 500-520 nm range of GFP. Adobe Photoshop and Microsoft PowerPoint were used to improve contrast, assemble serial sections of confocal images and for annotation.

## 2.3 Results

### 2.3.1 *unc-119* mutants exhibit fasciculation and branching defects

Transgenic strains were used which expressed reporters only in subsets of neurons. Using an integrated *Punc-129::GFP* reporter in both wild-type and *unc-119* strains, cell bodies and processes of DA and DB classes of motor neurons could be clearly identified. When pan-neural markers are used to image all axons, supernumerary branching is one of the most obvious characteristics of the *unc-119* mutants. However, individual DA and DB class motor neurons exhibited fairly weak penetrance of this defect (Table 2.2). While DA/DB axons are always unbranched in the wild type (White et al., 1986), in about 50% of *unc-119* mutant animals at least one neuron from the DA and DB classes had a branched commissure. About two-thirds of these animals exhibited multiple branching of single axons or had more than one neuron with a branched axon (data not shown). Different neurons were affected in different animals with both DA and DB class neurons being equally affected. Branching defects were slightly concentrated proximal to the vulva from DA4 to DA6. These data are consistent with those observed for DD and VD axons (Knobel et al., 2001).

Defasciculation of the VNC and DNC was highly variable (Figure 2.1). In about half of the animals observed, VNC defasciculation was not apparent or was only mild (Figure 2.1A, B). Severe defasciculation was only seen in about 10% of worms and tended to be most pronounced between the nerve ring and the vulva (Figure 2.1C). Occasionally disruption of the VNC was so severe that left and right bundles appeared to decussate (Figure 2.1C, small arrow). The DNC was almost always (90%) fasciculated to the same extent as in the wild type (data not shown), underlying its different origin from

axons that comprise the VNC.

### **2.3.2 Cell placement defects along the VNC are common**

In addition to the defasciculation defect, cell bodies were often displaced from their normal position along the VNC (Figure 2.1D-F). In 60% of *unc-119* mutants DA5 was displaced from its normal position immediately posterior to the vulva and was found, instead, beside DB5, immediately anterior to the vulva (Figure 2.1E). Because neural organization is developed embryonically to a large extent and vulval development occurs much later, the initial displacement of the embryonic DA5 neuron was probably not very large relative to its turning choice point. Alternatively the vulva may have been slightly displaced so that it developed to the posterior of DA5 and displaced the cell body anteriorly in the adult. Vulval displacement was not directly measured. Occasionally other cell bodies were displaced dorsolaterally from their normal position near the ventral midline (data not shown). No obvious migration defects were observed in the AVM and PVM mechanosensory neurons.

### **2.3.3 Commissures make choice point errors**

The commissures normally associated with any single motor neuron were not always observed at their expected A/P position within the worm, but rather aberrantly placed commissures were noted elsewhere in the animal (Figure 2.1A, B, C). This suggests that commissures in the mutant are not responding to the correct turn signal at their choice points and, failing to do so, they travel in an anterior or posterior direction until they respond to some other turn signal. Because such commissures turn from the VNC at an incorrect A/P position, they may target incorrect muscle cells, contributing to an inability to correctly coordinate movement. In general no correlation between

incorrect choice point and supernumerary branching was observed (see Figure 2.1E for an example), suggesting that the mechanisms regulating these processes are somewhat independent.

It was somewhat surprising, then, to find that the commissure arising from the displaced DA5 neuron was usually targeted correctly. The wild-type DA5 commissure sprouts from the ventral side of the cell body, crosses the ventral midline by passing over the hypodermal ridge, then projects circumferentially around the left side of the worm until it reaches the DNC (White et al., 1986). In *unc-119* mutant worms with displaced DA5 cell bodies, the commissural axon projected posteriorly (either fasciculating with the right or left VNC) until it reached the A/P position where it would normally turn dorsolaterally away from the VNC. At this point it turned correctly and projected to the DNC in a normal manner (Figure 2.1E,F). The correct projection was not affected by the presence of an additional branch on this axon (Figure 2.1F).

#### **2.3.4 Axon elongation defects in mechanosensory and chemosensory neurons**

A *Pmec-4::GFP* reporter was used to observe the anterior mechanosensory neurons (ALM and AVM) which are responsible for initiating the response to light touch in the head (Chalfie and Sulston, 1981; Chalfie et al., 1985). In the wild type, the cell bodies of ALML and ALMR are situated laterally near the mid-body and sensory processes extend anteriorly almost to the nose of the animal. Near the nerve ring one axon branches from each process, projects medially and then runs ventrally along the inside of the nerve ring, fasciculating with the neuropil and making several synapses until it meets the process arising from the ventral axon of AVM with which it forms a gap junction (Figure 2.2A, B, C; White et al., 1986). In an *unc-119(ed3)* mutant the anterior

elongation of the sensory processes of the ALMs appeared normal but the axons in the nerve ring terminated prematurely after extending medially to the nerve ring but before reaching the ventral side of the animal (Figure 2.2D, E). As a result, it would be impossible for the axons to synapse correctly with other neurons involved in effecting the touch response. These axons typically did not have terminal arbors.

A *Pdaf-7::GFP* reporter was used to visualize the chemosensory ASI amphid pair (Figure 2.3). Dendrites from these neurons terminate in sensory cilia within the amphid pore (White et al., 1986). In about 10% of *unc-119(ed3)* mutants examined, the dendrite ended in an abnormal forked structure (Figure 2.3D) compared to the wild type (Figure 2.3B). Wild type ASI neurons form gap junctions with each other and synapses with other amphids and with interneurons by means of an axon which extends ventrally from the cell body, joins the VNC via the amphid commissure and then turns anteriorly and enters the nerve ring (Figure 2.3A, C). In almost all *unc-119* animals examined the axons appeared highly malformed (Figure 2.3E). Not only were they prematurely terminated near the ventral midline where they would normally enter the nerve ring but they usually ended in highly-branched structures. This would make it impossible to form their normal gap junctions and synapses and they would be unable to communicate sensory input to downstream effector neurons. ASI amphids have an essential function in the initiation of the dauer larva (Bargmann and Horvitz, 1991) and these axonal defects may explain the inability of *unc-119* mutants to enter into dauer.

In the L1 larvae of both wild type and mutant worms ASI axons were fully elongated and appeared to contact each other medially (Figure 2.3F-H) but the axons were clearly misguided in the *unc-119(ed3)* strain (Figure 2.3G, H). Following correct

elongation to the ventral medial region, the axon failed to enter the nerve ring and projected either anteriorly (Figure 2.3G) or posteriorly (Figure 2.3H) to contact its contralateral partner. This structure was never observed in *unc-119* adults leading to the conclusion that it was likely not stable and retracted, subsequently forming the branched structure seen in the adult.

### 2.3.5 ASI axon defects are distinct in *unc-119* mutants

In order to place UNC-119 within the pathways of known axon guidance mechanisms, a comparison of ASI axons was made among mutant strains representing different components of these mechanisms (Figure 2.4). UNC-6 /netrin is a secreted signal which directs elongation towards or away from the ventral midline depending on growth cone UNC-5/DCC and UNC-40 receptors (Hedgecock et al., 1990; Chan et al., 1996). In 84 percent (16/19) of *unc-6* animals examined with a *Pdaf-7 ::GFP* reporter the ASI axons extended into the nerve ring, but not to the dorsal midline, and had extra processes. The remaining 16 percent were normal. UNC-44 is related to ankyrin, a spectrin binding protein that links integral membrane proteins (such as ion channels and cell adhesion molecules) to the actin cytoskeleton (Otsuka et al. 1995, Bennett, 1992). Seven out of twenty-three ASI axons observed in *unc-44* mutants were normal but sixteen appeared to turn anteriorly and fasciculate with their ipsilateral dendrite as they passed it. UNC-51 is a serine-threonine kinase thought to regulate axon elongation, possibly through vesicular transport (Ogura et al., 1994, Okazaki et al., 2000). All (16/16) ASI axons observed in an *unc-51* mutant strain extended to the dorsal midline though fifteen of these had characteristic varicosities and five had extra branches near the cell body. UNC-104 is a member of the kinesin family thought to transport synaptic

vesicles from the neuron cell body to the synapses (Hall and Hedgecock, 1991, Otsuka et al., 1991). All (13/13) ASI axons viewed in *unc-104* mutants extended to the dorsal midline, though four of these had varicosities or extra branches near the cell body. Unique among these various mutations, ASI axons in *unc-119* mutants frequently (40/51) terminated at the ventral entry to the nerve ring in extensive arbors; ASIs in the remaining animals (11/51) appeared normal. This suggests that UNC-119 acts through a mechanism that is distinct from several other processes important in nervous system development including netrin-based guidance, adhesion molecule clustering and synaptogenesis.

### **2.3.6 UNC-119 rescues some axonal defects cell-autonomously**

Cell-autonomous rescue of the supernumerary branching defect in *unc-119* mutants has been previously reported (Knobel et al., 2001). We hypothesized that UNC-119 expression in specific neurons should also rescue the elongation defects we observed in mechanosensory and chemosensory axons. However, because axons from these two neural classes travel through very different kinds of neural neighborhoods on their way to the nerve ring, we wondered whether there might be some qualitative difference in their rescue. We speculated that axons that elongate in a more pioneer-like manner (e.g. ALMs) might behave differently than axons that are guided by fasciculating with other pioneering axons (e.g. ASIs). In the latter case rescued axons that fasciculate along the length of aberrant primary axons might still not be able to elongate properly to find their final target beyond where the pioneering axon incorrectly terminates.

We expressed *unc-119 cDNA* behind the mechanosensory *mec-4* or chemosensory *daf-7* promoters and observed the effect the transgenes had on ALM and AVM or ASI

axons, respectively, in an *unc-119(ed3)* background (Figure 2.5). While expressing UNC-119 in ALM and AVM mechanosensory neurons rescued *unc-119* axon elongation defects (Figure 2.5A, B), expression in ASI chemosensory neurons did not (Figure 2.5C, D). The rescue of ALM and AVM axon defects was specific to the neurons in which UNC-119 was expressed. When this rescuing construct was expressed in an *unc-119* strain containing an unrelated DA/DB motor neuron GFP reporter (*Punc-129::GFP*), VNC defasciculation and cell-placement defects in the DA/DB neurons were still observed (Figure 2.5E).

### 2.3.7 UNC-119 in neural subset does not rescue gross phenotypic defects

While expression of *unc-119* cDNA only in mechanosensory neurons (ALM, AVM, PLM, PVM) was able to rescue *unc-119*-associated axon defects in those neurons, neither mechanosensory nor chemosensory (ASI) expression was able to rescue gross movement and dauer formation defects (Figure 2.6). This confirmed the observation that neural defects outside of those neurons in which UNC-119 is directly expressed are not also rescued. Thus gross phenotypic defects involving networks of neurons are not repaired by expression in only some of those neurons.

However, *unc-119* cDNA expressed either behind its native promoter (data not shown) or behind the pan-neural F25B3.3 promoter (Figure 2.6) was able to fully restore both movement and dauer formation defects in *unc-119* mutants. UNC-119::GFP driven by the F25B3.3 promoter is pan-neural but expression begins in post-mitotic neurons at the three-fold stage of embryo development, much later than the 80-cell stage at which UNC-119 expression is normally seen (Altun-Gultekin et al., 2001, S. Urban and D.P., unpublished observations). However rescue of gross *unc-119* phenotypic defects

resulting from expression under the control of this promoter is nearly complete suggesting that UNC-119 expression is not required until somewhat later in development.

### **2.3.8 Intronic elements expand expression of gDNA-based constructs**

We and others (Maduro and Pilgrim, 1995, Knobel et al., 2001) had previously observed that constructs containing the *unc-119* full-length genomic DNA (gDNA - consisting of coding sequence plus introns) did rescue gross movement defects seen in the mutant but had not previously quantified this rescue. We expressed *unc-119* gDNA behind the same promoters used above and observed a dramatic rescue of movement, particularly in younger larval stages, and full recovery of dauer formation capability.

This difference in behaviour between the gDNA and cDNA constructs might be explained by differences in their respective patterns of expression. Thus while an *unc-119* cDNA::GFP construct expressed behind the *mec-4* promoter was observed only in the expected mechanosensory neurons, the same construct incorporating *unc-119* gDNA had an expanded expression pattern (Figure 2.7A). Fluorescence was observed in all eight head muscles (Figure 2.7B) as well as in all three pairs of coelomocytes (Figure 2.7A, E). The expression of an *unc-119* gDNA::GFP reporter under the regulation of the *daf-7* promoter was similarly expanded beyond ASI chemosensory neurons into head muscles (Figure 2.7C) but was not observed in coelomocytes likely due to an overall lower signal level. Head muscle expression could be observed in three-fold embryos but not in two-fold embryos (Figure 2.7D and data not shown).

### **2.3.9 Muscle-specific UNC-119 rescues gross phenotypic defects**

To directly test the hypothesis that muscle expression of UNC-119 might be responsible for the gross phenotypic rescue, we expressed the *unc-119* cDNA under the

control of the muscle-specific *myo-3* promoter. Remarkably, this cDNA construct partially rescued both movement and dauer defects (Figure 2.6). Although movement of this strain was reduced relative to wild type it was significantly better than the *unc-119* mutant (t-test  $p < 0.01$ ;  $n = 10$ ). Rescue of these gross defects worsened as the animals aged so that transgenic adults were barely distinguishable from normal *unc-119* mutants. Strikingly, while expression of full-length genomic DNA behind neural promoters (*mec-4* and *daf-7*) fully rescued dauer formation and largely rescued movement (at least through L4), expression of *unc-119* gDNA behind a muscle promoter (*myo-3*) did not rescue either defect.

Direct observation of GFP fluorescence resulting from these constructs showed that the cDNA construct was highly expressed in body-wall muscle (Figure 2.8A). No neural expression was observed and coelomocytes could not be seen behind the very bright muscle expression. By contrast, the intronic enhancer coupled with the *myo-3* promoter to switch the gDNA expression into several neurons but at a very low level (Figure 2.8B). Strangely, this was insufficient to rescue movement and dauer defects. Thus, the precise expression of UNC-119 is controlled by a combination of promoter and enhancer elements in a manner that is not strictly additive but is a synthesis of signals from various regulatory elements.

## 2.4 Discussion

*C. elegans unc-119* mutants have multiple behavioural defects (Maduro and Pilgrim, 1995). Immuno-electron microscopy studies have shown that the rat homolog, Unc119/RRG4, is associated with pre-synaptic membranes in photoreceptors in the rat retina (Higashide et al., 1998), leading to the proposal that the mammalian homolog of UNC-119 may be involved in synaptic function. We have shown that severe structural defects in the nervous system including defasciculation of the VNC, choice point errors and elongation defects likely form the basis for the behavioural abnormalities in the *unc-119* mutant worm. Further, while commissures form supernumerary branches, their elongation to the dorsal midline is largely complete, unlike *unc-5* and *unc-6* mutants (Hedgecock et al., 1990, Siddiqui, 1990, Siddiqui and Culotti, 1991). In addition, ASI axon defects in *unc-119* mutants have a morphology that is distinct from those of *unc-6*, *unc-44*, *unc-51* or *unc-104* mutants. This suggests that netrin guidance mechanisms are unaffected in *unc-119* worms and that UNC-119 affects axons through a mechanism that is not related to these genes.

In adult *unc-119* mutants, axons of ASI amphid neurons frequently terminate in aberrant varicosities or highly branched structures near the ventral midline outside the nerve ring. In L1 mutant larvae these axons are fully elongated but fail to enter the nerve ring. ALM mechanosensory axons also fail to elongate along the inside of the nerve ring in *unc-119* mutants, although they appear to initiate medial projection into the nerve ring near the normal dorsolateral position. Elongation defects appear in these classes of axons at choice points in their pathways; ASI axons as they transit from the VNC into the nerve ring and ALM axons as they turn ventrally along the inside of the nerve ring. DD and

VD commissures exhibit a similar failure shortly following their turning at the dorsal midline along the DNC in *unc-119* mutants (Knobel et al., 2001).

As axons encounter choice points they must change either their response to guidance cues or their adhesive properties or both (Kaprielian et al., 2001). Axons could exhibit an incorrect response to a choice point in a number of ways, including: i) failing to detect the choice point, ii) failing to transduce the choice point signal to effector molecules, iii) failing to produce or localize new guidance cue receptor or adhesion molecules at the axon surface, or iv) failing to down regulate old guidance cue receptor or adhesion molecules. We hypothesize that failing to detect or process a choice point signal or failing to upregulate new receptor or adhesion molecules should result in axons that fail to defasciculate and overshoot their choice point, similar to choice point defects seen in *Drosophila* DLAR mutants (Krueger et al., 1996) or in Fasciclin II overexpressing transgenic flies (Lin et al., 1994). However axons in *unc-119* mutants exhibit fasciculation and fascicle stabilization defects that are more in keeping with a failure to downregulate the response to previous guidance and adhesion molecules at choice points.

In addition, while defects in ALM axons projecting medially into the nerve ring are repaired by expressing UNC-119 in ALMs, defects associated with ASI axons are not rescued by corresponding expression in ASIs. It is possible that the response to UNC-119 expression in different neurons depends on the time at which the neural-specific promoters used in these experiments become activated. UNC-119 is normally expressed at about the 80-cell stage of embryogenesis but *daf-7* reporters are not seen prior to hatching and *mec-4* reporters are not observed prior to the two-fold stage of

embryogenesis. Pan-neural expression of UNC-119 at the three-fold stage of embryogenesis under the F25B3.3 gene promoter was sufficient to rescue gross phenotypic defects, placing the requirement for the protein at a time that is between that observed for the *daf-7* and *mec-4* promoters. This may explain why *mec-4*-driven UNC-119 rescued ALM axon defects while *daf-7*-driven UNC-119 did not rescue ASI axon defects.

However, we may also attribute this difference in behaviour to differences in the local neighborhood through which these different axons extend in reaching the nerve ring. Axons elongate over different substrates; pioneer axons over hypodermis and basement membrane, and follower axons along the surface of other axons. We hypothesize that, for follower axons, guidance or elongation defects in the pioneering axon may affect the apparent pathfinding of the secondary axon by disrupting its supporting substrate. Thus axons in the VNC which ASIs follow into the nerve ring may be so disrupted in *unc-119* mutants that, even though UNC-119-regulated fasciculation is correct, the ASI axons are not correctly guided into the nerve ring. By contrast, ALM axons do not enter the nerve ring by fasciculating with pioneer axons but act as pioneers themselves.

Expressing an intron-containing construct under the regulation of either mechanosensory or chemosensory promoters caused an expansion in the pattern of expression outside that specified by the promoter fragment alone and resulted in overall rescue of the *unc-119* movement and dauer formation defects. Using such constructs, we observed expression in all four pairs of head muscles starting during the three-fold stage of embryonic development and continuing throughout adulthood. This suggests that

there is an enhancer element within the full-length *unc-119* gDNA that combines with certain promoters to drive expression in head muscles and that this expanded expression is sufficient to rescue the *unc-119* defects in larval stages but not throughout adulthood. A trivial explanation is that the *myo-3* promoter expresses at an undetectable, but sufficient, level in neurons, but we have never observed any transgenic animals (or their progeny) that were rescued but had no detectable GFP using any rescuing construct.

By immunohistochemistry UNC-119 has been found throughout the cytoplasm of worm neurons, including in axons and growth cones (Knobel et al., 2001). However, ectopic expression of UNC-119 in muscles was also able to substantially rescue the *unc-119* movement and dauer formation defects. This led us to conclude that UNC-119 must be able to repair neural defects in a cell-nonautonomous manner. In primary cultures UNC-119::GFP expressing cells are seen to adopt a muscle-like morphology at a low frequency (Christensen et al., 2002), raising the possibility the UNC-119 may normally be found in some muscles and may play some role there. Indeed, a full-length genomic UNC-119::GFP reporter has previously been observed in head muscles (Christensen et al., 2002) in addition to our own observations.

While it is theoretically possible that the movement defects associated with *unc-119* mutants may be, for example, simply due to defects in muscle arm pathfinding rather than neural defects *per se*, dauer larva formation has not been shown to be dependent in any way on muscles. Thus muscle expression of UNC-119 must be rescuing the L2 nervous system structure sufficiently to be able to respond to exogenous overcrowding and food availability cues and induce dauer formation. Indeed, expression of UNC-119 in head muscles alone may be necessary and sufficient in some unknown way for proper

formation of the nerve ring and restoration of both movement and dauer formation capability in *unc-119* mutants.

By contrast, the localization of GFP to coelomocytes was intriguing, as GFP reporters secreted into the coelomic cavity are absorbed into coelomocytes (Fares and Greenwald, 2001). This suggests that the ectopically expressed UNC-119(gDNA)::GFP was either being expressed directly in these cells or being taken up from the pseudo-coelomic cavity (Fares and Greenwald, 2001). UNC-119 does not have a secretory signal and has not previously been detected outside of neurons and head muscles. However, improperly-folded and, therefore, non-fluorescent GFP has been shown to be secreted by some types of cells utilizing a non-classical pathway (Tanudji et al., 2002) and ectopic UNC-119::GFP when expressed in muscles may find its way into the ECM via this route.

Alternatively, an UNC-119 homolog has been observed in association with synaptic vesicle membranes in rat photoreceptors (Higashide et al., 1998). Depending on its exact topology relative to the vesicle membrane this could lead to two possible models. i) Growth cones at the tips of elongating axons are dynamic regions (Sabo and McAllister, 2003) and vesicles undergo both exocytosis (adding plasma membrane and releasing proteins to the extra-cellular space) and endocytosis (e.g. during filopodial retraction). Thus UNC-119 may normally be secreted or presented extra-cellularly at the growth cone as vesicles fuse with the plasma membrane of the elongating axon. It may then be associated with the underlying extra-cellular matrix where it serves some unknown signaling function. Ectopic UNC-119 secreted by muscles into the region where axons are elongating would also be capable of serving the normal signaling function. ii) Alternatively UNC-119 may normally act as an adaptor for some extra-

cellular signal but may, itself, only be found intracellularly associated with both exocytosing and endocytosing vesicles. In this case ectopic extracellular UNC-119 in an *unc-119* mutant background may be taken up by endocytosing vesicles during axon elongation and transported into the cytoplasm by an unknown mechanism where it can serve some of its normal function.

Although there are many *C. elegans* strains mutant in genes required for endocytosis, defects in neural structure have not been reported. Mutations in molecules required for all endocytosis (e.g. clathrin, clathrin adaptors, dynamin) result in dead embryos, while temperature-sensitive mutants have generally only been studied for their impaired synaptic vesicle recycling (Harris et al., 2001). However, RNA interference of dynamin, a molecule essential for endocytosis, greatly impairs neurite formation in primary cultures of rat hippocampal neurons (Torre et al., 1994). Further, when primary neural cultures of temperature-sensitive *Drosophila shibire* mutants are raised at the restrictive temperature, outgrowth of processes is impaired (Masur et al., 1990).

One difficulty faced by our model is explaining the severe age-related reduction of movement observed with muscle UNC-119 transgenic animals. An ongoing requirement for UNC-119 in fully-elongated neurons to suppress the formation of supernumerary branches has previously been shown (Knobel et al., 2001). Sprouting of supernumerary branches in SAB motoneurons that innervate head muscle has been shown to be dependent on synaptic activity at the neuromuscular junction (Zhao and Nonet, 2000). Also abrogating sensory neural activity by mutations in a cyclic nucleotide-gated channel causes sprouting of additional axons in late larval stages (Coburn et al., 1998). This suggests that the ongoing requirement for UNC-119 in

neurons may be related to a role in synaptic activity and that this is required intracellularly.

Thus, muscle expression and secretion, whether by the *myo-3* promoter or as a result of the intronic enhancer present in *unc-119*, may be insufficient to maintain synaptic activity and suppress extensive axon branching in the adult. However, axon retraction similar to that seen in *unc-119* mutants has not been observed in mutants with altered neural activity, suggesting that a role in axon stability may be separated from synaptic activity. Also suppression of synaptic activity has not been shown to lead to the kind of fasciculation and choice point defects found in *unc-119* mutants. By contrast, a mutation in the worm homolog of p190 RhoGAP, RPM-1, does exhibit axon retraction and supernumerary branch formation similar to that found in *unc-119* (Schaefer et al., 2000; Billuart et al., 2001). This suggests that the axon instability in *unc-119* may be associated more with an instability in the actin and tubulin cytoskeleton, perhaps resulting from instability in axonal adhesion, than with neural activity.

**Acknowledgements.** We would like to thank the Caenorhabditis Genetics Center (supported by NIH's National Center for Research Resources) for providing some of the strains used in this work, Joe Culotti for the *Punc-129::GFP* and *PF25B3.3::GFP* strains and promoters, Monica Driscoll for the *mec-4* promoter and Andy Fire for providing GFP expression vectors. This work was supported by grants from the Canadian Institutes for Health Research. W.M. received support from the Natural Sciences and Engineering Research Council and the Alberta Heritage Foundation for Medical Research

<b>Strain</b>	<b>Genotype</b>	<b>GFP Expression</b>
DP328	<i>lin-15(n765ts); edEx141[WM006(Pmyo-3::unc-119 gDNA)::GFP; lin-15(+)]</i>	body wall muscle
DP329	<i>lin-15(n765ts); edEx142[WM008(Pmec-4::unc-119 gDNA)::GFP; lin-15(+)]</i>	mechanosensory neurons
DP330	<i>lin-15(n765ts); edEx143[WM009(Pdaf-7::unc-119 gDNA)::GFP; lin-15(+)]</i>	ASI chemosensory neurons
DP332	<i>lin-15(n765ts); edEx145[WM006b(Pmyo-3::unc-119 cDNA)::GFP; lin-15(+)]</i>	body wall muscle
DP333	<i>lin-15(n765ts); edEx146[WM008b(Pmec-4::unc-119 cDNA)::GFP; lin-15(+)]</i>	mechanosensory neurons
DP334	<i>lin-15(n765ts); edEx147[WM009b(Pdaf-7::unc-119 cDNA)::GFP; lin-15(+)]</i>	ASI chemosensory neurons
DP336	<i>unc-119(ed3); edEx141[WM006(Pmyo-3::unc-119 gDNA)::GFP; lin-15(+)]</i>	body wall muscle
DP337	<i>unc-119(ed3); edEx142[WM008(Pmec-4::unc-119 gDNA)::GFP; lin-15(+)]</i>	mechanosensory neurons
DP338	<i>unc-119(ed3); edEx143[WM009(Pdaf-7::unc-119 gDNA)::GFP; lin-15(+)]</i>	ASI chemosensory neurons
DP340	<i>unc-119(ed3); edEx145[WM006b(Pmyo-3::unc-119 cDNA)::GFP; lin-15(+)]</i>	body wall muscle
DP341	<i>unc-119(ed3); edEx146[WM008b(Pmec-4::unc-119 cDNA)::GFP; lin-15(+)]</i>	mechanosensory neurons
DP342	<i>unc-119(ed3); edEx147[WM009b(Pdaf-7::unc-119 cDNA)::GFP; lin-15(+)]</i>	ASI chemosensory neurons
DP376	<i>edEX148[WM014c(Punc-119::unc-119 cDNA)::GFP; Punc-129:: GFP]</i>	pan-neural
DP377	<i>unc-119(ed3); edEX148[WM014c(Punc-119::unc-119 cDNA)::GFP; Punc-129::GFP]</i>	pan-neural
DP381	<i>edEx150[PF25B3.3 gene::unc-119 cDNA::GFP]</i>	pan-neural
DP382	<i>unc-119(ed3); edEx150[PF25B3.3 gene::unc-119 cDNA::GFP]</i>	pan-neural

**Table 2.1 Transgenic strains used to test cell-autonomy**

Neuron	Percent with supernumerary branches
DA3	3
DB4	10
DA4	17
DB5	10
DA5	17
DB6	13
DA6	17
DB7	3
DA7	7
Any DB-class	50
Any DA-class	46

**Table 2.2 Quantification of supernumerary branches in DA/DB class motor neurons.**

Neurons were visualized using a *Punc-129::GFP* reporter. Branching defects were scored only when a commissure could unequivocally be assigned to a specific neuron. Numbers represent the percent of worms in which a branching defect of the commissure was observed (n=30). In the wild type, DA and DB axons are never branched.

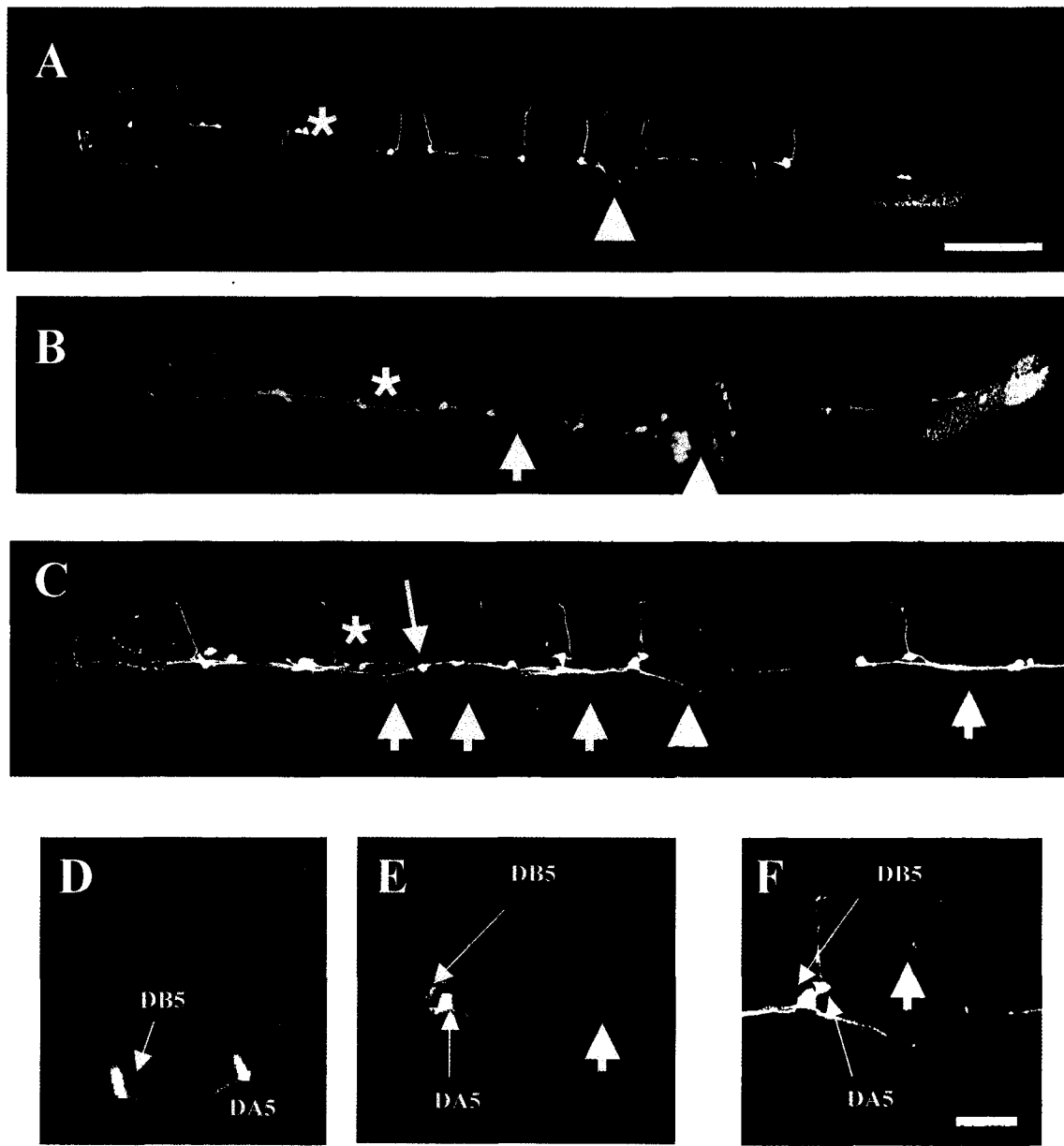


**Figure 2.1 *unc-119* mutants have VNC defasciculation and cell placement defect.**

Ventral aspects; anterior is to the left. A-C, Neurons are visualized with an integrated *Punc-129::GFP* reporter. Arrowhead – vulva. A. N2 (wild type) VNC shows characteristic tightly-fasciculated right VNC fiber similar to 50% of *unc-119* mutants. DA2 and DB3 commissures fasciculate and project to the right of the VNC (asterisk). Scale bar, 100 μm. B. 40% of *unc-119* mutants display moderately-defasciculated VNCs (large arrows) usually most noticeable anterior to the vulva. Only one commissure is seen at normal DA2/DB3 position. Other may be posteriorly displaced but still projects to right of VNC (asterisk). C. 10% of *unc-119* mutants exhibit severe defasciculation encompassing neurites in both the anterior and posterior regions of the animal. Thin arrow - Apparent decussation of VNC. One of DA2/DB3 commissures appears slightly posteriorly displaced but turns to left of VNC (asterisk). D-F. DA5 cell body is misplaced in about 60% of *unc-119* mutants. D. DB5 and DA5 at anterior and posterior (respectively) of vulva in wild type. E. DA5 cell body is misplaced anterior to vulva in *unc-119* worm but axon (large arrow) is targeted normally. F. Even when DA5 axon (large arrow) fasciculates with left VNC bundle and produces supernumerary branch, it is still targeted approximately correctly. Scale bar, 50 μm.

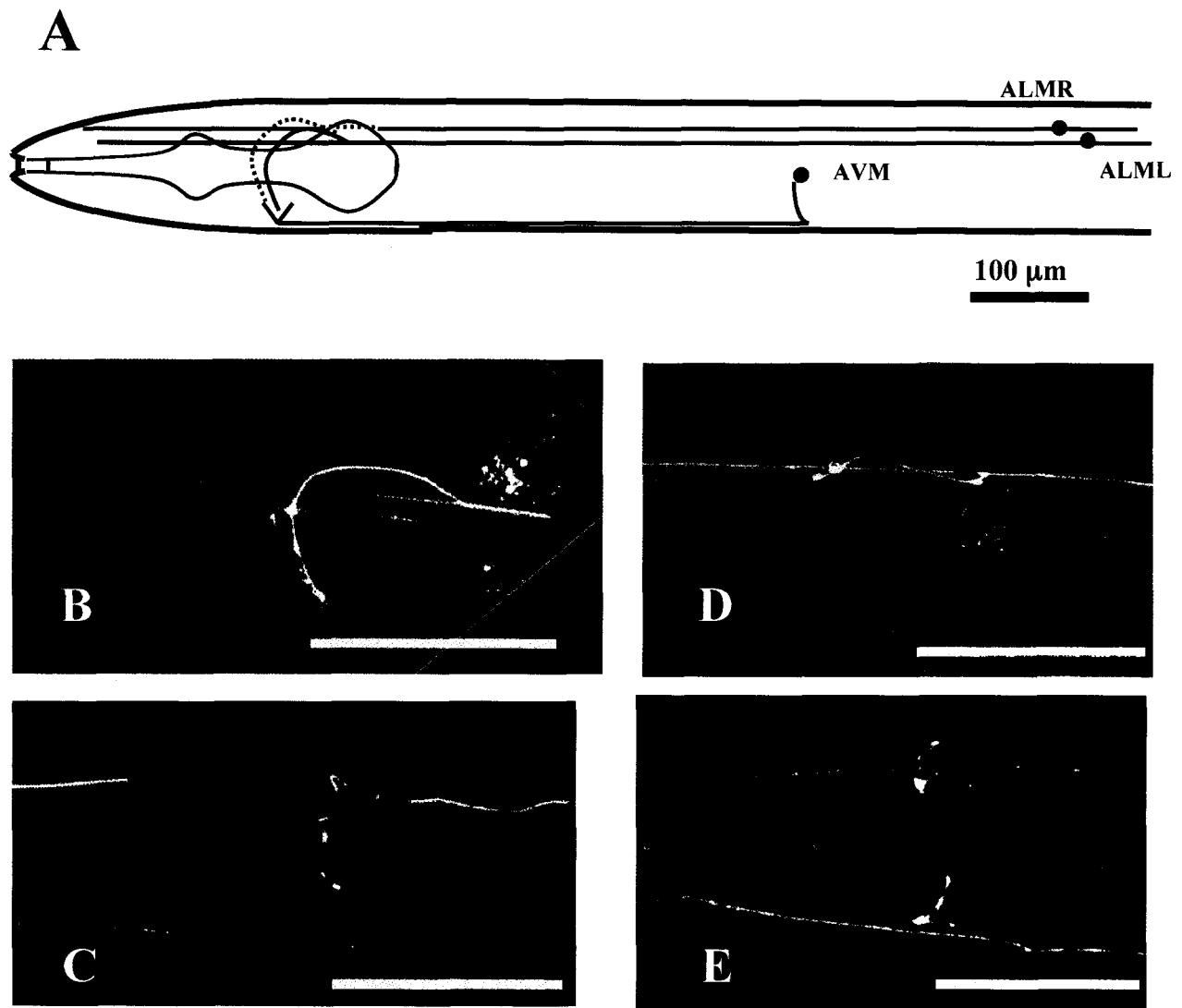


**Figure 2.2 Axons of mechanosensory neurons terminate prematurely in the nerve ring.**

A, Diagram of ALM mechanosensory neurons and processes. B and C are wild type. D and E are *unc-119(ed3)* mutants. Anterior is to left; ventral is down. The ALM neurons are visualized with a *Pmec-4::GFP* reporter. Scale bar, 100 μm. B. Lateral view of ALM processes as they pass by the nerve ring. While sensory processes continue anteriorly, axons branch off to project medially into the nerve ring then elongate along the inner periphery. Eventually these processes synapse with the forked terminus of AVM near the ventral midline. C. Ventral view of another pair of ALM anterior processes at the nerve ring showing their fasciculation at the dorsal midline. D. Lateral view of ALM processes in *unc-119* mutant showing premature termination. E. Ventral view of another pair of ALM process in *unc-119* mutant showing termination of axon in the nerve ring without ventral extension. AVM is not visible at ventral midline in B-E due to low GFP intensity and selection of optical slices (focal planes) for inclusion in confocal projections but see Figure 2.5 A and B. Scale bar, 100 μm.

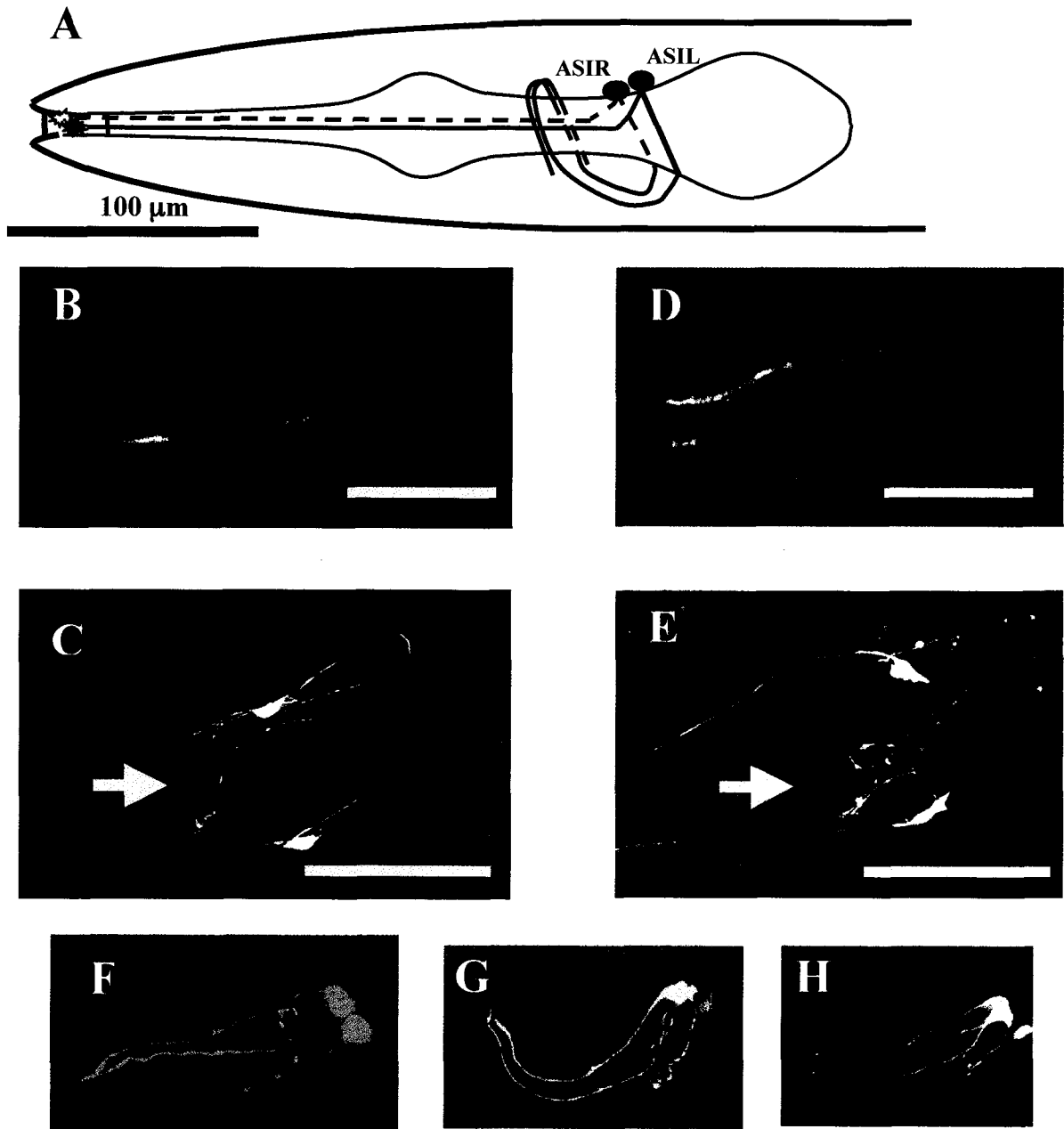


**Figure 2.3 Neurites of ASI amphid neurons are aberrant in *unc-119(ed3)* mutants.**

Neurons are visualized with *Pdaf-7::GFP* reporter. A, Diagram showing the location of the ASI amphid neurons and their processes. Note that axons fasciculate and are connected by gap junctions in the nerve ring. Figure adapted from White et al. (1986). B, C and F are wild type. D, E, G and H are *unc-119(ed3)* mutants. B and D show lateral close-ups of single ASIL amphid dendrites. Scale bar, 10  $\mu$ m. B, Unbranched wild-type morphology. D, Infrequent branched morphology in mutants. C and E are ventro-lateral views showing axons making contact (at arrowheads) as unbranched processes in the wild type (C) or terminating prematurely in non-contacting branched structures in the *unc-119* mutants (E). F – G show dorso-lateral views of ASI axons in L1 larvae. F, wild type ASIs have same morphology as adults. G, ASI axons in mutant fail to enter into nerve ring but meet at ventral midline anterior to cell bodies. H, ASI axons in mutant meet at midline posterior to cell bodies. Scale bars, 100  $\mu$ m.

	a) wild type	b) varicosities or branches near cell body	c) fasciculate with dendrites	d) terminal branches or varicosities
N2	24/24			
<i>unc-6</i>	8/19	11/19		
<i>unc-44</i>	7/23		16/23	
<i>unc-51</i>		16/16		
<i>unc-104</i>	9/13	4/13		
<i>unc-119</i>	11/51			40/51

**Figure 2.4 Comparison of ASI axon defects in several mutants.**

ASI axon morphologies fell into four categories: a) Wild type, b) Wild type but with branches or varicosities near cell body, c) Axon fails to fully elongate and appears to fasciculate with ipsilateral dendrite, d) Axon fails to enter nerve ring near ventral midline and ends in terminal arbor or varicosity. Ratios shown are number of axons observed in each category out of all animals observed with that genotype. Axons in *unc-119* mutants uniquely end in terminal arbors before entering nerve ring.

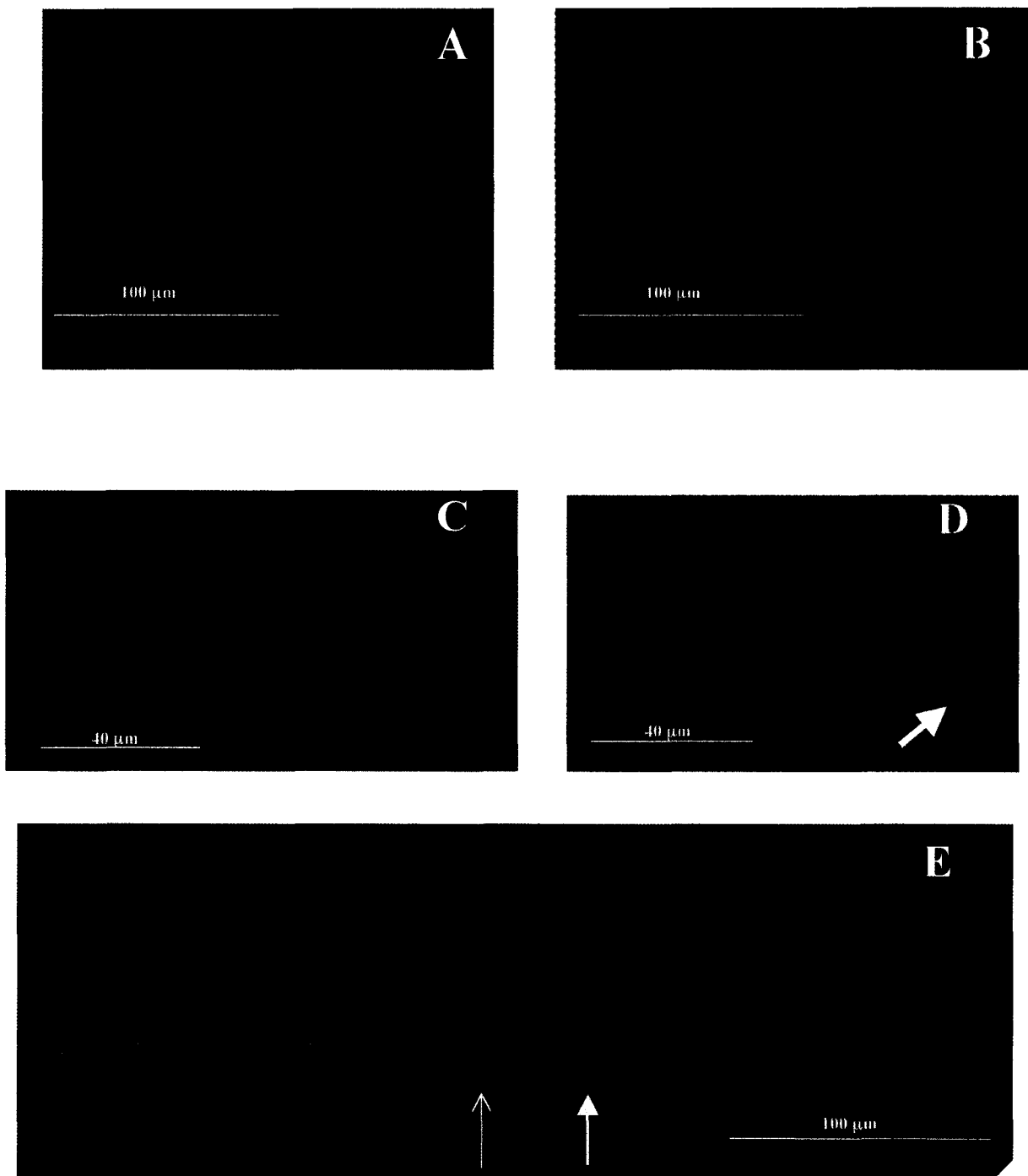


**Figure 2.5 Neural-specific expression of UNC-119 rescues defects cell-autonomously.**

A, ventral view of wild-type mechanosensory axons. B, rescuing *Pmec-4::unc-119::gfp* restores axons to wild-type morphology in *unc-119(ed3)* mutants (compare to Figure 2.2E). C, lateral view of wild-type ASI axon and dendrite. D, transgenic *Pdaf-7::unc-119::gfp* does not restore wild-type morphology to ASI axon. (compare to Figure 2.3E). Premature termination, varicosity and terminal arbor are visible at ventral position (arrow). E, DA/DB motorneuron defects are not rescued by mechanosensory UNC-119 expression. Closed head arrow points to defasciculated VNC in *Pmec-4::unc-119::gfp* transgenic worm also containing *Punc-129::gfp* reporter. Open head arrow points to normal DA5 position, though cell body appears to be displaced to anterior of vulva (compare to Figure 2.1C).

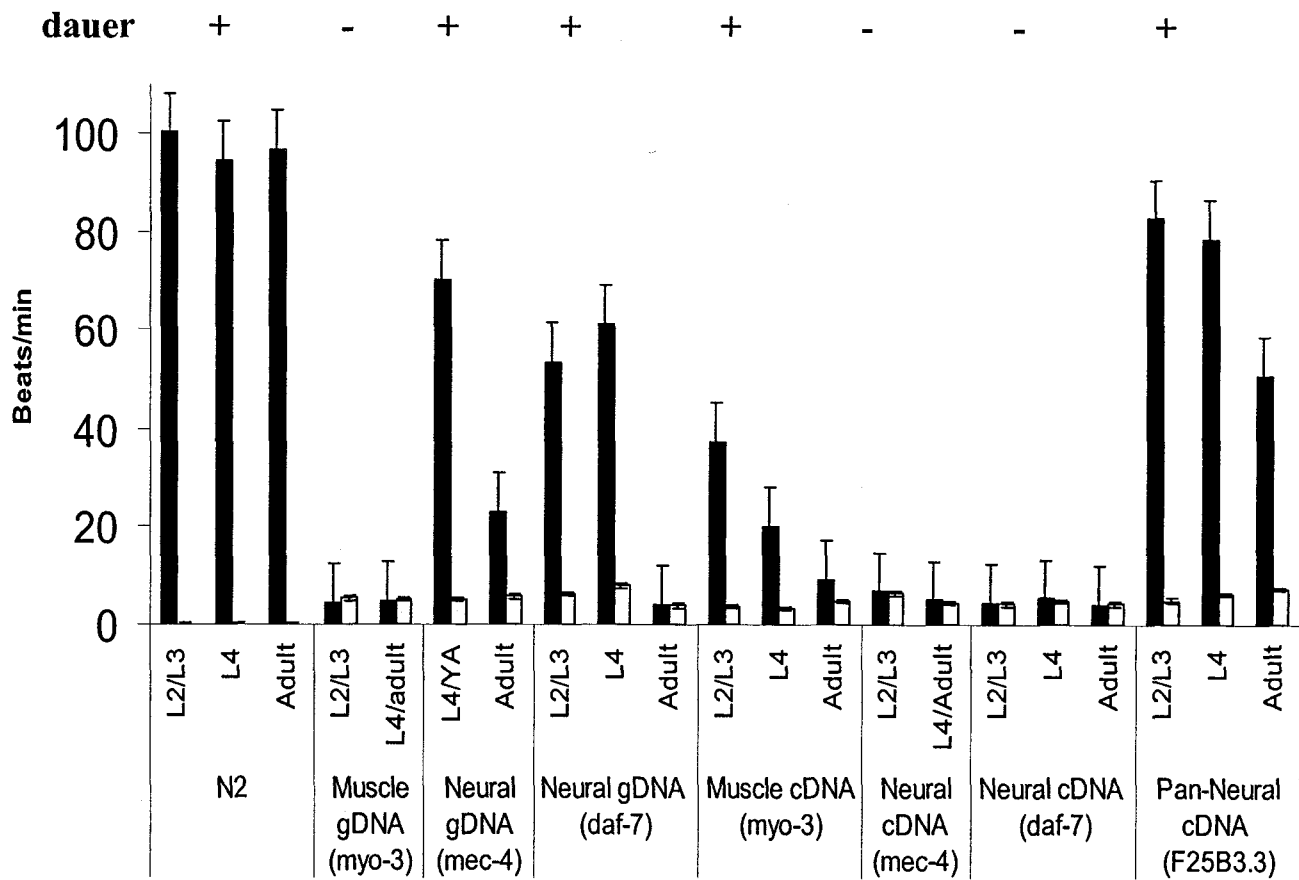


**Figure 2.6 Rescue of *unc-119* movement and dauer defects by tissue-specific UNC-119.**

Number of swimming movements of worms in M9 buffer was counted over one minute period. Various larval and adult stages were assayed for movement. Solid bars represent worms expressing the UNC-119::GFP transgene; hollow bars are non-transgenic *unc-119* siblings from same plate. Dauer formation ability was assayed by 2 hour incubation of plates 4 days after clearing in 2% SDS at 25 °C. Inability to form dauer larvae is indicated by - while dauer formation ability is indicated by + in line of text above graph. Wild type (N2) worms swim at approximately 100 beats/min. at all stages. Expression of UNC-119 (cDNA based) under the pan-neural F25B3.3 promoter almost completely rescues movement and dauer formation. Expression of cDNA-based UNC-119 in mechanosensory (*mec-4*) or chemosensory (*daf-7*) neurons does not rescue movement or dauer formation, but expression of gDNA-based UNC-119 under same promoters does. Expression of muscle-specific UNC-119 (gDNA-based) does not rescue movement or dauer-formation but the same promoter driving cDNA-based UNC-119 partially rescues movement and the strain can form dauers.

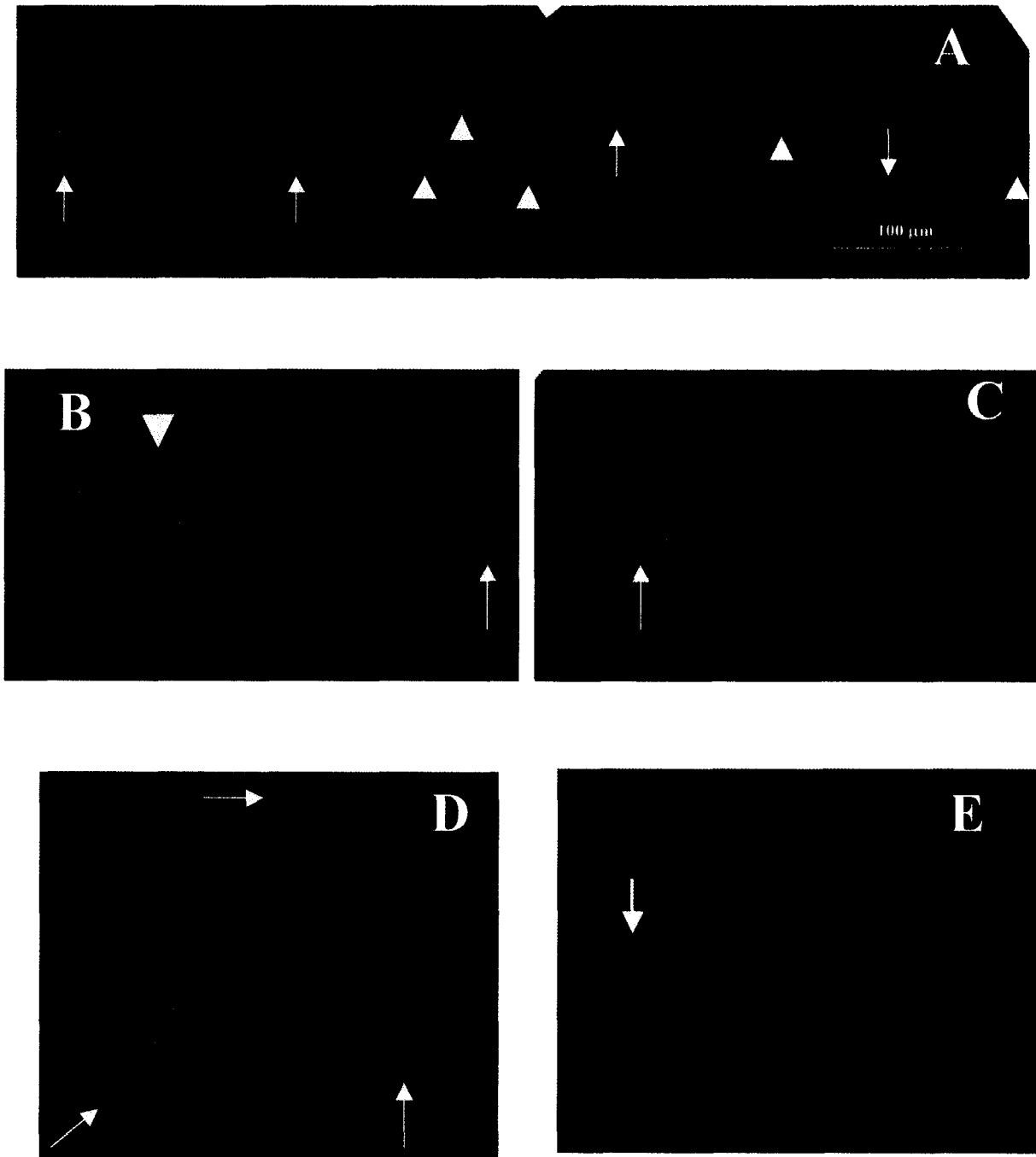


**Figure 2.7 Phenotypic rescue of transgenic *unc-119* mutants is due to UNC-119 in muscles.**

A, gDNA-based UNC-119::GFP under *mec-4* promoter expands beyond mechanosensory neurons (arrowheads) into other cells (arrows). B, higher magnification of worm in A, reveals expression in head of animal is due to UNC-119::GFP in head muscles. Arrow points to muscle arm projection into nerve ring and arrowhead points to punctate pattern similar to that of dense bodies. C, a gDNA-based UNC-119::GFP under *daf-7* promoter also has weak expression in head muscles. D, expression of this transgene is first apparent and is much stronger in three-fold embryos (arrow points to head muscles). E, apparent coelomocyte in posterior of worm shown in A containing UNC-119::GFP. Expression may have spread to coelomocytes or it may result from uptake of secreted protein from muscles.

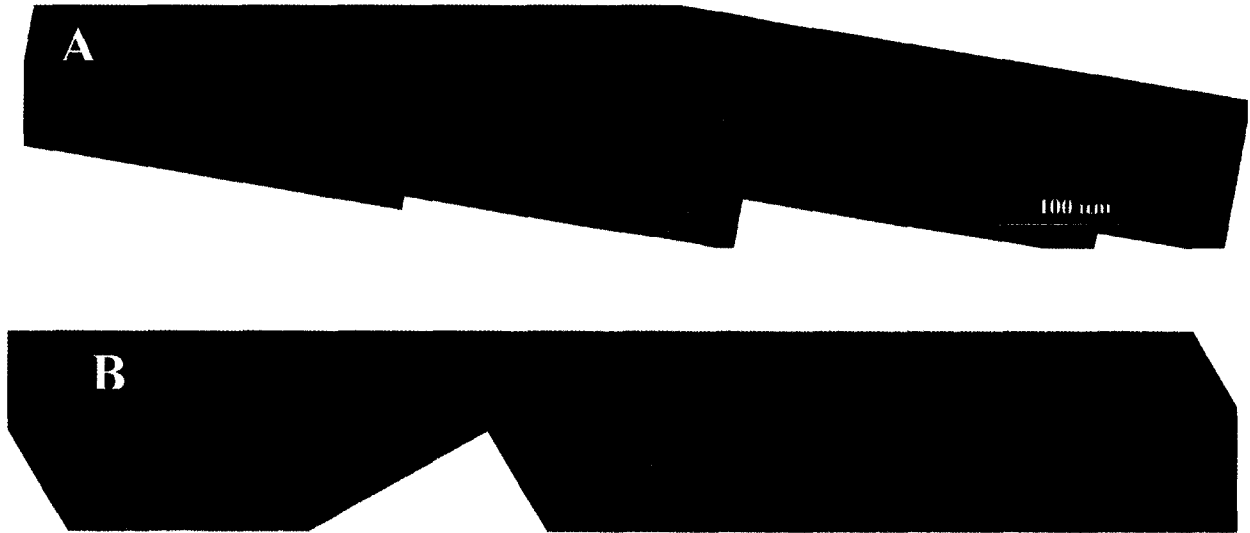


**Figure 2.8 UNC-119 expressed under muscle promoters**

A, cDNA-based UNC-119 under muscle-specific *myo-3* promoter is expressed only in body wall muscle. Expression is very high and occludes neural reporters (not shown) in DA/DB motorneurons. B, gDNA-based UNC-119 under same promoter shows weak expression only in some neurons. This does not rescue either movement or dauer formation defects.

## 2.5 References

- Ackley, B.D., Crew, J.R., Elamaa, H., Pihlajaniemi, T., Kuo, C.J. and Kramer, J.M. (2001), The NC1/endostatin domain of *Caenorhabditis elegans* type XVIII collagen affects cell migration and axon guidance, *Journal of Cell Biology*, **152**: 1219-32
- Altun-Gultekin, Z., Andachi, Y., Tsalik, E.L., Pilgrim, D., Kohara, Y. and Hobert, O. (2001), A regulatory cascade of three homeobox genes, *ceh-10*, *itx-3* and *ceh-23*, controls cell fate specification of a defined interneuron class in *C. elegans*, *Development*, **128**: 1951-69
- Bargmann, C.I. and Horvitz, H.R. (1991), Control of larval development by chemosensory neurons in *Caenorhabditis elegans*, *Science*, **251**: 1243-1246
- Barnes, W.M. (1994), PCR amplification of up to 35-kb DNA with high fidelity and high yield from  $\lambda$  bacteriophage templates, *Proceedings of the National Academy of Sciences*, **91**: 2216-2220
- Billuart, P., Winter, C.G., Maresh, A., Zhao, X. and Luo, L. (2001), Regulating axon branch stability: the role of p190 RhoGAP in repressing a retraction signaling pathway, *Cell*, **107**: 195-207
- Bennett, V. (1992), Ankyrins. Adaptors between diverse plasma membrane proteins and the cytoplasm, *Journal of Biological Chemistry*, **267**: 8703-6
- Brenner, S. (1974). The genetics of *Caenorhabditis elegans*, *Genetics*, **77**: 71-94.
- Chalfie, M. and Sulston, J. (1981), Developmental genetics of the mechanosensory neurons of *Caenorhabditis elegans*, *Developmental Biology*, **82**: 358-370
- Chalfie, M., Sulston, J.E., White, J.G., Southgate, E., Thomson, J.N. and Brenner, S. (1985), The neural circuit for touch sensitivity in *C. elegans*, *Journal of Neuroscience*, **5**: 956-964
- Chan, S.S-Y., Zheng, H., Su, M-W., Wilk, R., Killeen, M.T., Hedgecock, E.M. and Culotti, J.G. (1996). UNC-40, a *C. elegans* homolog of DCC (deleted in colorectal cancer), is required in motile cells responding to UNC-6 netrin cues, *Cell*, **87**: 187-195
- Christensen, M., Estevez, A., Yin, X., Fox, R., Morrison, R., McDonnell, M., Gleason, C., Miller, D.M. 3<sup>rd</sup> and Strange, K. (2002), A primary culture system for functional analysis of *C. elegans* neurons and muscle cells, *Neuron*, **33**: 503-514
- Coburn, C. M., Mori, I., Ohshima, Y. and Bargmann, C.I. (1998), A cyclic nucleotide-gated channel inhibits sensory axon outgrowth in larval and adult *Caenorhabditis elegans*: a distinct pathway for maintenance of sensory axon structure, *Development*, **125**: 249-258

- Colavita, A., Krishna, S., Zheng, H., Padgett, R.W. and Culotti, J.G. (1998), Pioneer axon guidance by UNC-129, a *C. elegans* TGF- $\beta$ , *Science*, **281**: 706-709
- Fares, H., and Greenwald, I. (2001) Regulation of endocytosis by CUP-5, the *Caenorhabditis elegans* mucolipin-1 homolog, *Nature Genetics*, **28**: 64-68
- Hall, D.H. and Hedgecock, E.M. (1991), Kinesin-related gene unc-104 is required for axonal transport of synaptic vesicles in *C. elegans*, *Cell*, **65**: 837-47
- Harris, T.W., Schuske, K. and Jorgensen, E.M. (2001), Studies of synaptic vesicle endocytosis in the nematode *C. elegans*, *Traffic*, **2**: 597-605
- Hedgecock, E.M., Culotti, J.G. and Hall, D.H. (1990), The *unc-5*, *unc-6*, and *unc-40* genes guide circumferential migrations of pioneer axons and mesodermal cells on the epidermis in *C. elegans*, *Neuron*, **2**: 61-85
- Higashide, T., Murakami, A., McLaren, M.J. and Inana G. (1996), Cloning of the cDNA for a novel photoreceptor protein, *Journal of Biological Chemistry*, **271**: 1797-1804
- Higashide, T., McLaren, M.J. and Inana, G. (1998), Localization of HRG4, a photoreceptor protein homologous to *unc-119*, in ribbon synapse, *Investigative Ophthalmology & Visual Science*, **39**: 690-698
- Kaprielian, Z., Runko, E. and Imondi, R. (2001), Axon guidance at the midline choice point, *Developmental Dynamics*, **221**: 154-81
- Knobel, K.M., Davis, W.S., Jorgensen, E.M. and Bastiani, M.J. (2001), UNC-119 suppresses axon branching in *C. elegans*, *Development*, **128**: 4079-4092
- Krueger, N.X., Van Vactor, D., Wan, H.I., Gelbart, W.M., Goodman, C.S. and Saito, H. (1996), The transmembrane tyrosine phosphatase DLAR controls motor axon guidance in *Drosophila*, *Cell*, **84**: 611-22
- Lin, D.M., Fetter, R.D., Kopczynski, C., Grenningloh, G. and Goodman, C.S. (1994), Genetic analysis of Fasciclin II in *Drosophila*: defasciculation, refasciculation, and altered fasciculation, *Neuron*, **13**: 1055-69
- Lai, C.C., Hong, K., Kinnell, M., Chalfie, M. and Driscoll, M., (1996), Sequence and transmembrane topology of MEC-4, an ion channel subunit required for mechanotransduction in *Caenorhabditis elegans*, *Journal of Cell Biology*, **133**:1071-81
- Lewis, J.A., Wu, C.H., Berg, H. and Levine, J.H. (1980), The genetics of levamisole resistance in the nematode *Caenorhabditis elegans*, *Genetics*, **95**: 905-928

- Maduro, M. and Pilgrim, D. (1995), Identification and cloning of *unc-119*, a gene expressed in the *Caenorhabditis elegans* nervous system, *Genetics*, **141**: 977-988
- Maduro, M.F., Gordon, M., Jacobs R. and Pilgrim, D.B. (2000), The UNC-119 family of neural proteins is functionally conserved between humans, *Drosophila* and *C. elegans*, *Journal of Neurogenetics*, **13**:191-212
- Masur, S.K., Kim, Y.T. and Wu, C.F. (1990), Reversible inhibition of endocytosis in cultured neurons from the *Drosophila* temperature-sensitive mutant *shibire<sup>ts1</sup>*, *Journal of Neurogenetics*, **6**: 191-206
- Mello, C.C., Kramer, J.M., Stinchcomb, D., and Ambros, V. (1991), Efficient gene transfer in *C. elegans*: extrachromosomal maintenance and integration of transforming sequences, *The EMBO Journal*, **10**: 3959-3970
- Ogura, K., Wicky, C., Magnenat, L., Tobler, H., Mori, I., Muller, F. and Ohshima, Y. (1994), *Caenorhabditis elegans unc-51* gene required for axonal elongation encodes a novel serine/threonine kinase, *Genes and Development*, **84**: 2389-2400
- Okazaki, N., Yan, J., Yuasa, S., Ueno, T., Kominami, E., Masuho, Y., Koga, H. and Muramatsu, M. (2000), Interaction of the UNC-51-like kinase and microtubule-associated protein light chain 3 related proteins in the brain: possible role of vesicular transport in axonal elongation, *Molecular Brain Research*, **85**: 1-12
- Otsuka, A.J., Franco, R., Yang, B., Shim, K.-H., Lan, Z.T., Yu, Y.Z., Boontrakulpoontawee, P., Jeyaprakash, A., Hedgecock, E., Wheaton, V.I. and Sobery, A. (1995), An ankyrin-related gene (*unc-44*) is necessary for proper axonal guidance in *Caenorhabditis elegans*, *Journal of Cell Biology*, **129**: 1081-1092
- Otsuka, A.J., Jeyaprakash, A., Garcia-Anoveros, J., Tang, L.Z., Fisk, G., Hartshorne, T., Franco R. and Born, T. (1991), The *C. elegans unc-104* gene encodes a putative kinesin heavy chain-like protein, *Neuron*, **6**: 113-22
- Ren, P., Lim, C.S., Johnsen, R., Albert, P.S., Pilgrim, D. and Riddle, D.L. (1996), Control of *C. elegans* larval development by neuronal expression of a TGF-beta homolog, *Science*, **274**: 1389-91
- Sabo, S.L. and McAllister, A.K. (2003), Mobility and cycling of synaptic protein-containing vesicles in axonal growth cone filopodia, *Nature Neuroscience*, **6**: 1264-1269
- Schaefer, A.M., Hadwiger, G.D. and Nonet, M.L. (2000), *rpm-1*, a conserved neuronal gene that regulates targeting and synaptogenesis in *C. elegans*, *Neuron*, **26**: 345-56
- Siddiqui, S.S. (1990), Mutations affecting axonal growth and guidance of motor neurons and mechanosensory neurons in the nematode *Caenorhabditis elegans*, *Neuroscience Research*, Supplement **13**: 171-190

- Siddiqui, S.S. and Culotti, J.G. (1991), Examination of neurons in wild type and mutants of *Caenorhabditis elegans* using antibodies to horseradish peroxidase, *Journal of Neurogenetics*, **7**: 193-211
- Swanson, D.A., Chang, J.T., Campochiaro, P.A., Zack, D.J. and Valle, D. (1998), Mammalian orthologs of *C. elegans unc-119* highly expressed in photoreceptors *Investigative Ophthalmology & Visual Science*, **39**: 2085-2094
- Tanudji, M., Hevi, S. and Chuck, S.L. (2002), Improperly folded green fluorescent protein is secreted via a non-classical pathway, *Journal of Cell Science*, **115**: 3849-57
- Thomas, J. (1993), Chemosensory regulation of development in *C. elegans*, *BioEssays*, **15**: 791-797
- Torre, E., McNiven, M.A. and Urrutia, R. (1994), Dynamin 1 antisense oligonucleotide treatment prevents neurite formation in cultured hippocampal neurons, *Journal of Biological Chemistry*, **269**: 32411-7
- White, J.G., Southgate, E., Thomson, J.N. and Brenner, S. (1986), The structure of the nervous system of *Caenorhabditis elegans*, *Philosophical Transactions of the Royal Society of London. Series B, Biological Science*, **314**: 1-340
- Wood, W.B. (1988), *The nematode Caenorhabditis elegans*, (ed. W. B. Wood) Cold Spring Harbor, NY: Cold Spring Harbor Laboratory Press.
- Zhao, H. and Nonet, M.L. (2000), A retrograde signal is involved in activity-dependent remodeling at a *C. elegans* neuromuscular junction, *Development*, **127**: 1253-1266

## Chapter 3 - Src, Arl, and Basement Membrane Collagen Interactions with *C. elegans* UNC-119

### 3.1 Introduction

*C. elegans* UNC-119 is required for correct nervous system development. *unc-119* mutant worms exhibit a variety of behavioural defects including paralysis, constitutive feeding, egg retention. These are likely caused by nervous system structural defects, including supernumerary branching of commissural axons, defasciculation of the Ventral Nerve Cord (VNC), axon elongation defects and choice point errors in commissural turning points (Maduro and Pilgrim, 1995; Knobel et al., 2001; Materi and Pilgrim, submitted). The human homolog (HsUnc119) is enriched in the retina where it has been reported to localize to ribbon synapses in the outer plexiform layer (Higashide et al., 1998). A patient heterozygous for a premature stop codon in HsUnc119 displays late-onset cone-rod dystrophy and a heterozygous mouse knocked-in with the same mutation also shows age-dependent retinal degeneration (Kobayashi et al., 2000). Lower levels of expression have also been detected by RT-PCR in many other human tissues, including the adrenal glands, cerebellum, cultured fibroblasts and kidney (Swanson et al., 1998).

UNC-119 in *C. elegans* contains no obvious conserved domains or motifs with known functionality. However, similar proteins are encoded in the genomes of all metazoans examined including flies, mice, rats, dogs and humans (Higashide et al., 1998, Maduro et al., 2000). These proteins all exhibit roughly equal levels of amino acid identity (approximately 51–55%) and similarity (approximately 81–85%) with *C. elegans* UNC-119. This remarkable structural conservation is paralleled by a functional homology; both *Drosophila* and human Unc119 are capable of fully rescuing *unc-119*

mutant worms (Maduro et al., 2000). A weakly-similar paralog, PDL-1 (26% identity, 51% similarity over a 92 amino acid domain – Maduro, 1998), has been identified in the worm but no nervous system structural defects have yet been detected in a *pdl-1* deletion mutant despite intense scrutiny (Smith, 2003). PDL-1 is named after its similarity to human phosphodiesterase  $\delta$  (PDE $\delta$ ) and some clues to the molecular function of UNC-119 have arisen through studies of this protein family.

Human PDE $\delta$  interacts with the constitutively activated forms of ARL1, ARL2 and ARL3 in directed yeast two-hybrid assays (Van Valkenburgh et al., 2001). HsUnc119 interacts with both active and inactive forms of ARL1-3 but not with members of the ARF family. An independent yeast two-hybrid screen of a human retinal cDNA library with HsUnc119 confirmed the interaction with ARL2 and subsequent co-immunoprecipitation and immunofluorescence studies demonstrated direct interaction and co-localization of ARL2 and RRG4, the rat homolog of UNC-119 (Kobayashi et al., 2003). Based on the co-crystallization structure of PDE $\delta$  and ARL2 it has been suggested that, in the retina, human HsUnc119 may interact with Arl2 via highly conserved residues and may interact with prenylated proteins via a conserved hydrophobic pocket (Kobayashi et al., 2003; Hanzal-Bayer et al., 2002).

Recently HsUnc119 has also been shown to interact with the cytoplasmic domain of the interleukin 5 receptor alpha sub chain (IL5R $\alpha$ ) in eosinophils and to thereby activate both Lyn and Hck Src-type non-receptor tyrosine kinases (Cen et al., 2003). In addition, HsUnc119 activation of the Src kinases Fyn and Lck is essential for T-cell activation (Gorska et al., 2004). HsUnc119 interacts with Src family members through SH2 and SH3 binding motifs (Figure 1.4). Members of the Src family have been shown

to play crucial roles in cytoskeleton dynamics (reviewed in Frame et al., 2002). Inactivated Src allows actin stress fibers to form within the cell resulting in surface adhesion while activated Src produces a loss of stress fibers and adherence. Src kinase activity is required for strengthening the F-actin linkage to NCAM during growth cone steering in *Aplysia* (Suter and Forscher, 2001) highlighting its role in axon elongation and guidance.

Given the structural and functional conservation of UNC-119 family members, it was expected that domains important for function in one organism would be important in all. Since the role of UNC-119 is best-characterized in *C. elegans*, we thought it would be an ideal organism in which to perform *in vivo* testing of the requirement for specific protein regions and residues.

Here we show that the putative SH2 and SH3 binding motifs in UNC-119 are not required for its function in nervous system development in the worm. In addition, we demonstrate that directed two-hybrid assays with worm UNC-119 and PDL-1 do not completely recapitulate the human interaction profile and reason that an ARL interaction is unlikely to be important in the worm. By contrast, the carboxyl domain (and many individual residues therein) are shown to be critical for UNC-119 function, though this is not in a region that is thought to interact with either Src or Arl family members. Indeed, our own two-hybrid screens of a worm cDNA library suggest that UNC-119 may interact with the basement membrane collagen IV family member, LET-2 and we propose a model for how such an interaction might be important in nervous system development.

## 3.2 Materials and Methods

### 3.2.1 PCR-based site-directed mutagenesis

pPD#MM051 contains *unc-119* cDNA fused downstream of the *unc-119* promoter region (Maduro, 1995). Specific conserved residues in putative SH2 and SH3 binding motifs were mutagenized using a modified PCR-based method (Weiner et al., 1994). Briefly, inverse long PCR was performed on pDP#MM051 using primers in Table 3.1. Some primers make one or more base changes in the cDNA and thus introduce specific amino acid changes into the encoded protein. The resulting PCR products were purified from a 0.8% agarose gel using the Sephaglass BandPrep Kit (Amersham) and subjected to DpnI digestion for 30 minutes at 37 °C to remove the methylated template and any hemi-methylated half-template double strands. They were treated with Pfu at 72 °C for 30 minutes to remove any single base overhangs left at the 3' ends of the PCR product and gel-purified again. The mutated double-stranded DNA was circularized with T4 DNA ligase (Invitrogen) per manufacturer's instructions and transformed into competent *E. coli*. Following verification of mutated constructs, plasmids were used to create transgenic strains for testing. Mutated plasmids are described in Table 3.2.

### 3.2.2 Single strand site-directed mutagenesis

pDP#UGF16 is a rescuing plasmid containing a full-length *unc-119* genomic DNA::*gfp* fusion under the control of the *unc-119* promoter (Maduro, 1998). Single strand site-directed mutagenesis of carboxyl residues in pDP#UGF16 was carried out using Muta-Gene Phagemid *In vitro* Mutagenesis based on manufacturer's instructions (Bio-Rad Laboratories). Briefly single-strand *unc-119>::gfp* DNA was isolated from *dut*<sup>-</sup>

*ung*<sup>-</sup> CJ236 *E. coli* cells transformed with pDP#UGF16 plasmid. These transformants were then superinfected with VCSM13 helper phage and single-stranded DNA containing high levels of dUTP base were isolated. 5' phosphorylated primers (Table 3.1 – Y201D, L207H, V208G, K212N and D214R) were annealed to this single strand template DNA and the complementary strand was synthesized with T4 DNA polymerase, then circularized using T4 DNA ligase. These heterodimers were then transformed into competent XL1-B cells (Stratagene) where the active uracil-N-glycosylase inactivates the dUTP-containing template strand allowing only the complementary strand to replicate. DNA was isolated from overnight cultures of selected transformants and subjected to restriction analysis and sequencing. Plasmids which contained the desired mutations (Table 3.2) were used to create transgenic strains in an *unc-119* mutant background and these were evaluated for rescue of the movement defect.

### 3.2.3 *Unc-119* domain deletion analysis

pDP#WM014 is a rescuing plasmid containing the full-length *unc-119* genomic DNA fused to GFP and under the regulation of the *unc-119* promoter (Materi and Pilgrim, submitted). A *Sall*-*BclI* fragment from the rescuing plasmid pDP#MM051 (Maduro and Pilgrim, 1995), containing almost the entire 1.2 kb upstream *unc-119* promoter region and cDNA was cloned into the corresponding sites in pDP#WM014 to make pDP#WM014b and the ability of this plasmid to rescue the mutant *unc-119* phenotype was tested by germline transformation. The construction of pDP#UBP2 (the corresponding two-hybrid bait vector) is described below.

Deletions of portions of the *unc-119* coding region in the rescuing plasmid pDP#WM014b and in the corresponding two-hybrid bait plasmid pDP#UBP2 were

created by long inverse PCR using primers in Table 3.3. Primers used with pDP#UBP2 introduced unique *ApaI* sites while those used with pDP#WM014b introduced unique *BglIII* sites which could be used to recircularize the PCR products. In adding these restriction sites to the PCR products new amino acids were added to this linker region as shown in Table 3.3. PCR reactions were carried out in 200 $\mu$ l tubes containing the following: 5 $\mu$ l 10 X PCR Buffer (500 mM Tris-HCl pH9.2, 160 mM (NH<sub>4</sub>)<sub>2</sub>SO<sub>4</sub>, 20mM MgCl<sub>2</sub>), 2  $\mu$ l 10 mM dNTPs, 5 $\mu$ l template DNA (approx. 50 ng/ $\mu$ l), 2  $\mu$ l Primer 1 (5pmol/ $\mu$ l), 2  $\mu$ l Primer 2 (5pmol/ $\mu$ l), 1  $\mu$ l Taq+Pfu (50:1), 33  $\mu$ l H<sub>2</sub>O (Milli-Q). The reactions were carried out as follows: 94°C for 30" then 35 cycles of (94 °C for 15", 54 °C for 20", 68 °C for 1'30") then hold at 4 °C. PCR product was isolated, treated with the appropriate restriction enzyme to expose cohesive sites at either end and recircularized with T4 DNA ligase (Invitrogen) as per manufacturer's instructions. Constructs were confirmed by sequencing across the join. In addition, domain deletion constructs based on pDP#WM014b were verified by confirming GFP expression in transgenic worms (see below). Constructs (referred to as Del1 through Del11) are diagrammed in Figure 3.1.

### 3.2.4 Transgenic strain construction

Germline transformation was accomplished as described (Mello *et al.*, 1991) by coinjecting a desired construct from above into N2 wild type worms. For non-GFP fusion constructs used in PCR-based site-directed mutagenesis a P<sub>F<sub>25B3.3</sub></sub>::GFP reporter was co-injected so that the entire nervous system could be observed by fluorescent microscopy (Altun-Gultekin *et al.*, 2001). F1 progeny expressing pan-neural GFP were selected. Table 3.4 shows the genotypes of transgenic strains constructed for this paper.

### 3.2.5 Genetic testing

Worms were maintained at room temperature on agar plates seeded with *E. coli* strain OP50 (Brenner, 1974) except for temperature sensitive (ts) strains which were maintained at 16°C . Upon verification of GFP expression in an injected strain *unc-119* worms were mated overnight to *him-8* males on a spot-seeded plate. Male F1 progeny from this cross should all be heterozygous for *unc-119*. These males were then mated overnight to transgenic hermaphrodites. The next day the hermaphrodites were singled on seeded plates and 20 F1 L4 hermaphrodite progeny were later selected from plates with many males and subsequently singled onto seeded plates. About one-half of these would be expected to be heterozygous for *unc-119*. After four days F2 progeny were examined for the presence of the Unc phenotype. If the *unc-119* construct in the transgenic array does not rescue, about one-quarter of the progeny of heterozygous worms should be Unc. If it does rescue, this number will be reduced as only those worms that have lost the array will be Unc. If Unc worms expressing GFP were observed some were singled and maintained and the construct was considered to be non-rescuing. If no GFP+ Unc worms were observed on a plate but non-GFP Unc worms were, then 40 GFP+ non-Unc hermaphrodites were singled from such plates. Approximately one-quarter of these should be homozygous for *unc-119*. The construct was considered to be rescuing if plates could be found on which all worms were either GFP+ non-Unc or non-GFP and Unc.

### 3.2.6 Microscopy

Worms were screened and maintained under a Zeiss Stemi SV 11 dissecting microscope equipped with a 100W UV fluorescent bulb, 6.6X zoom and a 10X objective.

### 3.2.7 Yeast two-hybrid screen

A two-hybrid bait plasmid (pDP#UBP2) producing a GAL4 binding domain::UNC-119 fusion protein was constructed by removing the *unc-119* cDNA from pDP#MMcDNA5 via a BamHI + NsiI double digest and ligating it into TRP+ pGBD-C1 (James et al., 1996) at the BamHI + PstI sites. The correct reading frame at the 5' end was confirmed by sequencing. A similar construct (pDP#HBP1) containing most of the human homolog HsUnc119 was made by removing the HsUnc119 cDNA from pDP#MM092R with a BamHI digest and ligating it non-directionally into the BamHI site in pGBD-C1. The correct orientation and reading frame were confirmed by sequencing.

Transformations into the yeast strain PJ69-4A (James et al., 1996) were performed as described (Agatep et al., 1998) except that LiAc and PEG were dissolved in TE instead of water and the heat shock duration was 40 minutes. Transformation efficiencies of  $10^5$  colonies per microgram of DNA were generally observed. Strains containing the pDP#UBP2 and pDP#HBP1 bait plasmids were constructed and absence of autoactivation of the *ade* reporter was confirmed by streaking colonies onto SC –TRP –ADE plates and verifying absence of growth. A *C. elegans* two-hybrid prey cDNA library (the kind gift of R. Barstead) was subsequently transformed independently into these two strains in ten separate transformations each, resulting in a total of approximately  $10^6$  transformants screened in total; this is expected to cover the entire worm genome of about 20,000 genes five to ten times over. Both RB1 (poly-T primed cDNA) and RB2 (random primed cDNA) libraries were used in five transformations each and positive interactions resulted from each library. Prey plasmids confer LEU prototrophism and interactions between proteins encoded by bait and prey plasmids

permit growth on –HIS –ADE media and express  $\beta$ -galactosidase.

Screening the *C. elegans* cDNA library with pDP#HBP1 resulted in over 1,000 transformants growing on selective quadruple knockout medium (SC –TRP –LEU –HIS –ADE) while the screen with UBP-2 had approximately 200 colonies, only 12 of which grew vigorously. All 12 of these colonies were used for subsequent steps while a  $\beta$ -galactosidase assay on colony lifts from the ten quadruple knockout plates containing cells from the pDP#HBP1 assay was used to select 34 strongly-interacting prey colonies.

Selected colonies were streaked on SC–LEU to relieve selection for the bait plasmid and four to thirty-two individual colonies were then replica-patched onto SC –LEU –TRP plates; replicates of colonies which fail to grow under this double knockout condition have lost their bait plasmid. Plasmids were extracted from the original colonies indicated by this assay and transformed into *E. coli* for amplification. DNA was extracted and sequenced at the 5' join using a GAL4 activation domain primer (GAL4AD 5' GTTTGGAATCACTACA GGGATG 3') to confirm translational frame then a BLAST search was performed to identify the original worm gene.

All in-frame prey plasmids were retransformed into both pDP#HBP1 and pDP#UBP2 containing strains to verify the original interaction. Because the human homolog of *unc-119* is functional in worms (Maduro et al., 2000), it was anticipated that it should demonstrate the same protein-protein interactions. Therefore all prey plasmids (whether identified in the screen with pDP#HBP1 or pDP#UBP2) were reconstructed as above into both bait-containing strains. The interaction between a SIR3 bait and RAD7 prey (kind gifts from R. D. Geitz, University of Manitoba) was used to rule out false positives.

### 3.2.8 Directed 2-hybrid assay

In order to test UNC-119 and PDE $\delta$  for interaction with Arl2, *C. elegans* and human UNC-119 as well as worm *pdl-1* cDNA were cloned into the Gal4 activating domain plasmid pGAD-C1 (James et al., 1996). Human Arl2, activated human Arl2(Q70L) (both the kind gifts of Richard Kahn) and activated *C. elegans* EVL-20(Q70L) (the kind gift of Min Han) were fused to the Gal4 DNA binding domain to make bait plasmids. Bait and prey constructs were co-transformed into PJ69-4A yeast and plated onto SC –TRP –LEU medium to select for transformants. Two colonies from each transformation were then tested for growth on SC –TRP –LEU –HIS –ADE medium. Growth on this medium indicates interaction between the bait and prey proteins. As well, individual colonies from each plate were patched onto SC –TRP –LEU and tested for expression of the lacZ reporter using a  $\beta$ -galactosidase assay.

For the  $\beta$ -galactosidase assay, patched yeast were lifted onto a circle of #1 Whatman filter paper. The filter was treated with three rounds of freeze-thaw with liquid nitrogen and then placed, yeast side up, onto another two rounds of filter paper saturated in Z-buffer (100mM sodium phosphate pH 7.0, 10 mM KCl, 1 mM MgSO<sub>4</sub>, 1% Xgal). The reaction was incubated in the dark at 30°C. Filters were inspected at 15 minutes, 30 minutes, and 3 hours and color changes were recorded.

### 3.3 Results

Putative SH2- and SH3-domain binding motifs have been identified in the human homolog HsUnc119 along with requisite phosphorylated tyrosine residues (Cen et al., 2003). Because Src tyrosine kinases are thought to be central to cytoskeletal dynamics in growth cones they were considered excellent candidates to interact with UNC-119. Table 3.2 relates these motifs to the worm homolog and shows that they are not all perfectly conserved.

#### 3.3.1 Src-interacting motifs not required for UNC-119 function in worms

In order to directly test whether an interaction between UNC-119 and an unknown Src family member is required for UNC-119 function in the worm, we used PCR-based site-directed mutagenesis to change conserved residues thought to be important for this interaction and which were shown to be important in human eosinophils (Table 3.2). Mutated plasmids were coinjected with a pan-neural GFP reporter to construct transgenic strains. Three independently-arising lines from each injection were crossed into an *unc-119* mutant background and assayed for the ability of the injected plasmid to rescue the near-total paralysis associated with mutant worms.

Only one SH3-binding motif is conserved in the worm. In constructing the mutated version of the conserved SH3-binding motif exactly 6 nucleotides were lost in addition to the intended changes so that the SQMPRPP motif beginning at residue 19 was modified to SQMAA deleting two amino acids and changing the remaining requisite prolines to alanines. Despite these changes, this construct was fully able to restore movement in an *unc-119* mutant background (Table 3.2). The nervous system had wild type morphology in a rescued *unc-119* background (Figure 3.2). The putative SH2

binding motif EHIYEF at position 172 was mutated to KHIYKF reversing the charge on the conserved glutamate residues by converting them to lysines. Again this modified construct was able to completely restore movement in an *unc-119* mutant background and the nervous system structure was wild type. Together, these experiments indicate that interaction with SH2 and SH3 domains through these putative binding sites is dispensable for UNC-119 function in worms.

Two tyrosine residues in the human HsUnc119 are located following putative phosphorylation signals but only the tyrosine in the putative SH2 binding motif is conserved in the worm; the other residue is a phenylalanine. The conserved tyrosine at position 175 was mutated to an aspartate but this did not reduce the ability of the transgene to rescue the mutant phenotype (Table 3.2). As a control we mutated the highly-conserved RMIERH motif at position 141 into RMIEGG. This motif immediately precedes the non-conserved putative phosphorylated tyrosine found in the human homolog. Because this tyrosine is not conserved in worms (and so the phosphorylation signal in this motif could not be important) we reasoned that it would serve as a good negative control. Surprisingly, changing this motif destroyed the ability of the resulting UNC-119 to function in worms, indicating that some residues not related to activating Src or to phosphorylating tyrosines are critical to the function of the protein. In addition, the nervous system morphology of *unc-119* worms expressing this transgene contained defects normally seen in *unc-119* mutant strains (Figure 3.2C).

### **3.3.2 ARL-2 interaction with UNC-119**

In humans, PDE $\delta$  and HsUnc119 have been shown to interact with Arl2 (Renault et al., 2001; Van Valkenburgh et al., 2001; Hanzal-Bayer et al., 2002; Kobayashi et al.,

2003). EVL-20 is the closest sequence homolog of Arl2 in the worm genome and mutant worms exhibit defects in vulva and gonad formation as well as in hypodermal enclosure and elongation (Anotshechkin and Han, 200). As well, *evl-20* worms have been previously rescued by transgenic expression of Arl2, suggesting that EVL-20 and Arl2 are functionally conserved. If this is true, then the binding partners of Arl2 could reasonably be expected to be conserved between worm and human.

We tested this hypothesis using directed yeast 2-hybrid between Gal4 binding domain fusions of Arl2(Q70L), Arl2, and EVL-20(Q70L) and Gal4 activation domain fusions of PDL-1, UNC-119, HsUnc119, and PDE $\delta$ . Arl2(Q70L) and EVL-20(Q70L) are mutant protein forms that are thought to be constitutively GTP-bound and therefore constitutively active. Specifically, the Q70L mutation should be deficient in GTP hydrolysis based on its analogy to the Ras Q61L mutation, which has been shown to lack GTPase activity (Temeles et al., 1985; Frech et al., 1994).

PDE $\delta$  has previously been shown to interact only with the activated form of Arl2 while HsUnc119 interacts with either activated or wild-type Arl2 (Van Valkenburgh et al., 2001; Hanzal-Bayer et al., 2002). Under our assay conditions, the only combinations that grew well were PDE $\delta$  and PDL-1 with Arl2(Q70L). HsUnc119 showed a weak interaction with Arl2(Q70L) that was visible as poor growth after several days at room temperature. None of the other combinations allowed growth in the assay (Table 3.5).

The previously published reports used HIS selection and a lacZ reporter to indicate protein interaction whereas our strains allow the use of both HIS and ADE as selectable markers in addition to the lacZ reporter (James et al., 1996). It is theoretically possible that ADE provides more stringent selection that eliminates all but the strongest

of interactions. Therefore, we assayed for  $\beta$ -galactosidase expression (which is regulated by a different promoter) to determine if there were weaker interactions that might have been missed by assaying only for growth. After permitting transformants to grow on SC –TRP –LEU media (selecting only for the presence of both bait and prey plasmids) strains were assayed for  $\beta$ -galactosidase activity (Table 3.5). The strains that had grown on ADE and HIS selective medium showed stronger  $\beta$ -galactosidase staining than those which had not, but all combinations showed some degree of staining. This confirmed that there may be a weak interaction between PDE $\delta$ /PDL-1 and Arl2/EVL-20 and suggested that any similar interaction between UNC-119 family members and Arl2/EVL-20 is likely even weaker.

### **3.3.3 Interaction with LET-2**

In order to identify other candidates with which UNC-119 might interact we conducted two independent two-hybrid screens of worm cDNA libraries using either worm UNC-119 or human HsUnc119 as bait. Because HsUnc119 is a functional homolog of UNC-119 in the worm we reasoned that it should interact with the same proteins. In general HsUnc119 was a more promiscuous bait generating over a thousand vigorous colonies in the initial screen compared to only twelve with the worm homolog as bait. Selection using a second reporter (*lacZ*) narrowed this number to thirty-four.

We identified a total of 46 colonies exhibiting strong interactions from these two screens but were only able to isolate prey plasmids from 32 of these. We confirmed that the two-hybrid prey interacted with both UNC-119 and HsUnc119 but not with an unrelated Rad7 bait. Seven of the fifteen prey that met these criteria contained in-frame fragments from the 450 carboxyl residues of the basement membrane collagen LET-2, a

region containing the non-collagenous NC1 domain. Four of these were identified in an interaction with the human homolog while the other three arose in the screen using the worm homolog as bait.

Previous work has shown that the amino portion of UNC-119 preceding Domain A is dispensable for function while the more highly-conserved carboxyl function in Domain B is critical (Maduro et al., 2000). If the interaction with LET-2 has biological and not just biochemical relevance then perturbations to UNC-119 that abrogate its interaction with LET-2 in a directed two-hybrid assay should lose the ability to rescue the *unc-119* mutant when expressed as a transgene. Thus we constructed a series of domain deletion constructs based on either the two-hybrid bait plasmid pDP#UBP2 or the rescuing UNC-119::GFP fusion plasmid pDP#WM0014b and assayed these for function (Figure 3.1).

All deletions tested lost the ability to rescue the mutant phenotype except for a small 33 residue deletion amino to Domain A. Neither Domain A (Del7) nor Domain B (Del3) by themselves were sufficient for UNC-119 function in the worm. Losing either the 95 amino-most residues of Domain B (Del11) or the 28 carboxy-most residues (Del8) completely abolished the ability of the protein to rescue movement in the mutant worm.

In yeast, deleting either all of Domain A (Del10) or just the 33 residues amino to this (Del2) did not remove the interaction with LET-2. However deleting both these regions (Del3) resulted in an auto-activating construct. Similarly removing all of Domain B also led to an auto-activating construct suggesting that either of these domains alone is capable of recruiting transcription machinery in the yeast nucleus but that they interact to suppress this. The amino-most 95 residues of Domain B are required for the LET-2

interaction (Del8 and Del10). Thus, while it is clear that proteins that are unable to interact with LET-2 also lose their functionality in the worm, it is also obvious that UNC-119 function in the worm requires more than just a LET-2 interaction.

### **3.3.4 Other highly conserved residues are required**

In order to determine important residues in the carboxyl portion of Domain B, we carried out site-directed mutagenesis on specific, highly-conserved residues in this domain (Table 3.2) then assayed transgenic strains containing mutagenized plasmids for rescue of the movement defect in an *unc-119* background. All five residues tested were found to be absolutely required for UNC-119 function as transgenic strains containing mutagenized plasmids moved no better than untransformed mutant worms.

While we were conducting these tests a new allele of *unc-119* with a weaker phenotype was brought to our attention (C. Bargmann, personal communication). We obtained the strain, sequenced all the exons and discovered a single missense mutation changing a conserved histidine at position 210 to tyrosine. Thus there is clearly a critical domain containing the carboxyl-most twenty residues that is unrelated to any putative Src, Arl2/EVL-20 or LET-2 interacting domains.

### 3.4 Discussion

Members of both Src and Arl protein families have recently been proposed to interact with HsUnc119, the human homolog of the *C. elegans* protein UNC-119. Src family members are implicated in cytoskeletal remodeling mechanisms (Frame et al., 2002) as well as in cell survival, the latter particularly in cells of the immune system (Zamoyska et al., 2003). The functions of Arl family members are not well understood although they have been implicated in regulation of the golgi apparatus (Lu et al., 2001), tubulin stabilization (Bhamidipati, Lewis and Cowan, 2000), male fertility (Schurmann et al., 2002), and hypodermal enclosure of the worm embryo (Antoshechkin and Han, 2002).

HsUnc119 has recently been shown to transduce a signal between the interleukin 5 receptor alpha subunit and downstream Src family members, including Fyn, Lyn, Lck and Hck, thus promoting eosinophil survival (Cen et al., 2003) and activation of T cells (Gorska et al., 2004). In this study we have shown that the SH3- and SH2-binding motifs in HsUnc119 which mediate Src activation are completely dispensable for UNC-119 function in *C. elegans*. This is somewhat surprising as both the SH2 binding motif (EHIYEF at position 172) and one of the two SH3 binding motifs (SQMPRPP at position 19) are well conserved from humans to worms. Yet neither the tyrosine nor the surrounding residues in the SH2 binding motif are required for *in vivo* function in the worm. Further, while an oligopeptide corresponding to the RKQPIGP SH3-binding motif at position 56 in HsUnc119 has been shown to be the most effective Src activator in eosinophils, this motif is not conserved in worms. In addition, we have shown that the other, more highly-conserved, SH3-binding motif SQMPRPP at position 19 is also not

required for UNC-119 function in the worm.

A directed two-hybrid assay (Van Valkenburgh et al., 2001) and an independent two-hybrid screen (Kobayashi et al., 2003) have both implicated Arl2 in a biologically important interaction with HsUnc119. Using a different yeast strain from these studies we have shown that the interaction between worm UNC-119 and EVL-20 (the worm homolog of Arl2) is weak and reporter-dependent. By contrast the interaction between the UNC-119 paralog PDL-1 (the worm homolog of PDE $\delta$ ) and constitutively activated Arl2 is considerably more robust, indicating that this interaction is likely to be more biologically relevant in the worm. Unlike *unc-119* mutants, *pdl-1* mutant worms have no visible phenotype (Smith, 2003).

In a sensitized strain, RNAi against either *arl-1* or *evl-20* results in embryonic lethality, suggesting that these Arls have important roles outside of neurons, while *arl-3* RNAi worms have no visible phenotype (Simmer et al., 2003). A co-crystal structure of PDE $\delta$  and GTP-bound Arl2 has been solved and residues important for their interaction have been identified (Hanzal-Bayer et al., 2002). Many of these residues are conserved in UNC-119 but their role in protein function is unknown.

Although other two-hybrid screens have suggested an UNC-119/EVL-20 interaction, our own screens pointed to an interaction with LET-2, a basement membrane collagen type IV. While collagens are normally thought to play only structural roles, type IV collagens are known to promote adhesion of cultured neurons (Wildering et al., 1997), to induce neurite outgrowth in peripheral neurons (Tonge et al., 1997) and to enhance action potential production (Kowtha et al., 1998). Type IV collagens are characterized by a long coiled-coil domain and a globular NC1 domain that contains a region similar to

canstatin or tumstatin, both potent inhibitors of angiogenesis (Kamphaus et al., 2000; Maeshima et al., 2002). The NC1 domain of LET-2 is most like canstatin (73% identical, 83% similar) while tumstatin is most like the NC1 domain of the other worm collagen IV member, EMB-9 (61% identical, 75% similar).

The NC1 domain of an unrelated collagen XVIII known as CLE-1 contains a region homologous to a different angiogenesis inhibitor, endostatin (Ackley et al., 2001). Loss of the NC1 domain of this protein in *cle-1(cg120)* mutants leads to a mild Unc phenotype probably due to axon defasciculation and guidance defects. Three different isoforms of CLE-1 are expressed in different tissues during embryogenesis including body wall muscles, pharynx, GLR glia and neurons in the nerve ring, ventral and dorsal nerve cords. Beginning in the L4 larva, secreted CLE-1 accumulates in basement membrane surrounding the intestine, gonad, and pharynx as well as in the underlying body wall muscle. Expressing the entire NC1 domain in mechanosensory neurons rescues migratory defects associated with these neurons in the mutant. Expressing only the endostatin subdomain not only phenocopies the mechanosensory migration defect but also causes ectopic gonad migration defects similar to those seen in the *cle-1* mutant. This is a clear reflection of the cell nonautonomous mode of action of CLE-1 and is the first example of a basement membrane collagen involved in neural development in the worm.

The *cle-1* mutant phenotype is milder than found in *unc-119* mutants but is otherwise similar and we might have reasonably expected that, if UNC-119 were to interact with any basement membrane collagen in our two-hybrid screens, CLE-1 would be a likely candidate. The NC1 domains of CLE-1 and LET-2 are about 18% identical

and 45% similar while those of LET-2 and EMB-9 are much more highly conserved (60% identity, 85% similarity). Nevertheless, our screen only identified an interaction with LET-2. While *cle-1(cg120)* mutants exhibit a low level of embryonic lethality *let-2* temperature-sensitive mutants are 100% embryonic lethal at restrictive temperatures. If LET-2 also plays a role in axonogenesis during embryonic development it is impossible to detect against this background lethal phenotype. However, it may be possible to rescue the *let-2* lethal phenotype with a transgenic LET-2 lacking the canstatin region of the NC1 domain and thus reveal other putative non-lethal phenotypes. Alternatively, it may be possible that expressing a secreted form of the NC1 domain of LET-2 alone will act as a dominant-negative for a putative role in axonogenesis but still permit embryogenesis.

In worm neurons, UNC-119 is normally found throughout the cytoplasm, including axons (Knobel et al., 2001). We have previously shown that when UNC-119 is expressed ectopically in body-wall muscle it appears to be secreted and to partially rescue both movement and dauer formation defects found in the *unc-119* mutant (Materi and Pilgrim, submitted). This suggests that this ectopic UNC-119 is somehow able to rescue at least some of the neural defects that are responsible for these phenotypic defects. It was initially unclear how a cytoplasmic protein might also be able to function from within the extracellular space. However, the possible interaction with LET-2 (a basement membrane collagen) indicated by our yeast two-hybrid screen and domain deletion analysis, suggests a mechanism.

We propose that UNC-119 may act as an adaptor protein linking basement membrane signaling components with intracellular response effectors. The ability of

extracellular UNC-119 to rescue neural defects suggests that this mechanism is likely to involve endocytosis at the growth cone. Such endocytosis has been shown to be critical for axon formation by examining RNAi phenotypes in cultured hippocampal neurons (Torre et al., 1994) and through an analysis of axon outgrowth in *Drosophila shibire* mutants (Masur et al., 1990). No mechanism has been proposed to date to explain why endocytosis at growth cones may be required and we do not know what ECM components may be brought inside the neurons through this process. Our work here suggests that basement membrane collagens (or, likely, their proteolysis products) may be included among endocytosed components and that UNC-119 may help mediate this process.

**Acknowledgements.** The directed two-hybrid analysis of the interaction between ARL-2 and UNC-119 reported in Sections 3.2.8 and 3.3.2 and in Table 3.5 was performed by Jessica Smith and is adapted from Smith (2003). The work on single-stranded site-directed mutagenesis in Sections 3.2.2 and 3.3.4 was performed by Leanne Sayles as part of the requirements for an undergraduate Honours project. Kathy Bueble sequenced the new *unc-119(ky571)* allele. This work is reported here for completeness and cohesiveness and will be submitted as a multi-author paper. Interpretation of the data and any errors introduced during writing are my responsibility.

Name	Sequence (5' to 3')	Residues modified
SH2MODU	AAA CAT ATC TAT AAA TTT CCA CAA CTT TCA	E172K, E176K
YSH2MODL	ACA GTT GTT TCT CGA ATT TGG CAT ACA GAA	none
YMODU	GAA CAT ATC GAT GAA TTT CCA CAA CTT TCA	Y175D
SH3MODU	CGA GCC GCA CCG GTA ACC GAA CAG G	P24A, P25A
SH3MODL	GGC CAT CTG AGA CGG GAA GGT TGC C	P22A
RH145GGU	GGG GGC TTT TTC AAG GAT CGT TTA T	R145G, H146G
RH145GGL	TTC AAT CAT TCG AAA ATG TGT GAT C	none
NNCE169	CCA AAT TCG AGA AAC AAC TGT GAA CAT ATC TAT GAA TTT CCA	none
FDFEFGF156	CAT ACA GAA TCC AAA TTC AAA ATC AAA GCA TTT CAA TAA ACG	none
169CENN	CCA AAT TCG AGA TGT GAA AAC AAC CAT ATC TAT GAA TTT CCA	N169C, C170E, C171N, E172N
169GGGG	CCA AAT TCG AGA GGC GGC GGT GGA CAT ATC TAT GAA TTT CCA	N169G, N170G, C171G, E172G
156ADAEAGA	CAT ACA GGC TCC AGC TTC AGC ATC AGC GCA TTT CAA TAA ACG	F156A, F158A, F160A, F162A
ATVEF126	GCG ACG GTC GAG TTC AAG GTC GGC GAT GTG	none
126AKDEA	GCG AAG GAC GAG GCA AAG GTC GGC GAT GTG	T127K, V128D, F130A
FLKLKTV118	GCC GAC CGT CTT TAA TTT CAG AAA ATT CGG	none
118RRKLTKE	GCC GTC CGT CTT TAA TTT CCT TCT ATT CGG	F118F, L119R, V124E
Y201D	CGA TAG CTT CGA TTT TGT GG	Y201D
L207H	GAA TAA GCA CGT AAT GCA C	L207H
V208G	GAA TAA GCT CGG AAT GCA A	V208G
K212N	GCA CAA TAA TGC CGA CTA C	K212N
D214R	CAA TAA GGC CCG CTA CTC G	D214R

**Table 3.1 Primers used for Site-directed Mutagenesis**

Primers were used to mutate specific UNC-119 residues through site-directed mutagenesis of a pDP#MM051 (PCR-based reactions) or pDP#UGF-16 (single-stranded reactions) DNA template. pDP#MM051 contains the putative *C. elegans unc-119* promoter followed by *unc-119* cDNA (Maduro, 1998). pDP#UGF-16 contains the entire *unc-119* coding sequence plus introns fused upstream of the GFP coding sequence all under the regulation of the worm *unc-119* promoter (Maduro, 1998). PCR-based reactions were used to produce mutations in residues thought to be in UNC-119 SH2 and SH3 binding motifs as well as putative phosphorylation signals. Single-stranded reactions were used to modify single residues in the carboxyl region of the protein.

Mutation name	Motif	Consensus sequence	Potential Motif(s) from HsUnc119	Potential Motif(s) from UNC-119	Modified motif in UNC-119	Reqd for UNC-119 function
Mut1	SH2 binding	[DE]-X <sub>2,3</sub> -Y*-[DE]-[FWP]	EHIYDF (191-196)	EHIYEF (172-177)	KHIYKF	-
Mut2	Tyrosine phosphorylation	[RK]-X <sub>2,3</sub> -[DE]-X <sub>2,3</sub> -Y*	RMIERHY (160-166) KNTCEHIY (187-194)	RNNCEHIY (168-175)	RNNCEHID	-
Mut3	Conserved		RMIERH (160-165)	RMIERH (141-146)	RMIEGG	+
Mut4	SH3 binding	RX <sub>2</sub> PX <sub>2</sub> P	APIRQPP (26-32), RQKPIGP (56-62)	SQMPPRP (19-25)	SQM-AA	-
Y201D	Conserved			Y201	D	+
L207H	Conserved			L207	H	+
V208G	Conserved			V208	G	+
K212N	Conserved			K212	N	+
D214R	Conserved			D214	R	+

**Table 3.2 Site-directed mutagenesis of motifs in HsUnc119 and Unc-119**

Specific mutations were introduced into *C. elegans* UNC-119 using either PCR-based or single-strand site-directed mutagenesis with primers in Table 3.1. Related motifs from the human homolog, HsUnc119, are shown for comparison. The regular expression in the "Consensus sequence" column is read as follows: only one of the residues in [] brackets is in the final sequence, subscripted residues appear in the final sequence the number of times indicated by the subscript or subscripts, X means any residue, Y\* is an obligate phosphorylated tyrosine. Thus [DE]-X<sub>2,3</sub>-Y\*-[DE]-[FWP] specifies a peptide sequence containing a D or E, followed by any 2 or 3 residues, followed by a phosphorylated tyrosine, then another D or E and ending with a F or W or P. The dashes in SQM-AA in the "Modified motif in UNC-119" column represent two deleted residues in the mutated sequence. + in the "Reqd for UNC-119 function" column indicates that, if residues are mutated as in the previous column, a construct encoding such a protein cannot rescue the mutant phenotype. - indicates that mutated residues do not abolish protein function as determined by phenotypic rescue

Template	Name	Sequence (5' to 3')	a.a. added
UBP-2	119Parts2	CAG TGG GGG CCC GGA GCA ACC TTC CCG TCT CAG ATG	PG
	119Parts2'	CAG TGG GGG CCC AGA CGA GCC GGG TGC GAT CGA TTG	SG
	119Parts1A	CAG TGG GGG CCC GGA CTC GCG AAA AAT CAA ATT ACA	PG
	119Parts1A'	CAG TCG GGG CCC TCC AAG CTC CGC CTC GGT GGT TAT	GG
	119Parts1B	CAG TGG GGG CCC GGA ACG GAA GAG AAT CTG CAG GCG	PG
	119Parts3B'	CAG TGG GGG CCC TCC TCC TTG CAG ATT CTC TTC CGT	GG
	119Parts1C	CAG TGG GGG CCC GGA AAT CCA AAC GAG ACC CGC TCC	PG
	119Parts1C'	CAG TGG GGG CCC TCC GGA GCG GGT CTC GTT TGG ATT	GG
	119Parts2D	CAG TGG GGG CCC GGA GCC GAC TAC TCG TAT GAT GCA	PG
WM014b	119Parts4	CGA TAG ATC TGG ATC AGC AAC CTT CCC GTC TCA G	SG
	119Parts4'	GCA TAG ATC TAA TGC CGG GTG CGA TAG ATT GTT G	IR
	119Parts4A	CGA TAG ATC TGG ACT CGC GAA AAA TCA AAT TAC A	SG
	119Parts4A'	GCA TAG ATC TAA TAA GCT CCG CCT CGG TGG TTA T	IR
	119Parts4B	CGA TAG ATC TGG AAC GGA AGA GAA TCT GCA GGC G	SG
	119Parts4B'	GCA TAG ATC TAA TCG CCT GCA GAT TCT CTT CCG T	IR
	119Parts4C	CGA TAG ATC TGG AAA TCC AAA CGA GAC CCG CTC C	SG
	119Parts4C'	GCA TAG ATC TAA TGG AGC GGG TCT CGT TTG GAT T	IR
	119Parts4D	CGA TAG ATC TGG AGC CGA CTA CGC GTA TGA TGC A	SG

**Table 3.3 Primers used for domain deletion**

The domain deletions shown in Figure 3.1 were produced using these primers in long inverse PCR reactions with either pDP#WM014b (a construct that expresses UNC-119 in worms under the control of its native promoter) or pDP#UBP-2 (a yeast two-hybrid bait construct containing the UNC-119 coding sequence fused carboxyl to the yeast GAL-4 DNA binding domain). Primer pairs used to generate a specific deletion are listed in Figure 3.1.

Strain name	Genotype
DP344	<i>lin-15(n765); edEx149[WM014bDel1; lin-15(+)]</i>
DP345	<i>lin-15(n765); edEx150[WM014bDel2; lin-15(+)]</i>
DP346	<i>lin-15(n765); edEx151[WM014bDel3; lin-15(+)]</i>
DP347	<i>lin-15(n765); edEx152[WM014bDel4; lin-15(+)]</i>
DP348	<i>lin-15(n765); edEx153[WM014bDel5; lin-15(+)]</i>
DP349	<i>lin-15(n765); edEx154[WM014bDel6; lin-15(+)]</i>
DP350	<i>lin-15(n765); edEx155[WM014bDel7; lin-15(+)]</i>
DP351	<i>lin-15(n765); edEx156[WM014bDel8; lin-15(+)]</i>
DP352	<i>lin-15(n765); edEx157[WM014bDel9; lin-15(+)]</i>
DP353	<i>lin-15(n765); edEx158[WM014bDel10; lin-15(+)]</i>
DP354	<i>lin-15(n765); edEx159[WM014bDel11; lin-15(+)]</i>
DP355	<i>unc-119(ed3); lin-15(n765); edEx149[WM014bDel1; lin-15(+)]</i>
DP356	<i>unc-119(ed3); lin-15(n765); edEx150[WM014bDel2; lin-15(+)]</i>
DP357	<i>unc-119(ed3); lin-15(n765); edEx151[WM014bDel3; lin-15(+)]</i>
DP358	<i>unc-119(ed3); lin-15(n765); edEx152[WM014bDel4; lin-15(+)]</i>
DP359	<i>unc-119(ed3); lin-15(n765); edEx153[WM014bDel5; lin-15(+)]</i>
DP360	<i>unc-119(ed3); lin-15(n765); edEx154[WM014bDel6; lin-15(+)]</i>
DP361	<i>unc-119(ed3); lin-15(n765); edEx155[WM014bDel7; lin-15(+)]</i>
DP362	<i>unc-119(ed3); lin-15(n765); edEx156[WM014bDel8; lin-15(+)]</i>
DP363	<i>unc-119(ed3); lin-15(n765); edEx157[WM014bDel9; lin-15(+)]</i>
DP364	<i>unc-119(ed3); lin-15(n765); edEx158[WM014bDel10; lin-15(+)]</i>
DP365	<i>unc-119(ed3); lin-15(n765); edEx159[WM014bDel11; lin-15(+)]</i>
DP312	<i>unc-119(ed3); edEx137[MM051(Mut1);SU006];</i>
DP313	<i>unc-119(ed3); edEx138[MM051(Mut2);SU006];</i>
DP314	<i>unc-119(ed3); edEx139[MM051(Mut3);SU006];</i>
DP315	<i>unc-119(ed3); edEx140[MM051(Mut4);SU006];</i>

**Table 3.4 Strains used**

Transgenic *C. elegans* strains were constructed using standard germline transformation methods. Some transgenic strains were constructed in a *lin-15(n765)* background strain (a kind gift of Erik Jorgensen, University of Utah) and transgenic animals were detected by rescue of the temperature-sensitive *lin-15* ectopic vulva phenotype due to co-injection with wild-type *lin-15(+)*. Del 1 through Del11 are domain deletion constructs created through long inverse PCR reactions and described in Figure 3.1. Mut1 through Mut4 are site-directed mutation constructs described in Table 3.2. SU006 is a pan-neural reporter construct which expresses GFP under the regulation of the F25B3.3 (a *C. elegans* RasGRP homolog) promoter (Altun-Gultekin et al., 2001).

	hsPDE $\delta$	PDL-1	HsUnc119	UNC-119
hsArl2	+	+	+	+
hsArl2(Q70L)			++	++
EVL-20	+	+	+	+

**Table 3.5 Directed yeast 2-hybrid  $\beta$ -galactosidase staining results.**

A directed yeast two-hybrid assay was used to evaluate the strength of interactions between Unc-119 homologs and Arl2 homologs. Bait (columns) and prey (rows) constructs were co-transformed into yeast cells and plated on double knockout media. The hs prefix indicates the human homolog. PDE $\delta$  is phosphodiesterase delta. PDL-1 is *C. elegans* PDE delta-like 1. Arl2 is the ADP ribosylation factor like gene; the Q70L mutant is a constitutively active isoform. EVL-20 is the worm Arl2 homolog. Colonies containing both bait and prey plasmids were streaked on quadruple knockout media to assay interaction by HIS and ADE reporter expression. Shading indicates combinations which grew on quadruple knockout plates. Dark shading indicates robust growth while light shading indicates weak growth. Colonies from the double knockout media were also assayed for  $\beta$ -galactosidase reporter expression. +++ indicates development of blue within 15 minutes (strong interaction), ++ indicates development of blue within 30 minutes (moderate interaction) and + indicates development of blue within 3 hours (weak interaction). With the exception of worm UNC-119 all bait constructs interacted with activated human Arl2 to permit growth as well as to display a  $\beta$ -galactosidase dependent color change. UNC-119 exhibited indication of interaction with Arl2 only using the  $\beta$ -galactosidase reporter. Previous reports of interaction have depended on this reporter only.

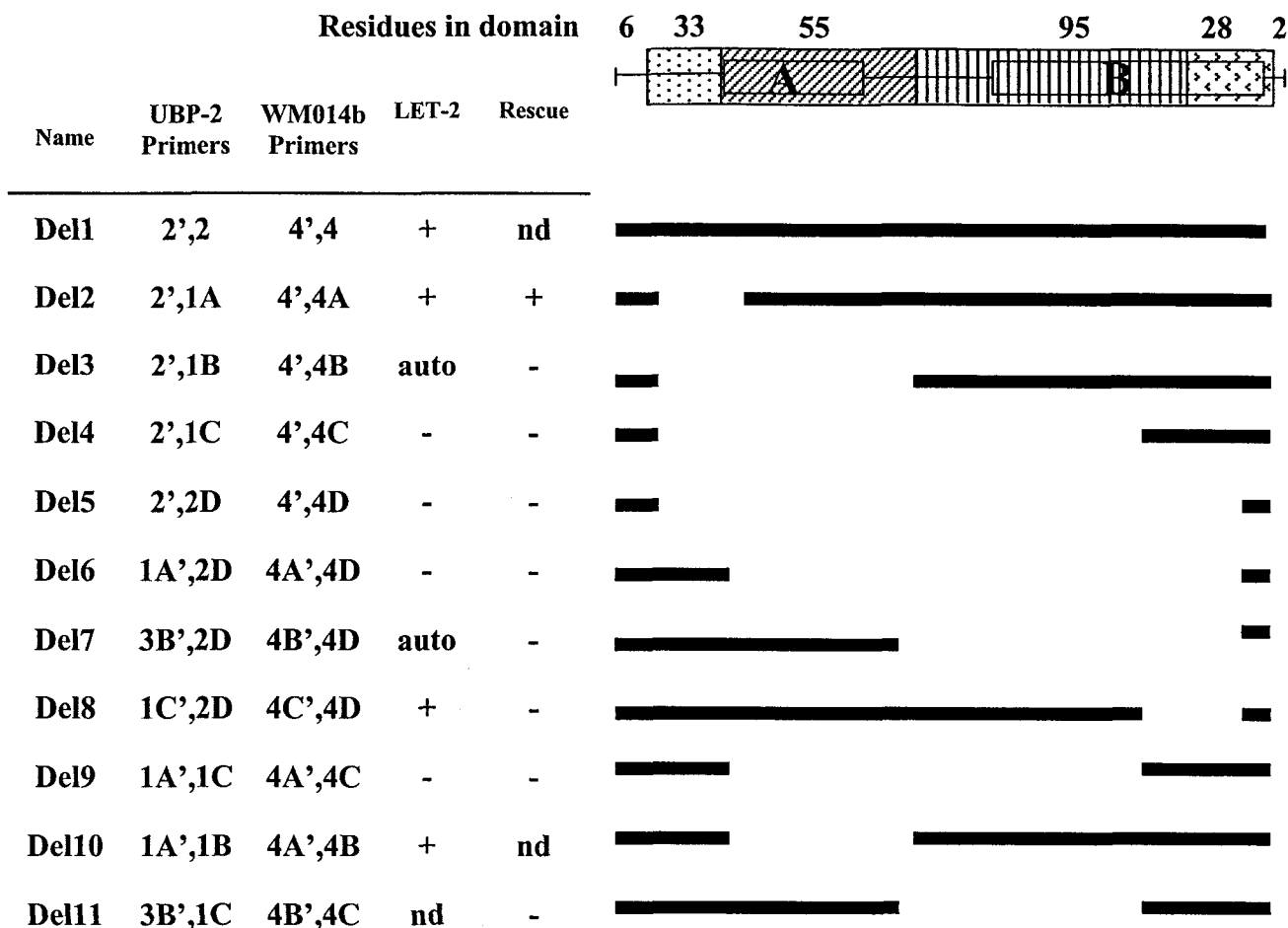


**Figure 3.1 Domain deletion analysis of UNC-119**

Deletions were made using long inverse PCR with the indicated primers and either using the yeast two-hybrid bait plasmid, UBP-2 or the rescuing UNC-119 (cDNA)::GFP fusion plasmid (pDP#WM0014b). A diagram of the protein is shown at top right. The shaded areas represent segments that could be removed using various primer combinations (the number of residues in each segment is shown above the segment). The black bars on the right represent segments of the protein that remain following deletion of each segment. The LET-2 column indicates the result of a directed yeast two-hybrid assay testing the interaction between the deletion-bearing bait plasmid and three different LET-2 prey plasmids from the screen. + indicates interaction (growth on quadruple knockout medium), - indicates no interaction, auto indicates auto-activation of reporter in absence of prey plasmid, nd indicates test not done. The Rescue column indicates the ability of a deletion-bearing plasmid to restore movement when expressed as a transgene in an *unc-119* mutant background. + indicates restoration of movement, - indicates no improvement over *unc-119*, nd indicates not done. Expression of deleted UNC-119 protein was not tested in yeast but GFP expression was confirmed in transgenic worms.

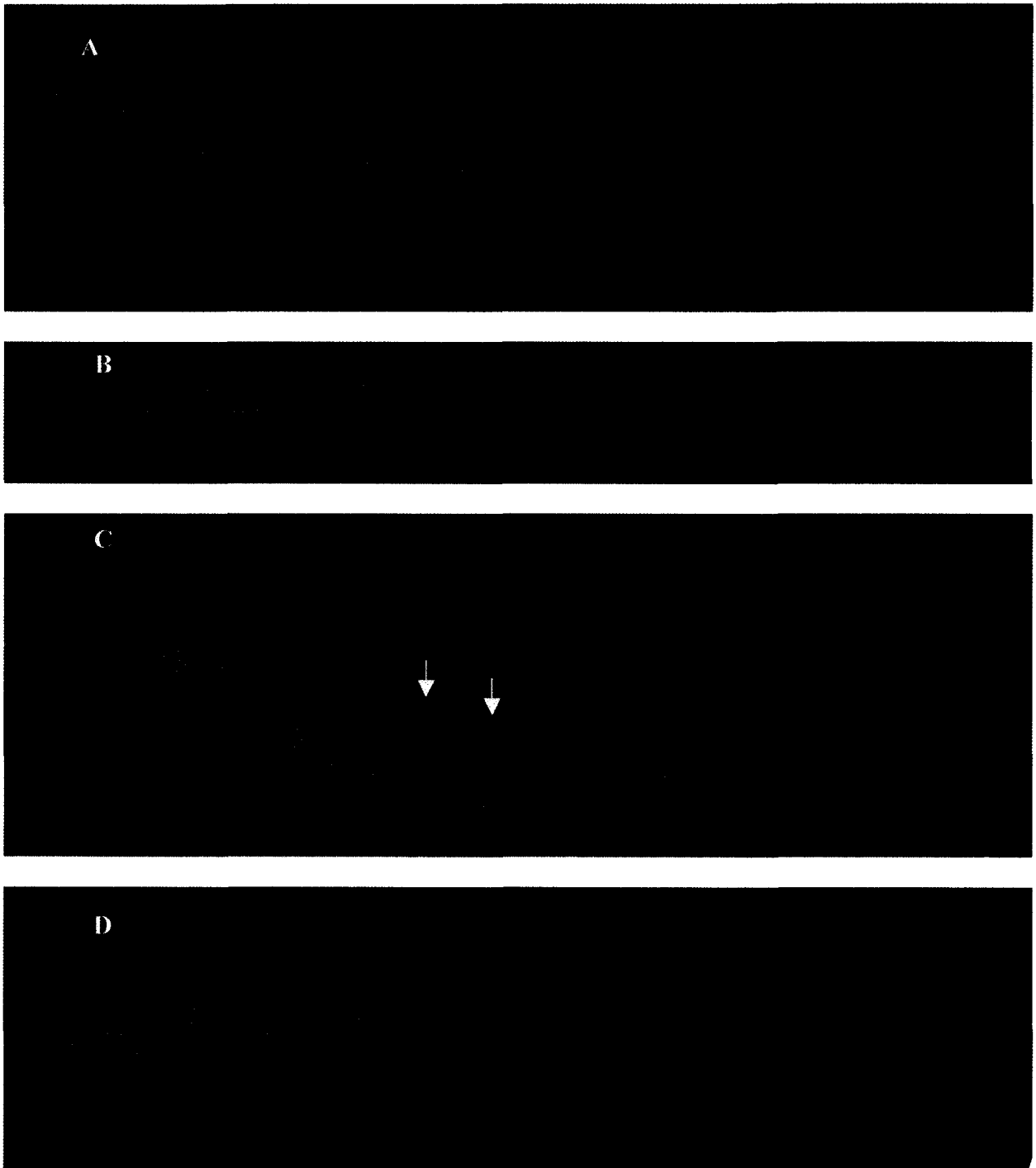


**Figure 3.2 Nervous system of transgenic worms with mutagenized SH2 or SH3 binding motifs**

A – DP312 contains mutated SH2 binding motif, B – DP313 contains mutated tyrosine phosphorylation motif, C- DP314 contains mutated conserved RMIERH motif, D – contains mutated SH3 binding motif. Anterior is to left and ventral is down. Nervous system is visualized with pan-neural pDP#SU006 reporter. Transgenic worms were created by germline transformation into wild type strain then crossed into an *unc-119* background. Commissures in A,B and D are wild type while some supernumerary branching of commissures (arrows) can be seen in C.

### 3.5 References

- Ackley, B.D., Crew, J.R., Elamaa, H., Pihlajaniemi, T., Kuo, C.J. and Kramer, J.M. (2001), The NC1/endostatin domain of *Caenorhabditis elegans* type XVIII collagen affects cell migration and axon guidance, *Journal of Cell Biology*, **152**: 1219-32
- Agatep, R., Kirkpatrick, R.D., Parchaliuk, D.L., Woods, R.A. and Gietz, R.D. (1998), Transformation of *Saccharomyces cerevisiae* by the lithium acetate/single-stranded carrier DNA/polyethylene glycol (LiAc/ss-DNA/PEG) protocol, *Technical Tips Online* (<http://tto.trends.com>)
- Altun-Gultekin, Z., Andachi, Y., Tsalik, E.L., Pilgrim, D., Kohara, Y. and Hobert, O. (2001), A regulatory cascade of three homeobox genes, *ceh-10*, *ttx-3* and *ceh-23*, controls cell fate specification of a defined interneuron class in *C. elegans*, *Development*, **128**: 1951-69
- Antoshechkin, I. and Han, M. (2002), The *C. elegans evl-20* gene is a homolog of the small GTPase ARL2 and regulates cytoskeleton dynamics during cytokinesis and morphogenesis, *Developmental Cell*, **2**: 579-591
- Bhamidipati, A., Lewis, S.A. and Cowan, N.J. (2000), ADP ribosylation factor-like protein 2 (Arl2) regulates the interaction of tubulin-folding cofactor D with native tubulin, *Journal of Cell Biology*, **149**: 1087-96
- Brenner, S. (1974), The genetics of *Caenorhabditis elegans*, *Genetics*, **77**: 71-94
- Cen, O., Gorska, M.M., Stafford, S.J., Sur, S. and Alam, R. (2003), Identification of UNC119 as a novel activator of Src-type tyrosine kinases, *Journal of Biological Chemistry*, **278**: 8837 - 8845
- Frame, M.C., Fincham, V.J., Carragher, N.O. and Wyke, J.A. (2002) V-Src's hold over actin and cell adhesions, *Nature Reviews. Molecular Cell Biology*, **3**: 233-245
- Frech, M., Darden, T.A., Pedersen, L.G., Foley, C.K., Charifson, P.S., Anderson, M.W., and Wittinghofer, A. (1994). Role of glutamine-61 in the hydrolysis of GTP by p21H-ras: an experimental and theoretical study, *Biochemistry*, **33**: 3237-44
- Gorska, M.M., Stafford, S.J., Cen, O., Sur, S. and Alam, R. (2004), Unc119, a novel activator of lck/fyn, is essential for T cell activation, *Journal of Experimental Medicine*, **199**: 369-79
- Hanzal-Bayer, M., Renault, L., Roversi, P., Wittinghofer, A. and Hillig, R.C. (2002), The complex of Arl2-GTP and PDE $\delta$ : from structure to function, *The EMBO Journal*, **21**: 2095-2106

- Higashide, T., McLaren, M.J. and Inana, G. (1998), Localization of HRG4, a photoreceptor protein homologous to *unc-119*, in ribbon synapse, *Investigative Ophthalmology & Visual Science*, **39**: 690-698
- James, P., Halladay, J. and Craig, E.A. (1996), Genomic libraries and a host strain designed for highly efficient two-hybrid selection in yeast, *Genetics*, **144**: 1425-1436
- Kamphaus, G.D., Colorado, P.C., Panka, D.J., Hopfer, H., Ramchandran, R., Torre, A., Maeshima, Y., Mier, J.W., Sukhatme, V.P. and Kalluri, R. (2000), Canstatin, a novel matrix-derived inhibitor of angiogenesis and tumor growth, *Journal of Biological Chemistry*, **275**: 1209-15
- Knobel, K.M., Davis, W.S., Jorgensen, E.M. and Bastiani, M.J. (2001) UNC-119 suppresses axon branching in *C. elegans*, *Development*, **128**, 4079-4092
- Kobayashi, A., Higashide, T., Hamasaki, D., Kubota, S., Sakuma, H., An, W., Fujimaki, T., McLaren, M.J., Weleber, R.G. and Inana, G. (2000), HRG4 (UNC119) mutation found in cone-rod dystrophy causes retinal degeneration in a transgenic model, *Investigative Ophthalmology & Visual Science*, **41**: 3268-77
- Kobayashi, A., Kubota, S.K., Moria, N., McLaren, M.J. and Inana, G. (2003), Photoreceptor synaptic protein HRG4 (UNC119) interacts with ARL2 via a putative conserved domain. *FEBS Letters*, **534**: 26-32
- Kowtha, V.C., Bryant, H.J., Pancrazio, J.J. and Stenger, D.A. (1998), Influence of extracellular matrix proteins on membrane potentials and excitability in NG108-15 cells, *Neuroscience Letters*, **246**: 9-12
- LaVallie, E.R., DiBlasio, E.A., Kovacic, S., Grant, K.L., Schendel, P.F. and McCoy, J.M. (1993), A thioredoxin gene fusion expression system that circumvents inclusion body formation in the *E. coli* cytoplasm, *Biotechnology*, **11**: 187-93
- Lu, L., Horstmann, H., Ng, C. and Hong W. (2001), Regulation of Golgi structure and function by ARF-like protein 1 (Arl1), *Journal of Cell Science*, **114**: 4543-55
- Maduro, M. and Pilgrim, D. (1995), Identification and cloning of *unc-119*, a gene expressed in the *Caenorhabditis elegans* nervous system, *Genetics*, **141**: 977-88
- Maduro, M. (1998), Characterization of the *unc-119* gene of *Caenorhabditis elegans*, PhD. Thesis, University of Alberta, Canada
- Maduro, M.F., Gordon, M., Jacobs, R. and Pilgrim, D.B. (2000), The UNC-119 family of neural proteins is functionally conserved between humans, *Drosophila* and *C. elegans*, *Journal of Neurogenetics*, **13**: 191-212

- Maeshima, Y., Sudhakar, A., Lively, J.C., Ueki, K., Kharbanda, S., Kahn, C.R., Sonenberg, N., Hynes, R.O. and Kalluri, R. (2002), Tumstatin, an endothelial cell-specific inhibitor of protein synthesis, *Science*, **295**: 140-3
- Masur, S.K., Kim, Y.T. and Wu, C.F. (1990), Reversible inhibition of endocytosis in cultured neurons from the *Drosophila* temperature-sensitive mutant *shibire<sup>ts1</sup>*, *Journal of Neurogenetics*, **6**: 191-206
- Renault, L., Hanzal-Bayer, M. and Hillig, R.C. (2001), Coexpression, copurification, crystallization and preliminary X-ray analysis of a complex of ARL2-GTP and PDE delta, *Acta Crystallographica. Section D, Biological Crystallography*, **57**: 1167-70
- Rigaut, G., Shevchenko, A., Rutz, B., Wilm, M., Mann, M. and Séraphin, B. (1999), A generic protein purification method for protein complex characterization and proteome exploration, *Nature Biotechnology*, **17**: 1030 - 1032
- Schurmann, A., Koling, S., Jacobs, S., Saftig, P., Krauss, S., Wennemuth, G., Kluge, R. and Joost, H.G. (2002), Reduced sperm count and normal fertility in male mice with targeted disruption of the ADP-ribosylation factor-like 4 (*Arl4*) gene, *Molecular and Cellular Biology*, **22**: 2761-8
- Simmer, F., Moorman, C., Van Der Linden, A.M., Kuijk, E., Van Den Berghe, P.V., Kamath, R., Fraser, A.G., Ahringer, J. and Plasterk, R.H. (2003), Genome-Wide RNAi of *C. elegans* using the hypersensitive *rrf-3* strain reveals novel gene functions, *PLoS Biology*, **1**: 77-84
- Smith, J. (2003), Characterization of PDE $\delta$  in *Caenorhabditis elegans* and *Danio rerio*, PhD. Thesis, University of Alberta, Canada
- Suter, D.M. and Forscher, P. (2001), Transmission of growth cone traction force through apCAM-cytoskeletal linkages is regulated by Src family tyrosine kinase activity, *Journal of Cell Biology*, **155**: 427-438
- Swanson, D.A., Chang, J.T., Campochiaro, P.A., Zack, D.J. and Valle, D. (1998) Mammalian Orthologs of *C. elegans unc-119* Highly Expressed in Photoreceptors, *Investigative Ophthalmology & Visual Science*, **39**: 2085-2094
- Temeles, G.L., Gibbs, J.B., D'Alonzo, J.S., Sigal, I.S., and Scoln, E.M. (1985). Yeast and mammalian *ras* proteins have conserved biochemical properties, *Nature*, **313**: 700-703
- Tonge, D.A., Golding, J.P., Edbladh, M., Kroon, M., Ekstrom, P.E.R. and Edstrom, A. (1997), Effects of extracellular matrix components on axonal outgrowth from peripheral nerves of adult animals in vitro, *Experimental Neurology*, **146**: 81-90
- Torre, E., McNiven, M.A. and Urrutia, R. (1994), Dynamin 1 antisense oligonucleotide treatment prevents neurite formation in cultured hippocampal neurons, *Journal of Biological Chemistry*, **269**: 32411-7

Van Valkenburgh, H., Sher, J.F., Sharer, J.D., Zhu, X. and Kahn, R.A. (2001), ADP-ribosylation factors (ARFs) and ARF-like 1 (ARL1) have both specific and shared effectors, *Journal of Biological Chemistry*, **276**: 22826–22837

Weiner, M.P., Costa, G.L., Schoettlin, W., Cline, J., Mathur, E. and Bauer, J.C (1994), Site-directed mutagenesis of double-stranded DNA by the polymerase chain reaction, *Gene*, **151**: 119-23

Wildering, W.C., Hermann, P.M. and Bulloch, A.G.M. (1997), Neurite outgrowth, RGD-dependent, and RGD-independent adhesion of identified molluscan motorneurons on selected substrates, *Journal of Neurobiology*, **35**: 37-52

Zamoyska, R., Basson, A., Filby, A., Legname, G., Lovatt, M. and Seddon, B. (2003), The influence of the src-family kinases, Lck and Fyn, on T cell differentiation, survival and activation, *Immunology Reviews*, **191**: 107-18

## Chapter 4 - UNC-119 Protein and Antibody

### 4.1 Introduction

UNC-119 is required for development of the *C. elegans* nervous system but little is known about the underlying molecular mechanism of its action. HsUnc119, the human homolog, is associated with vesicles in photoreceptor ribbon synapses (Higashide et al., 1998). Affinity chromatography of rat retinal lysate with an HsUnc119::GST fusion protein identified an unknown coprecipitating 23 kDa protein (Kubota et al., 2002). Western analysis using antibodies to twelve known synaptic vesicle and docking proteins (including synaptotagmin, synaptogyrin, syntaxin, rabphilin and UNC-18) did not detect this protein, suggesting it was either novel or not involved in synaptic function.

By yeast two-hybrid analysis, HsUnc119 has been shown to interact with human Arl1, Arl2 and Arl3 (Van Valkenburgh et al., 2001). In addition Arl2 co-precipitates from rat retinal extract with HsUnc119 (Kobayashi et al., 2003). However recent studies (Smith, 2003) have indicated that the interaction between UNC-119 and EVL-20 (the worm homolog of Arl2) are weak and unreliable, at best. An interaction between HsUnc119 and Src non-receptor tyrosine kinases has also recently been observed in cultured eosinophils (Cen et al., 2003). However in Chapter 3 - we showed that the motifs which mediate Src-HsUnc119 interaction are not required for UNC-119 function in the worm.

Unlike human HsUnc119, worm UNC-119 holoprotein is insoluble in bacterial expression systems so antibodies have previously been raised using only portions of the protein (Knobel et al., 2001). In this section, I describe my efforts to express soluble UNC-119 holoprotein and attempts to produce antibodies to representative oligopeptides.

## **4.2 Materials and Methods**

### **4.2.1 Oligopeptide-based antibodies**

15-residue peptides were designed based on the UNC-119 primary amino acid sequence. Hydrophilic regions with a high degree of sequence divergence were selected from amino (U119N = PVTEQAITTEAELLA), central (U119M = NETEENLQAQAESAR) and carboxyl (U119C = QLSQQLMDDMINNPN) regions of the protein (Figure 4.1). These were synthesized (Research Genetics) on 8-branch MAP (Multiple Antigen Peptide) backbones, dissolved in water at 1 mg/ml, mixed 50% with Freund's Adjuvant and injected into rabbits monthly over a one year period. Rabbits 9M1 and 9M5 were injected with U119N, 9M3 and 9K4 were injected with U119M and 9K2 and 9K5 were injected with U119C. Test bleeds were performed two weeks after each booster injection and rabbits were exsanguinated following the ninth injection.

A dotblot was used to verify the specificity of antisera to the oligopeptide against which it was raised. Briefly, oligopeptides were dissolved to a final concentration of 1 mg/ml in Laemmli loading buffer and boiled for 10 minutes. 2  $\mu$ l of each oligopeptide were applied in a grid pattern directly to a nitrocellulose strip and allowed to dry. The blot was cut into strips, and antibody binding was detected using Western analysis.

### **4.2.2 Expressing UNC-119 in bacteria**

Initial attempts to express UNC-119 in several bacterial systems failed. Either bacteria transformed with the expression construct could not be recovered or, if they could, induction of protein expression completely impeded growth. These results suggested that the holoprotein was toxic to *E. coli* possibly due to insolubility. An antibody to the amino-most 50 residues has been previously described (Knobel et al.,

2001) but it had very low sensitivity and immunostaining was only accomplished by filleting worms. A tightly-regulated thioredoxin fusion at the amino end of the protein has been found to improve solubility and reduce toxicity for some proteins (La Vallie et al., 1993). *unc-119* cDNA from pDP#cDNA5 (Maduro, 1998) was cloned into the ThioFusion Expression System kit (Invitrogen) pTrxFus vector to make pDP#WM020. The thioredoxin fusion is expected to add 11.7 KDa to the predicted size of the UNC-119 protein (25.3 KDa). Expression of the cloned gene is tightly regulated by thymine in this system. The cloned plasmid was transformed into the GI698 and GI724 *E. coli* strains provided in the kit; GI698 is used for expressing fusion proteins below 30°C while GI724 expresses proteins above 30°C. Initial analysis indicated that the Thioredoxin::UNC-119 fusion protein was expressed best in GI698 so that was used for subsequent analysis.

Expression of the fusion protein was induced as per manufacturer's directions. Briefly, RM media containing 75 ug/ml ampicillin was inoculated and incubated O/N at 30°C with 260 rpm shaking. 5 ml of this was used to inoculate 50 ml of IM (Induction Media) and this was grown at 30°C with shaking to an  $A_{550}$  of 0.5 (approximately 3 hours). A sample was taken and tryptophan was added to a final concentration of 0.1 mg/ml to induce expression. Samples were taken at 2, 3 and 5 hours.

Protein was extracted from the bacteria using the BugBuster extraction reagent (Novagen) as follows. Samples of cells were centrifuged for 10 min. at 3700 rpm and the supernatant decanted. The pellet was resuspended in 1.0 ml lysis solution/gram of pellet. The lysis solution was composed of 1 X BugBuster, 1  $\mu$ l of Benzonase (Novagen) to degrade DNA and 1 Compleat Mini EDTA free tablet (Roche) plus 4 mM Pefabloc

(Roche) to inhibit endogenous proteinases. Cells were incubated at RT for 20 minutes with vortexing every 5 minutes then transferred to 1.5 ml tubes and spun at 13,000 rpm for 20 minutes. The supernatant was transferred to a fresh tube and the pellet resuspended in the same volume of lysis buffer.

#### **4.2.3 Purification of antisera**

The TrxFus vector, containing only the Thioredoxin coding sequence was expressed in GI698 bacteria and an acetone powder prepared from collected cells. Pre-immune and final bleed antisera were incubated along with approximately 5 mg of this acetone powder at RT with rocking for 30 minutes. The mixture was then spun at 13,000 rpm for 5 minutes and the supernatant transferred to a fresh tube; this should no longer contain antibodies to any common bacterial proteins nor to the Thioredoxin portion of the Thioredoxin::UNC-119 fusion protein.

Alternatively, antisera was affinity-purified over a Sepharose column containing conjugated oligopeptides. The affinity columns, one for each of U119N, U119M and U119C were prepared by conjugating each of the oligopeptides to NHS-activated Sepharose 4 Fast Flow (Amersham Pharmacia Biotech) according to the manufacturer's directions. NHS adds a 6-aminohexanoic acid spacer arm between the Sepharose matrix and the oligopeptide and is considered superior to cyanogen bromide-activated Sepharose for oligopeptide columns. The reaction was monitored by measuring  $A_{280}$  at various time points and was complete (no change in  $A_{280}$  from previous timepoint) within 3 hours.

Affinity purification was conducted as directed and fractions collected and analyzed by measuring  $A_{280}$ . Briefly, the column was washed 3 times with 1 column volume (5 ml) of PBS. 1 ml of crude antisera was clarified by centrifuging at 13,000 rpm

for 5 minutes then applied to the top of the column and allowed to run into the column bed. Following a 60 minute incubation binding period at RT the column was washed 6 times with 3 column volumes of PBS. Bound antibodies were then eluted with 3 column volumes of glycine-HCl (pH 2.3) and 750  $\mu$ l samples collected into 750  $\mu$ l of neutralizing Tris-HCl (pH 9.2). Finally the column was washed 4 times with 3 column volumes of PBS. All liquid flowing through the columns was collected and  $A_{280}$  measurements taken. Sequential eluate fractions with roughly equivalent  $A_{280}$  values were pooled.

#### **4.2.4 Construction of Multi-epitope tag**

Cassettes in three reading frames were designed with multiple epitopes, including Myc, HIS-6, TAP (Tandem Affinity Protocol), and FLAG. These epitopes were placed in-frame between multi-cloning sites derived from Fire Lab Vector pPD102.33 (the kind gift of Andrew Fire, Stanford University) as follows. First pDP#NOGFP was constructed by removing the GFP coding sequence from pPD102.33 using inverse PCR. Primers NOGFPU and NOGFPL were also designed to conserve the unique AgeI restriction site and introduce a new unique NheI site (Table 4.1). This also removed an in-frame stop codon in the 3' MCS. Three double-stranded oligonucleotide linkers with AgeI overhangs at each end and containing the Myc tag in one of three reading frames were created by annealing single-stranded oligonucleotides. MycF1U and MycF1L were annealed to create the MycF1 linker. MycF2U and MycF2L were annealed to create the MycF2 linker. MycF3U and MycF3L were annealed to create the MycF3 linker. These were annealed by mixing 20  $\mu$ l each of approximately 50 - 100  $\mu$ M single-stranded oligonucleotides, heating to 96  $^{\circ}$ C for 2 minutes then cooling to RT at 2  $^{\circ}$ C/minute. These double-stranded linkers were then inserted non-directionally into the AgeI site in

pDP#NOGFP and, following transformation into XL1-B *E. coli*, single colonies containing linkers in the correct frame and orientation were isolated. The three constructs were named NOGFP + MycF1 (Figure 4.2), NOGFP + MycF2 (Figure 4.3) and NOGFP + MycF3 (Figure 4.4) according to their insert.

The TAP tag was extracted from pREP-NTAP (K. Gould, Vanderbilt University Medical Center) by PCR using NTAPFUP and NTAPFLO primers which added *NheI* sites at each end of the PCR product (Table 4.1). NTAPFUP also added a HIS-6 coding sequence upstream of the TAP tag while NTAPFLO added a FLAG coding sequence downstream. This PCR product was then inserted non-directionally into the unique *NheI* site of NOGFP + MycF1, NOGFP + MycF2 or NOGFP + MycF3 to give pDP#STF1, pDP#STF2 or pDP#STF3 respectively. Correct construction of the plasmids was verified by sequencing across both upstream and downstream joins. The final tags contain the following epitopes (in amino to carboxyl order): Myc, HIS-6, IgG-Binding Protein (IgG-BP), TEV cleavage site, Calmodulin Binding Protein (CBP), FLAG (Figure 4.5).

#### **4.2.5 Construction of tagged UNC-119 in insect cells**

Sf9 cells, derived from pupal ovarian tissue of *Spodoptera frugiperda* (Invitrogen) were maintained at 27°C in 25 ml flasks with ESF921 Insect Cell Culture Medium, Protein Free (Expression Systems). Cells were passaged at 1:10 dilution when confluent (i.e. every 5 to 7 days).

The UNC-119 coding sequence was PCR-amplified from pDP#MM051 using primers cDNATRXUb (5' CAAGGTACCGCTATGGGAGCAGAGCAACAA) and cDNATRXL (5' GCTCTAGAGGTGCATCATACGAGTAGTCGGC). These primers add upstream *KpnI* and downstream *XbaI* sites at the ends of the PCR product and adds a

Kozak consensus sequence at the translational START. This also changes the lysine residue at position 2 to a glycine. This fragment was inserted into the same sites of a KpnI/XbaI fragment of pIB/V5-HIS insect cell expression vector from the Insect Select BSD System (Invitrogen) and transformed into XL1-B *E. coli*. The resulting pDP#WM025b plasmid was verified by sequencing across both joins. The multi-epitope tagged pDP#WM025e was then constructed by inserting a KpnI fragment of pDP#STF1 non-directionally into the corresponding sites of pDP#WM025b. Again, construction was verified by sequencing across both joins. The expected size of the recombinant tagged protein is 59.9 kDa.

Sf9 cells were transiently transfected with pDP#WM025e as directed (Invitrogen). Briefly, cells were passaged as per above into 4 flasks marked Dy2, Dy3, Dy4 and Mock Transfection, then grown until about 80% confluent. The medium was replaced with 2ml of Grace's Insect Cell Medium and incubated for 30 minutes at 27°C. Approximately 2 ug of pDP#WM025e was mixed with 1 ml of Grace's Insect Cell Medium in a 1.5 ml tube then 10 µl of CellFectin (Invitrogen) was added and the entire transfection solution was mixed by inversion and incubated 30 minutes at RT to allow complexes to form. The Grace's Medium was aspirated from the flasks and the transfection solution was added dropwise directly onto the cells. The cells plus transfection solution were incubated for 6 hours at 27°C with rocking every hour. Finally 2.5 mls of ESF921 Medium were added and the cells grown for 2, 3 or 4 days (3 days for the Mock Transfection).

Protein was extracted from transfected cells with Insect Cell Lysis buffer (50mM Tris HCl pH7.8, 150 mM NaCl, 1% Nonidet P-40) containing Mini-Compleat (1

tablet/10 mls) and 2mM Pefabloc as proteinase inhibitors. Medium was aspirated from the cells and 100 µl of this lysis buffer was added. Cells were scraped off the inside surface of the 25 ml flask, collected in a 1.5 ml microfuge tube and allowed to incubate with rocking at RT for 5 minutes. The tubes were centrifuged at 13,000 rpm for 2 minutes and the supernatant transferred to a fresh tube. The pellets were resuspended in the same volume of lysis buffer and samples of pellet and supernatant were subjected to further analysis.

Stable transfection of pDP#WM025e in Sf9 cells was accomplished by treating transfected cells with 70 ug/ml Blasticidin through two complete passages. Stably transfected cells were maintained in 10 ug/ml Blasticidin.

#### **4.2.6 Construction of tagged UNC-119 in worms**

Transgenic worms containing the pDP#WM014b Del2 construct were observed to rescue the *unc-119* movement defects. The construction of this Del2 plasmid introduced a unique BglII site in the linking sequence. pDP#STF1 contains three compatible BamHI sites but one of them is upstream of the FLAG epitope. I used degenerate PCR with primers BamBglIU (5' AGTAGATCTCCCGGGCTGCAGGAATT) and BamBglL(5' GCCCGGGAGATCTACTAGTTCTAGAG) to amplify the complete tag in pDP#STF1, converting the required BamHI sites into BglII sites. This fragment was then inserted non-directionally into the BglII site in pDP#WM014b Del2 to make pDP#WM0014f. Following sequencing to confirm the plasmid was constructed correctly, it was injected into N2 worms along with the pRF4 plasmid and rolling transgenic animals (edEx71) with pan-neural GFP were isolated. The expected size of the tagged UNC-119 protein is 70 kDa.

#### 4.2.7 Worm lysates

Transgenic worms (*unc-119; edEx71[pPD#WM014f/pRf4]*) were raised in two liters of liquid culture as specified (Lewis and Fleming, 1995). Worms that lost the rescuing transgene were Unc and did not grow as well as the wild type rescued worms in liquid culture conditions. Thus, without integrating, this method slightly selected for and concentrated worms expressing multi-epitope-tagged UNC-119::GFP.

A large mortar and pestle were cooled to -80°C then set on top of dry ice in a Styrofoam container and further cooled by adding liquid Nitrogen. Worms were floated on 35% sucrose to isolate living animals from corpses and bacterial debris. Floating worms were pipetted from the top of the sucrose, washed twice with M9 buffer and pelleted by centrifugation. Worm pellets were dropped into the liquid Nitrogen pool at the bottom of the mortar and ground with the pestle for several minutes, adding liquid Nitrogen as needed to maintain a slurry in the mortar. Grinding was monitored by sampling the worm powder under a dissecting microscope for intact bodies. Grinding was considered complete when no intact bodies were visible in the 10 µl sample.

#### 4.2.8 SDS-PAGE and Western Analysis

An equivalent volume of 2 X Laemmli SDS-PAGE loading buffer was added to the lysate, which was then boiled for 10 minutes and analyzed on 12 – 15% SDS-PAGE gels. Protein was electrophoretically transferred to nitrocellulose at 90V for 1 hour. Blots were stained with Ponceau S Red following transfer then sectioned as appropriate and blocked using 5% BLOTTO (in PBST or TBST buffer). Sections of the blot were incubated with appropriate 1° Ab at dilutions ranging from 1/500 to 1/10,000 in 0.5% BLOTTO for two hours at RT. Following three 5 minute washes in buffer, strips were

incubated for one hour in 1/10,000 anti-rabbit or anti-mouse secondary (HRP-conjugated – Amersham Biosciences) then washed three more times in buffer for 5 minutes each. Antibody binding was detected using SuperSignal West Pico Chemiluminescent Substrate (Pierce) according to manufacturer's instructions. Two different pre-stained molecular weight markers were used (Kaleidoscope Prestained Standards and Precision Plus Protein Standards, both from BioRad) and differences in apparent mobility may be responsible for some differences in estimated molecular weights on different gels.

#### **4.2.9 Tandem Affinity Purification and pull-down**

Protein was purified using the Tandem Affinity Purification (TAP) protocol (Rigaud et al., 1999). Because this is carried out using buffers that preserve native protein conformations, isolating the desired protein also isolates other proteins with which it is complexed. Briefly, the soluble lysate fraction of an appropriately-tagged protein was diluted in IgG binding buffer and applied to IgG agarose beads (Sigma). This was incubated overnight at 4°C with continuous rotation. Unbound (FT – flow-through) lysate was allowed to drain and the beads were washed 3 times with 150 column volumes of buffer. Bound protein complexes were released from the beads by cleavage with TEV protease, leaving the fragment containing Myc, HIS-6 and IgG-BP epitopes bound to the column. Calmodulin binding buffer was added to the eluate (containing CBP, FLAG, UNC-119 and GFP protein fragments) and it was incubated with Calmodulin-agarose beads (Sigma) for 1 hour at 4°C with continuous rotation. The unbound fraction was drained, the column washed 3 times with 150 column volumes of buffer and the bound complexes eluted with Calmodulin Elution Buffer.

#### 4.2.10 Co-immunoprecipitation

Myc-tagged UNC-119 and complexed proteins were immunoprecipitated from lysate with Protein G Sepharose. Briefly, 100  $\mu$ l of Protein G Sepharose (Amersham Biosciences) was washed with immunoprecipitation buffer. Lysate was mixed with 50  $\mu$ l of rabbit pre-immune serum and added to the Protein G Sepharose then incubated overnight at 4°C. This mixture was then precipitated by spinning for 30 seconds at 10.4k rpm at RT to remove the beads. Any proteins that bound non-specifically to the pre-immune serum or to the Protein G beads themselves were also removed.

The supernatant was transferred to a fresh tube to which 2  $\mu$ l of  $\alpha$ -Myc monoclonal antibodies and 100  $\mu$ l of fresh equilibrated Protein G Sepharose were added. This was incubated 1 hour at 4°C with rocking then spun 30 seconds at 10.4 k rpm to isolate the unbound fraction. Following 2 washes with 10 column volumes of buffer, the bound protein was eluted by adding 30  $\mu$ l of TBS and 30  $\mu$ l of Laemmli loading buffer, then heating to 85°C for 10 minutes.

## 4.3 Results

### 4.3.1 UNC-119 Antibodies

Polyclonal antibodies were raised to oligopeptides from the amino (U119N), central (U119M) and carboxyl (U119C) regions of the UNC-119 protein. A dotblot verified that antisera specifically reacted with its cognate peptide except that 9K2 (raised against U119C) also recognized U119M with similar affinity (Figure 4.6). At very low dilutions (1/500) most antisera cross-reacted with at least one other oligopeptide.

In order to show that our antisera recognized UNC-119 and not just oligopeptide fragments, we wanted to isolate recombinant UNC-119 protein. Initial attempts to express UNC-119 holoprotein in a variety of bacterial protein expression systems failed. Either transformed colonies could not be recovered or induction killed the growing cells. This suggested that UNC-119 was toxic to bacteria likely due to insolubility. We constructed a plasmid (pDP#WM020) that expressed a tightly-regulated Thioredoxin::UNC-119 fusion protein, as such fusions have been previously shown to increase protein solubility in some cases.

We probed a Western blot of lysate from bacteria transformed with pDP#WM020 using the antisera. The recombinant protein was initially expressed in two strains of bacteria (GI698 and GI724) which have slightly different regulation of protein expression and were, thus, grown at different temperatures (25°C and 30°C, respectively). GI698 lysate contained the recombinant protein at higher levels than GI724 lysate, though it was detected only in the insoluble pellet fraction, and was used for subsequent analysis (Figure 4.7). Preliminary results suggested all the antisera exhibited high levels of cross-reactivity with endogenous bacterial proteins (data not shown). We used acetone powder

from a bacterial strain expressing thioredoxin only to pre-clear the antisera to these endogenous proteins and to thioredoxin, itself, in an effort to reduce this background reactivity. In addition, we also tested the relative efficacy of affinity-purification of antisera using a Sepharose column to which different oligopeptides used to raise the various antisera was bound.

Pre-clearing the antisera with bacterial acetone powder reduced cross-reactivity to endogenous proteins but two bands (one slightly larger than the expected size of 37 KDa and the other approximately 23 KDa) were observed (Figure 4.8). Affinity-purification of the antisera resulted in only the single expected band. UNC-119 was detected in the pellet fraction from the lysate, indicating continued poor solubility of the recombinant protein. Unfortunately, none of the antisera detected native UNC-119 in worm lysate (data not shown). This may indicate that the epitope recognized by the antisera was not exposed in the native protein or that the worm lysate was of poor quality.

#### **4.3.2 Epitope-tagged UNC-119 proteins**

The poor solubility of recombinant UNC-119 in bacteria may be due to misfolding or lack of correct post-translational processing in the prokaryotic expression system. We expressed the protein in a eukaryotic system by constructing a multi-epitope tagged UNC-119 insect cell expression plasmid (pDP#WM025e) and stably transfected Sf9 insect cells with this plasmid. Western analysis of lysates showed relatively high expression levels of a soluble recombinant protein at 2, 3 or 4 days post-transfection (Figure 4.9) which was detectable with antibodies to a vector epitope and with antibodies to the Myc epitope in the tag. Although the protein appeared slightly larger than the predicted size, a similar discrepancy has been reported previously for HsUnc119

(Higashide et al., 1998; Denholm, 2003; A. Manning, personal communication).

Transgenic worms bearing a similar plasmid expressing multi-epitope tagged UNC-119 under the control of its native promoter were constructed. A Western blot of worm lysate from this strain (edEx71) had a band of the expected size which was detectable with  $\alpha$ -Myc and  $\alpha$ -FLAG antibodies though most of the protein was in the pellet fraction (Figure 4.10). Non-transgenic control worms (N2) did not show this band.

#### **4.3.3 Pull-down and co-immunoprecipitation assays**

One of the main objectives of this work was to enable protein pull-down or co-immunoprecipitation assays of worm lysates to verify yeast two-hybrid results *in vitro*. As a preliminary test of the protocol, we pooled lysates from twenty 75 ml flasks of stably-transfected pDP#WM025e Sf9 cells and attempted a TAP (Tandem Affinity Protocol) pulldown assay (Figure 4.11). The tagged UNC-119 protein was detected in the original lysate by both  $\alpha$ -Myc and  $\alpha$ -FLAG antibodies. Most of the tagged protein apparently bound to the IgG column as a reduced amount was detected in the concentrated flow-through fraction. Release of the carboxyl portion of the fusion protein (including CBP [Calmodulin Binding Protein], FLAG and UNC-119 regions) by TEV protease was verified by eluting the IgG-bound fragment with glycine (pH 2.3) following cleavage.  $\alpha$ -Myc antibody detected the Myc + IgG BP (IgG Binding Protein) fragment left bound to the IgG column following TEV cleavage (see Lane 3 of  $\alpha$ -Myc blot in Figure 4.11) but no protein was detected by  $\alpha$ -FLAG in any of the individual fractions eluted from the Calmodulin column. Pooling all five fractions of eluate and concentrating them 20-fold permitted the weak detection of the CBP + FLAG + UNC-

119 fragment by  $\alpha$ -FLAG (Lane 10 of  $\alpha$ -FLAG blot in Figure 4.11).

We created a transgenic strain of worm expressing a tagged UNC-119::GFP fusion protein under the control of its native promoter in an *unc-119* mutant background. The tagged UNC-119 rescued gross movement and phenotypic defects and pan-neural GFP was observed (data not shown). We grew gram quantities of this strain in liquid media and extracted protein by grinding in liquid nitrogen. Expression of the fusion protein in the soluble fraction of the lysate was verified by Western blot using both  $\alpha$ -Myc and  $\alpha$ -FLAG Ab's (Figure 4.12). However, following TAP pulldown or co-immunoprecipitation with Sepharose-bound  $\alpha$ -Myc, no tagged protein was detectable in any fractions either by Western or Coomassie staining (data not shown).

#### 4.4 Discussion

We have expressed UNC-119 protein in both prokaryotic and eukaryotic expression systems. Bacterial expression of UNC-119 produces insoluble holoprotein while a portion of the UNC-119 produced in an insect cell expression system is soluble. Using a complex multi-epitope tag for UNC-119 fusion protein detection and purification we have been able to purify small amounts of the holoprotein from insect cells. However, the purified protein is undetectable by Coomassie staining in the purified eluate and is only weakly detectable using Western blotting. This could be due to poor binding efficiency of the tagged protein to the second column in the TAP procedure or to poor affinity for Coomassie stain.

However, attempts to determine the binding efficiency to the second column by comparing amounts in flow-through, wash or elution fractions using the FLAG epitope failed to detect any protein in any fractions. This may be due to the placement of the FLAG epitope carboxyl to the CBP epitope as FLAG antibodies do not detect internal FLAG epitopes with high efficiency. An improved design of the tag would place FLAG immediately carboxyl to the TEV protease cleavage site, amino terminal to the CBP epitope. This should be followed by a Thrombin cleavage site so that the entire purification epitope domain can be removed from the final protein.

We have also been able to similarly tag UNC-119 in a transgenic worm strain and verified that the protein is expressed and is functional. However, depending on the method of extraction, the majority of tagged protein was often detected in the insoluble fraction of the lysate. Attempts to purify or pull-down UNC-119 and other complexed proteins from the soluble fraction, even when the tagged protein was detectable there,

failed to produce detectable levels of UNC-119 protein.

UNC-119 has been previously shown to localize to the cytoplasm of worm neurons including the cell body, axon shaft and growth cone (Knobel et al., 2001). In addition, we have suggested that UNC-119 may interact with LET-2, a basement membrane collagen. Thus, it is possible that UNC-119 protein strongly associates with both intracellular and extracellular components that are largely insoluble and that our lysis methods are not solubilizing the protein. Alternatively the quality of our worm lysate as a whole may be poor. We have attempted several methods of producing worm lysate and found that grinding for several minutes in liquid Nitrogen results in acceptable disruption of the worm body. Supernatant produced in this method contains detectable UNC-119 using  $\alpha$ -Myc or  $\alpha$ -FLAG though cross-reactivity with endogenous worm proteins using the  $\alpha$ -FLAG antibody is high, leading us to qualify this result. Other methods of producing lysate, including high-pressure French Press, should be explored.

In addition, although our worm lysate was of acceptable quality, insufficient quantity of lysate may have been used in pull-down/co-immunoprecipitation assays. UNC-119::GFP expression under the control of its native promoter is typically observed at relatively low levels of apparent abundance, suggesting it is not normally highly-expressed. Thus using all available lysate from several liters of liquid-cultured worms may be necessary to produce detectable levels of UNC-119. It is also possible that UNC-119 is rapidly degraded in worm lysate leading to loss of the amino-terminal epitopes and making the protein undetectable. Optimization of protease inhibitors may be required to overcome this problem. Finally, although UNC-119 is overexpressed in transgenic worms, putative binding partners are not, so they may not achieve detectable levels in

pull-down assays.

Given an additional six-to-twelve months in which to complete this project, I would redesign the multi-epitope tag to place the FLAG epitope immediately carboxyl to the TEV protease cleavage site, remove the extraneous restriction sites immediately carboxyl to the original CBP epitope, and add a Thrombin cleavage site at the carboxyl end of the tag. I would place this improved tag into insect-cell constructs expressing UNC-119 as described above. After verifying correct expression of the protein in stably-transfected Sf9 insect cells, I would grow liter quantities of cells in a spinner flask suspension culture and use lysate from these cells to optimize the Tandem-affinity purification protocol. Because Sf9 cells are largely undifferentiated, I would not expect any proteins to co-purify with UNC-119 as its normal neural partners should not be expressed in these cells. This purified protein could be injected into rabbits to produce anti-UNC-119 Ab.

After successful optimization of this protocol in Sf9 cells, I would produce a transgenic worm carrying a similarly-tagged UNC-119::GFP driven by the *unc-119* promoter in an *unc-119* background. I would optimize a protein extraction protocol on a control strain of worms (using, for example, an anti-myosin Ab) then produce lysate from a large liquid culture of this transgenic strain and attempt the TAP pull-down on the entire soluble fraction. The eluate from the final purification step would then be concentrated and subjected to 2D-SDS PAGE and developed with a Silver stain. Isolated dots would be identified by mass spectrometry and interactions confirmed independently with standard genetic methods.

```

Human      -----MKVK--KGGGGAGTATESAPGPSQSVAPIQPPAEESESGSESEPDAGPGPRP
Zebrafish  -----MKVK--KG---CNT-TD-----LG---VPVT-----T---EEE-----
Xenopus    ----MNRLKARRVQGKE-SGT-SDQ----SS-----IT-----RFFREEE-----
Drosophila MSVVGKQLNPVQSSGAG-AVTTSSSAAAGSSSSNSGVEANGGSGGSSGAAAAGAGASGDA
C. elegans -----MKAEQQQQSIAPGSATFP-----SQMPRPPPVTEQAITTEAE-----
C. briggsae -----MKAEQQQ-SIPPGSATFP-----SQMPRPPPSTEQGITTESE-----
          ::      .      :      :      .

Human      -GPLQRKQPIGPEDVLGLQRITGDYLCSPENIYKIDFVRFKIRDMSGTVLFEIKKPPVS
Zebrafish  ---LLANKTISPEDVLGLQKITENYLCSPEDNLYNIDFTRFKIRD METGTVLFEITKPPST
Xenopus    ---LLGLNELRPEHVLGLSRVTDNYLCKPEDNIFGIDFTRFKIRDLETGTVLFEISKPCSE
Drosophila MKRPAESSSVTPDEVLLHLTKITDDYLCSANANVFEIDFTRFKIRDLESGAVLFEIAKPPSE
C. elegans ---LLAKNQITPNDVLALPGITQGFCLCSPSANVYNI EFTKFQIRDLDTEHVLFEIAKPENE
C. briggsae ---LAKKAQITPNDVLALPGITQGFCLCSPSANIYNI EFTKFQIRDLDTEQVLFEIAKPEND
          : *:.** *  :* .:***... *:: *:.:***:***:***:***:  ***** **

Human      -ERLPINRRD-----LDPNAGRFVRYQFTPAFLRLRQVGATVEFTVGDKPV
Zebrafish  -DRG--DKRD-----VDPNAGRFVRYQFTPAFLRLRQVGATVEFTVGDIPI
Xenopus    -QEEEEESTH-----LDASAGRFVRYQFTPAFLRLRQVGATVEFTVGDKPV
Drosophila MQYPEGLSSDETMLAAA EKLSLDDTADPNAGRYVRYQFTPAFLNLKTVGATVEFTVGSQPL
C. elegans -TEE---NLQ-----AQAESARYVRYRFAPNFLKLTVGATVEFKVGDVPI
C. briggsae --QE---NDE-----SPQESARYVRYRFAPNFLKLTVGATVEFKVGDVPI
          .                               .:.*:***:***:***:***:  *:.: *  * *:*:*

Human      -NNFRMIERHYFRNQLLKSFDHFGFCIPSSKNTCEHIYDFPPLSEELISEMIRHPYETQS
Zebrafish  -NNFRMIERHYFREQLLKSFDHFGFCIPSSKNTCEHIYEFPLSEDLIREMILHPYETQS
Xenopus    -KSFMIERHYFRDRILKSFDFDFGFCIPNSRNTCEHMYEFPQLSEELIRLMTENPYETRS
Drosophila MNNFRMIERHFFRDRLLKTFDFDFGFCFPFSKNTVEHIYEFPNLPPDLVAEMISSPFETRS
C. elegans -THFRMIERHFFKDRLLKCFDFDFGFCMPNSRNNCEHIYEFPQLSQQLMDDMINNPNETRS
C. briggsae -HHFRMIERHFFKDRLLKCFDFDFGFCIPNSRNNCEHIYEFPQLSQQLMDDMINNPNETRS
          *****:*.:.:*** ***.*****:* *:.:***:***:***: * .:*: *  * *:*:*

Human      -DSFYFVDDRLVMHNKADYSYSGTP--
Zebrafish  -DSFYFVDNKLVMHNKADYSYSGGP--
Xenopus    -DSFYFVDKKLIMHNKADYAYNGRP--
Drosophila MDSFYFVGNRLVMHNKADYAYDGGNIV
C. elegans -DSFYFVENKLVMHNKADYSYDA----
C. briggsae -DSFYFVDNKLVMHNKADYSYDA----
          ***** .:.*:*****:*.:.

```

**Figure 4.1 Oligopeptides used to raise UNC-119 antibodies**

The 15 residue peptides (U119N, U119M, U119C) used to produce polyclonal antisera are indicated in **bold italics** in amino, middle and carboxyl regions of the protein shown on the *C. elegans* line. Other family members are shown to demonstrate the divergence of the selected peptides.

Name	Sequence (5' to 3')
NOGFPU	GCGCACCGGTATGGCATGGACGAACTATACAA
NOGFPL	CGCGACCGGTGGGACAACCTCCAGTGAAAAGTT
MYCF1U	CCGGAATGGAGCAGAAGCTCATCTCCGAGGAGGACCTCGCTAGCAAA
MYCF1L	CCGGTTTGCTAGCGAGGTCCTCCTCGGAGATGAGC TTCTGCTC
MYCF2U	CCGAAAATGGAGCAGAAGCTCATCTCCGAGGAGGAC CTCGCTAGCAA
MYCF2L	CCGGTTGCTAGCGAGGTCCTCCTCGGAG ATGAGCTTCTGCTCCATT
MYCF3U	CCGGAAAATGGAGCAGAAGCTCATCTCCGAGGAGGACCTCGCTAGCA
MYCF3L	CCGGTGCTAGCGAGGTCCTCCTCGGAGATGAGCTTCTGCTCCATTTC
NTAPFUP	GGACGTCGAAATGCACCACCACCACCACGAATTAATGAAAGCTGATG
NTAPFLO	CGACGTCCTTGTCATCGTCGTCCTTGTAGTCGGATCCGTCGACATAT

**Table 4.1 Primers used to construct multi-epitope tag**

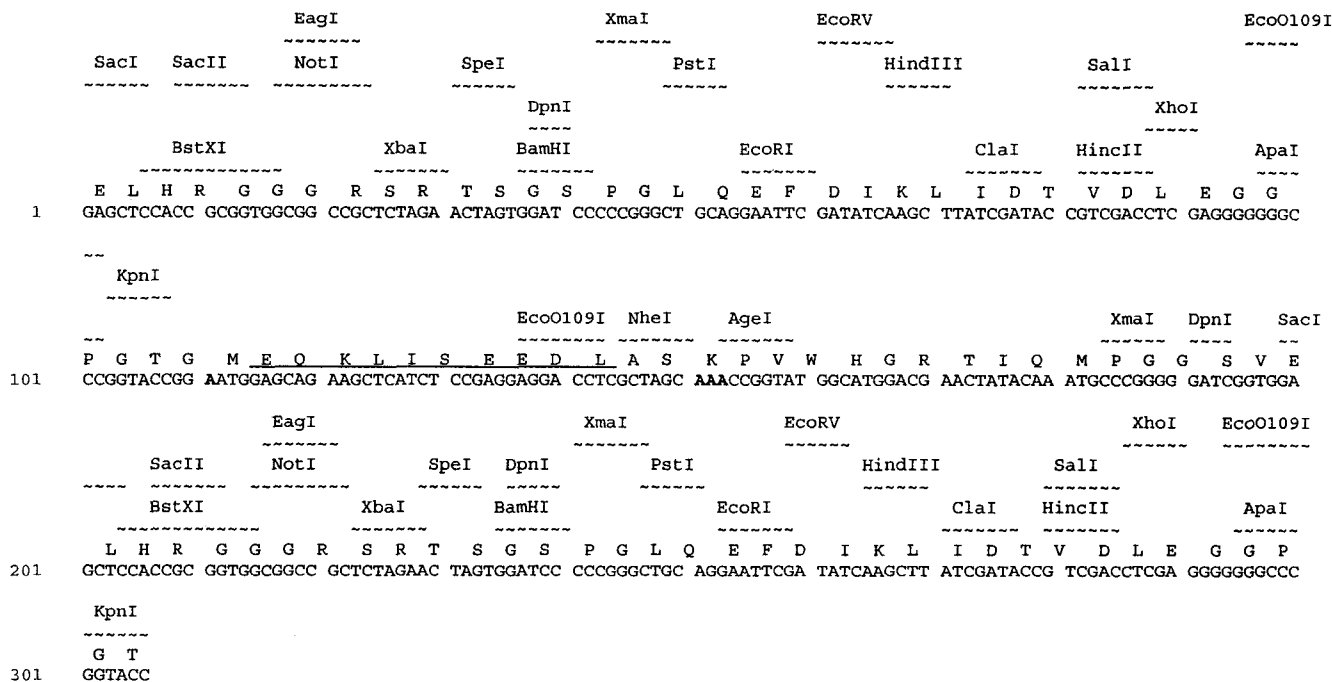


**Figure 4.2 NOGFP + MycF1**

The entire region from the start of the first MCS to the end of the second MCS is shown with restriction sites and translation above the nucleotides. The amino acid sequence of the Myc epitope is indicated by thick, wavy underline. A translational START (ATG) with Kozak consensus sequence (G/A NN ATG G) immediately precedes it. Nucleotides added to maintain or shift the reading frame are shown in bold near the Myc coding sequence.

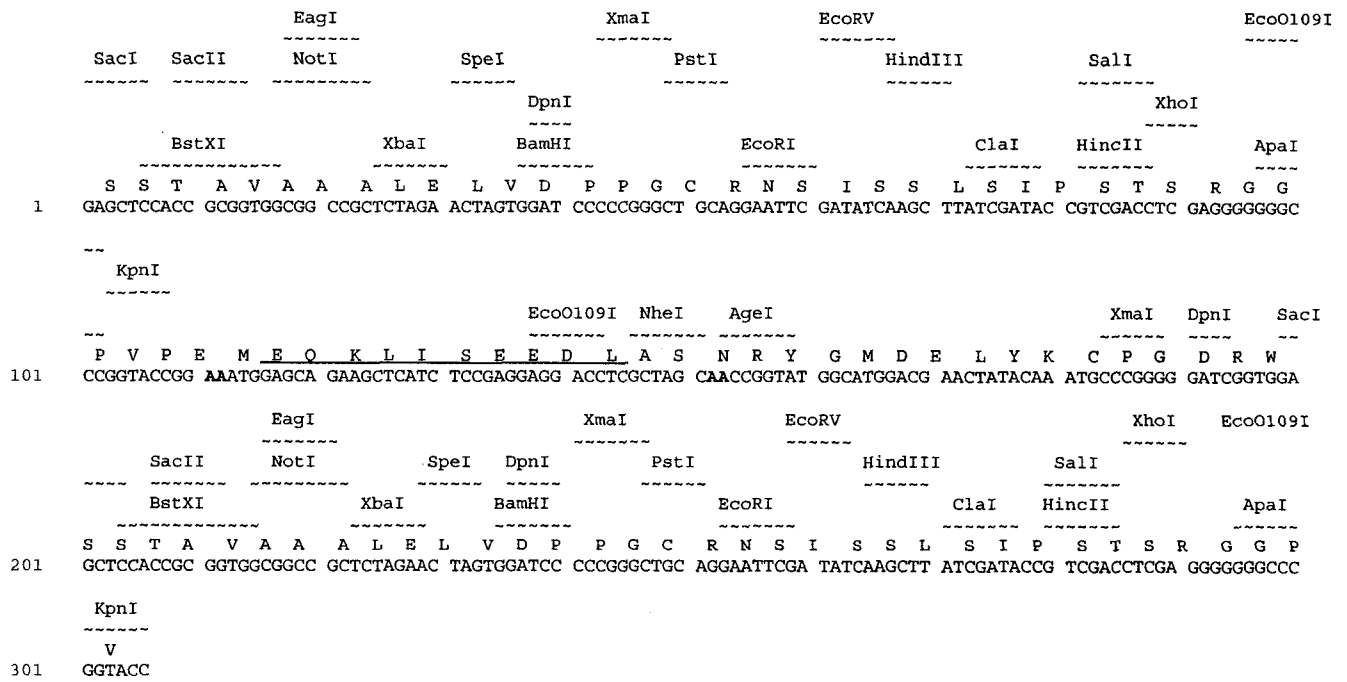


**Figure 4.3 NOGFP + MycF2**

The entire region from the start of the first MCS to the end of the second MCS is shown with restriction sites and translation above the nucleotides. The amino acid sequence of the Myc epitope is indicated by thick, wavy underline. A translational START (ATG) with Kozak consensus sequence (G/A NN ATG G) immediately precedes it. Nucleotides added to maintain or shift the reading frame are shown in bold near the Myc coding sequence.

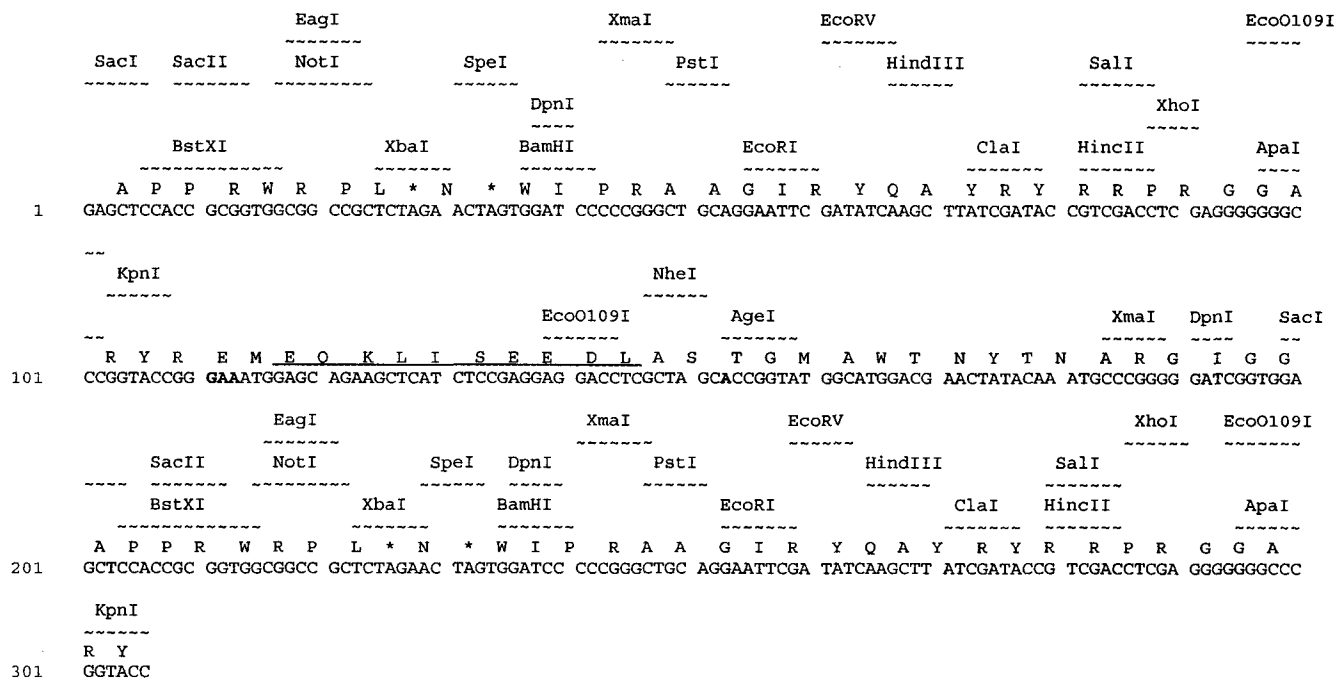


**Figure 4.4 NOGFP + MycF3**

The entire region from the start of the first MCS to the end of the second MCS is shown with restriction sites and translation above the nucleotides. The amino acid sequence of the Myc epitope is indicated by thick, wavy underline. A translational START (ATG) with Kozak consensus sequence (G/A NN ATG G) immediately precedes it. Nucleotides added to maintain or shift the reading frame are shown in bold near the Myc coding sequence. Notice that XbaI and SpeI restriction sites contain translational STOP sites in this frame.

```

----- His-6 -----
237  H H H H H H E L M K A D A Q Q N N F N K D
    CACC ACCACCACCA CCACGAATTA ATGAAAGCTG ATGCGCAACA AAATAACTTC AACAAAGATC
-----
301  Q Q S A F Y E I L N M P N L N E A Q R N G F I Q S L K D D P S Q S T
    AACAAAGCGC CTTCTATGAA ATCTTGAACA TGCCTAAGCTT AAACGAAGCG CAACGTAACG GCTTCATTCA AAGTCTTAAA GACGACCCAA GCCAAAGCAC
-----
----- IgG-Binding Protein -----
401  N V L G E A K K L N E S Q A P K A D N N F N K E Q Q N A F Y E I L
    TAACGTTTTA GGTGAAGCTA AAAAAATTAAA CGAATCTCAA GCACCGAAAG CTGATAACAA TTTCACAAA GAACAACAAA ATGCTTTCTA TGAAATCTTG
-----
501  N M P N L N E E Q R N G F I Q S L K D D P S Q S A N L L S E A K K
    AATATGCCTA ACTTAAACGA AGAACACGC AATGGTTTCA TCCAAAGCTT AAAAGATGAC CCAAGCCAAA GTGCTAACCT ATTGTCAGAA GCTAAAAAGT
-----
----- TEV Cleavage -----
601  L N E S Q A P K A D N K F N K E S S T P T T A S E N L Y F Q G E L K
    TAAATGAATC TCAAGCACCG AAAGCGGATA ACAAATTCAA CAAAGAATCT AGTACCCCAA CTAAGCTTTC TGAAAATCTA TATTTTCAAG GTGAACTAAA
-----
----- Calmodulin Binding Protein -----
701  T A A L A Q H A L E K M K R R W K K N F I A V S A A N R F K K I S
    AACTGCTGCT TTGGCTCAAC ATGCGCTCGA GAAGATGAAG CGACGATGGA AAAAGAATTT CATAGCCGTC TCAGCAGCCA ACCGCTTTAA GAAAATCTCA
-----
----- FLAG -----
801  S S G A L D Y G A P H M S T D P D Y K D D D D K A S
    TCCTCCGGGG CACTTGATTA TGCGCGGCCC CATATGTCGA CGGATCCAGA CTACAAGGAC GACGATGACA AGGCTAGC

```

**Figure 4.5 Epitopes common to STF1, STF2, STF3**

This segment is inserted into the NheI site of NOGFP+MycF1, NOGFP+MycF2 and NOGFP+MycF3 to give STF1, STF2 and STF3, respectively. The frame of this multi-epitope tag relative to the MCS in each construct is shifted by the linker fragments shown in Figure 4.2, Figure 4.3 and Figure 4.4. This allows this tag to be inserted as a cassette, into a selected sequence in any of three reading frames.

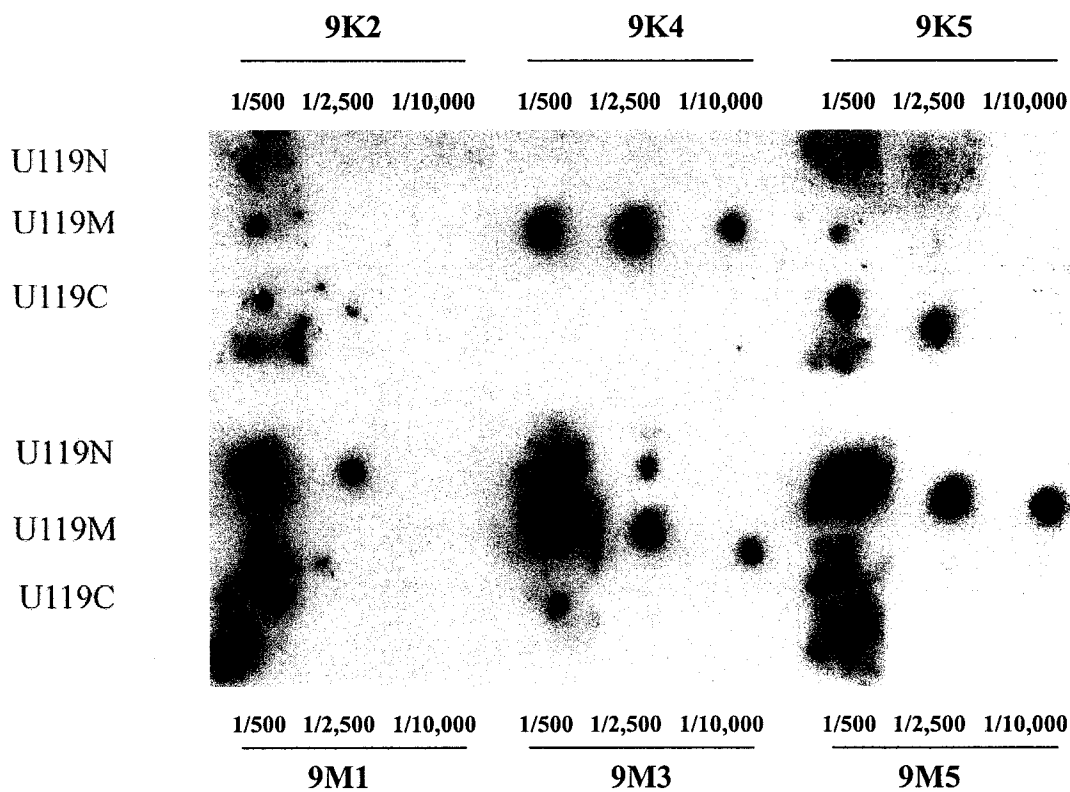


**Figure 4.6 Dot blot of antibodies versus oligopeptides**

Various oligopeptides were dotted on nitrocellulose then probed with peptide-specific polyclonal antisera. 9K2 reaction is not specific to U119C. 9K4 is highly specific to U119M at all dilutions. 9K5 is specific to U119C at 1/2,500. 9M1 is specific to U119N. 9M3 recognizes all 3 oligopeptides at high concentration but becomes specific to U119M at 1/10,000. 9M5 is also non-specific at high concentration but specifically recognizes U119N at 1/2,500 and 1/10,000 dilutions.

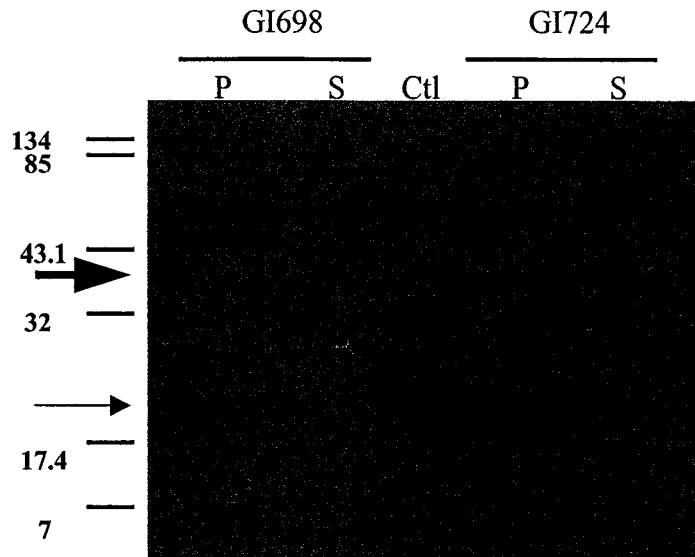


**Figure 4.7 GI698 expresses recombinant Thioredoxin::UNC-119 better than GI724**

Acetone-powder purified 9K2 antiserum was used to probe this Western blot. P- pellet, S – Osmotic shock supernatant, Ctl - Combined pellet and supernatant from control lysate expressing Thioredoxin only. Large arrow – Expected size of Thioredoxin::UNC-119 fusion protein (Band above this likely reflects actual mobility of fusion protein). Small arrow – non-specific recognition of endogenous protein (also seen in negative control lysate). Relative molecular weight is shown at left ( $\times 10^3$ ).

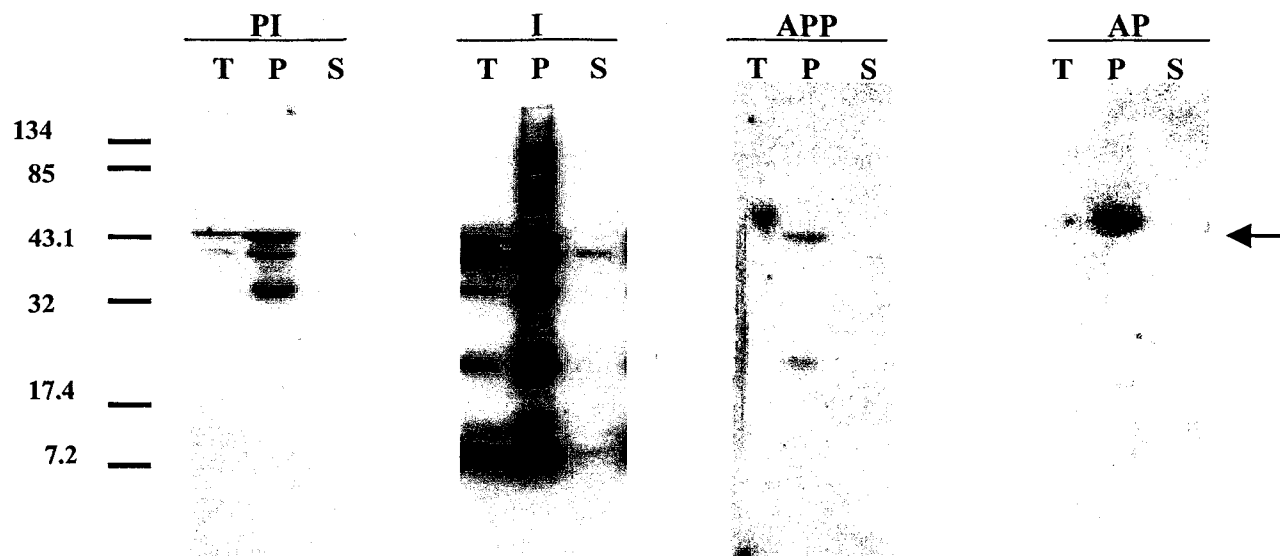


**Figure 4.8 Purified 9M5 antisera show improved specificity**

Composite from several Western blots has been normalized for spacing in this representative series using antiserum 9M5. PI – Pre-immune, I – Non-purified antisera, APP – Acetone Powder Purified/Cleared antisera, AP – Affinity Purified antisera. T – Lysate from GI698 expressing Thioredoxin only, P – Pellet of pDP#WM020 lysate, S- Supernatant of pDP#WM020 lysate. Relative molecular weights are shown at left ( $\times 10^3$ ). High cross-reactivity of antiserum to endogenous proteins is shown in I blot. Acetone powder purification reduces background reactivity and affinity purification abolishes it completely. All antisera are at 1/1,000 dilution but, due to relative differences in Ab concentration, different exposure times were required for signals (PI = 30", I = 30", APP = 1', AP = 15'). Images were adjusted in Photoshop to improve contrast. Arrow indicates expected size of recombinant UNC-119.

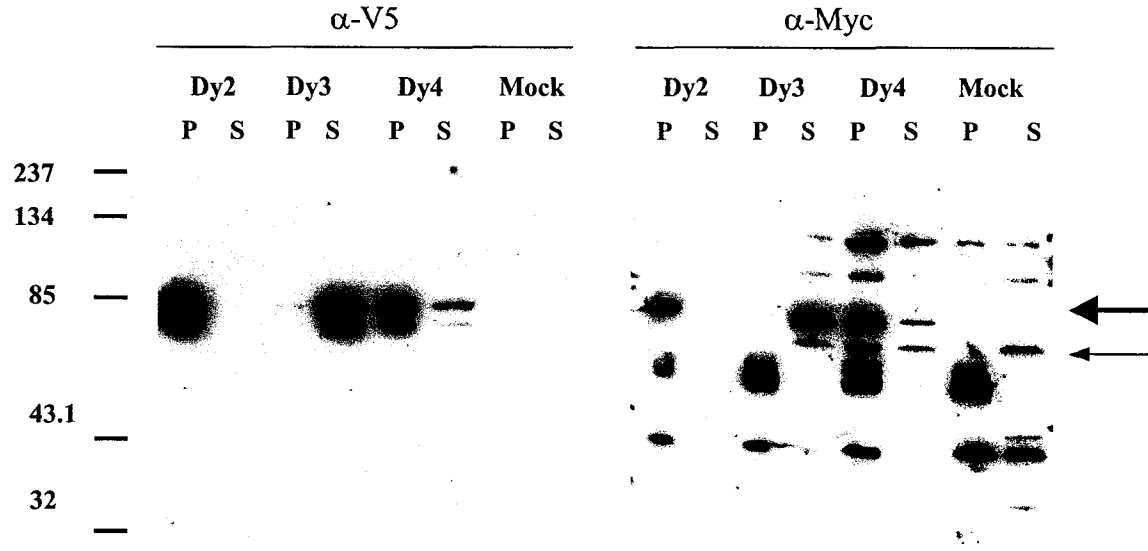


**Figure 4.9 Insect cells express soluble recombinant tagged UNC-119**

Sf9 insect cells transiently transfected with pDP#WM025e (multi-epitope tagged UNC-119) express soluble protein that can be detected using  $\alpha$ -V5 (intrinsic to expression vector) or  $\alpha$ -Myc antibodies. Protein is sometimes found in pellet rather than supernatant, indicating incomplete cell lysis. Dy2, Dy3, Dy4 – 2, 3 or 4 days post-transfection lysate, respectively. Mock – Mock transfection lysate. P – pellet, S – supernatant. Thin arrow – expected size of recombinant UNC-119. Thick arrow – apparent recombinant UNC-119. Relative molecular weights are shown at left ( $\times 10^3$ ).

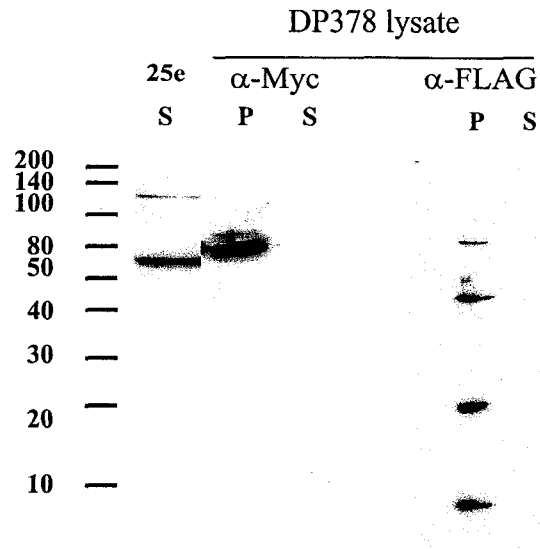


**Figure 4.10 Multi-epitope tagged UNC-119 is detected in worm lysate**

Western blots of worm lysate from strain DP378, containing an extrachromosomal array (edEx71) expressing the multi-epitope tagged UNC-119 shows band slightly larger than expected size (70 kDa) in pellet (P) fraction which is also just barely detectable in supernatant (S) fraction using  $\alpha$ -Myc 1<sup>o</sup>Ab. Probing same lysate with  $\alpha$ -FLAG 1<sup>o</sup>Ab shows some cross-reactivity with endogenous worm proteins (or, possibly, degradation products of tagged protein). Smaller band is shown in supernatant of lysate from stably-transfected Sf9 cells (25e) for comparison. Relative molecular weights are shown at left ( $\times 10^3$ ).

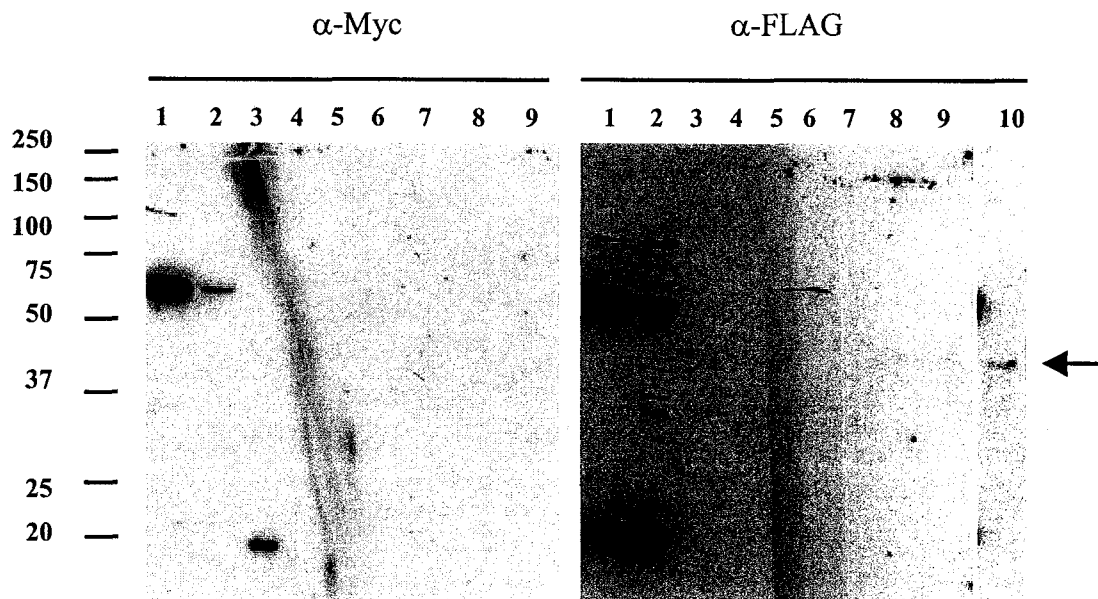


**Figure 4.11 TAP purification of pDP#WM025e lysate**

Western analysis of various fractions during TAP purification/pulldown of pDP#WM025e insect cell lysate with both  $\alpha$ -Myc and  $\alpha$ -FLAG primary Ab's shows effectiveness of purification steps. Separate SDS-PAGE and Westerns were performed in parallel to produce each blot. 1- Supernatant from pDP#WM025e lysate. 2 - Fraction that did not bind to IgG column. 3 - Following TEV protease cleavage to elute CBP + FLAG + UNC-119 fragment, the bound Myc + IgG BP was eluted with glycine (pH 2.3). This fragment shows as a band of 18.8 kDa in  $\alpha$ -Myc blot. 4 to 8 - Five fractions of EGTA elution from Calmodulin column. No protein is detectable. Band in lane 6 of  $\alpha$ -FLAG blot is likely artifact or non-specific FLAG binding. 9 - Glycine (pH 2.3) elution from Calmodulin column. 10 - Five fractions of EGTA elution were pooled, concentrated 20-fold and run on separate Western. Arrow points to band that is detectable with  $\alpha$ -FLAG that represents purified CBP + FLAG + UNC-119 (41.1 kDa). Relative molecular weights are shown at left.

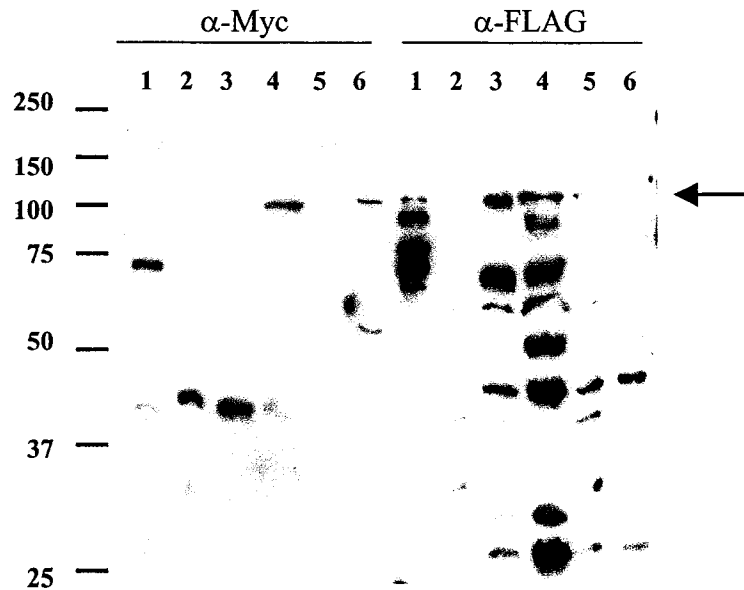


**Figure 4.12 Soluble tagged-UNC-119 extracted by grinding method**

Protein was extracted from DP378 worms by grinding in liquid nitrogen. 1- Supernatant from pDP#WM025e insect cell lysate. Pellet from first grinding was ground a second time. 2- Pellet following second grinding. 3 – Supernatant following second grinding. 4 – Supernatant following first grinding. 5 – N2 pellet (also from grinding) 6 – N2 supernatant. Soluble protein (arrow) can be detected in DP378 lysate with both  $\alpha$ -Myc (lane 4, left) and  $\alpha$ -FLAG antibodies (lanes 3 and 4, right).  $\alpha$ -Myc is more specific than  $\alpha$ -FLAG. N2 lysate (lanes 5 and 6) also contain an unidentified endogenous protein of similar size to tagged UNC-119 which likely is due to spillover from adjacent lanes. Relative molecular weights are shown at left ( $\times 10^3$ ).

## 4.5 References

- Cen, O., Gorska, M.M., Stafford, S.J., Sur, S. and Alam, R. (2003), Identification of UNC119 as a novel activator of src-type tyrosine kinases, *Journal of Biological Chemistry*, **278**: 8837 - 8845.
- Denholm, C. (2003), Characterization of the UNC-119 family in mammals, MSc. Thesis, University of Alberta, Canada
- Higashide, T., McLaren, M.J. and Inana, G. (1998), Localization of HRG4, a photoreceptor protein homologous to *unc-119*, in ribbon synapse, *Investigative Ophthalmology & Visual Science*, **39**: 690-698
- Knobel, K.M., Davis, W.S., Jorgensen, E.M. and Bastiani, M.J. (2001), UNC-119 suppresses axon branching in *C. elegans*, *Development*, **128**: 4079-4092
- Kobayashi, A., Kubota, S.K., Moria, N., McLaren, M.J. and Inana, G. (2003), Photoreceptor synaptic protein HRG4 (UNC119) interacts with ARL2 via a putative conserved domain. *FEBS Letters*, **534**: 26-32
- Kubota, S., Kobayashi, A., Mori, N., Higashide, T., McLaren, M.J. and Inana, G. (2002), Changes in retinal synaptic proteins in the transgenic model expressing a mutant HRG4 (UNC119), *Investigative Ophthalmology & Visual Science*, **43**: 308-13
- Lewis, J.A. and Fleming, J.T. (1995), Basic culture methods in methods in cell biology, Vol. 48, *Caenorhabditis elegans: modern biological analysis of an organism*, Epstein, H.F. and Shakes, D.C. ed's. Academic Press, San Diego, CA
- Rigaut, G., Shevchenko, A., Rutz, B., Wilm, M., Mann, M. and Séraphin, B. (1999), A generic protein purification method for protein complex characterization and proteome exploration, *Nature Biotechnology*, **17**: 1030 - 1032
- Van Valkenburgh, H., Sher, J.F., Sharer, J.D., Zhu, X. and Kahn, R.A. (2001), ADP-ribosylation factors (ARFs) and ARF-like 1 (ARL1) Have Both Specific and Shared Effectors, *Journal of Biological Chemistry*, **276**: 22826–22837

## Chapter 5 - General Discussion

This work has suggested that UNC-119 is involved in transducing a signal required for axon elongation and stability. Further, I have shown that this signal may particularly play a role in the interaction between an elongating axon and the substrate over which it extends, either another axon or the extracellular matrix. Thus, neurons in *unc-119* mutants exhibit axon elongation defects that might specifically be associated with down-regulating guidance cue receptor or adhesion molecules following encounter with a choice point.

- i) The VNC is often moderately to severely defasciculated. As axons elongate within the VNC they encounter changes in neighbouring axons. For example when neighbouring axons terminate or neighbouring commissures turn away from the VNC, follower axons undergo a change in neighbourhood that may act as a choice point.
- ii) Lateral mechanosensory axons can extend medially into the nerve ring but do not elongate ventrally along the nerve ring in association with other axons. The medial extension pioneers entry into the nerve ring while the ventral elongation represents a change in direction as well as substrate.
- iii) Chemosensory axons can project ventrally but do not project anteriorly into the nerve ring in association with the VNC. ASI axons initially fasciculate with the amphid commissure then the VNC before entering the nerve ring. Many other axons also enter the nerve ring at this point and changes in neighbourhood are frequent.
- iv) Pioneering commissures elongate normally from the VNC to the DNC but

fail to stabilize. Instead they retract from the DNC and subsequently generate supernumerary branches. This is likely to be a result of signaling or adhesion as failure to form functional synapses (as in *ttx-2*, *ttx-4* or *unc-104* mutant strains) does not lead to similar axon retraction. In particular, the change from circumferential elongation over the ECM to anterior or posterior elongation by fasciculation with the DNC potentially represents a major choice point.

It is interesting to note the change in underlying substrate associated with some of these choice points, particularly in relation to the findings from protein-protein interaction experiments. Yeast two-hybrid screens detected an interaction between UNC-119 and the basement membrane collagen IV family member, LET-2. Deleting domains of UNC-119 that abrogate the interaction with LET-2 also made it unable to rescue the mutant phenotype. Although LET-2 is produced by both body wall muscle and somatic gonad, it is secreted into the pseudocoelomic cavity and localizes to basement membranes underlying body wall muscles, the intestine, the gonad, the pharynx and GLR glia beneath head muscle near the nerve ring. The choice points at which axons exhibit defects in *unc-119* mutants are near LET-2 deposits in the basement membrane. Thus filopodial contact with LET-2 may be acting as the choice point signal for medially-projecting ALM axons near the pharynx along the inside of the nerve ring, for ASI axons entering the nerve ring as they bypass GLR glia, or for commissures as they pass underneath dorsolateral body wall muscles and contact the DNC.

UNC-119 may act as an adaptor protein mediating an extracellular LET-2 choice point signal and downstream cytoplasmic signal transduction mechanisms. At choice

points axons modulate their adhesion properties as well as their receptors for extracellular guidance molecules. The axonal response to a choice point is complex and includes: i) sensing the choice point signal, ii) transducing the choice point signal, iii) expressing new adhesion or receptor molecules on the growth cone, and iv) removing old adhesion and receptor molecules from the growth cone. While UNC-119 might act at any point in this process we could predict that an absolute failure to sense or process the choice point signal is likely to result in ignoring the choice point altogether. If this were the case, we should observe commissures failing to defasciculate from the VNC altogether. However, the observed behaviour of ALM, ASI and commissural axons in *unc-119* mutants does not reflect this prediction but is closer to what we would expect if adhesion and receptor molecules were not properly down-regulated at choice points. This should lead to a failure of some axons to switch from one substrate to another in a stochastic or probabilistic manner.

UNC-119 normally acts cell-autonomously; expressing an UNC-119::GFP fusion protein in a neural subset in a mutant background specifically restores wild-type axon morphology only for neurons in which it is expressed. Immunohistochemistry has demonstrated that UNC-119 is normally found cytoplasmically in almost all neurons in the worm. In the rat, UNC-119 has been associated with the plasma membrane of pre-synaptic vesicles in photoreceptors. However, UNC-119 expressed ectopically in body wall muscles also rescues the mutant phenotype, particularly in early larval stages. Concentration of the ectopic protein in coelomocytes suggests that it may be secreted when it is expressed in muscles, perhaps by a non-classical pathway that is dependent on improper folding of the GFP moiety. The mechanism by which extracellular UNC-119

might restore intracellular function in neurons is unknown but could involve endocytosis by recycling vesicles in growth cones. How this might permit transduction of an extracellular choice point signal must also be the subject of future research.

UNC-119 also has activity that is independent of its interaction with LET-2 because single missense mutations in residues in the highly-conserved carboxyl region, which do not lose the ability to interact with LET-2, completely abolish the ability to rescue the mutant phenotype. Although it is not yet known whether these mutations also block the interaction with LET-2, this region is not sufficient, by itself, for that interaction. Other intracellular signal transduction roles that have been proposed for UNC-119 in humans include a role in activating Src during cytoskeletal remodeling and a role as a downstream effector of Arl signaling. However, mutating residues that are thought to be critical for activating Src, does not affect the ability of UNC-119 plasmids to rescue the mutant phenotype. While we have not yet similarly tested putative Arl-interacting motifs, directed two-hybrid assays indicate that any UNC-119 – Arl-2 interaction must be very weak, if, in fact, it exists at all. Again, UNC-119 must play a role outside of any putative interaction with Src or Arl as single residue mutations in regions outside of those required for the interaction are critical for UNC-119 function.

### **5.1 Future Directions**

This work has raised several interesting questions and hypotheses. In this section I will discuss possible future directions for this research to take. There were technical difficulties that prevented the completion of some experiments. Attempts to purify the protein and raise an antibody certainly fall into this category. Initial attempts to express the protein in various bacterial constructs indicated it is insoluble and toxic to bacteria.

Adding a thrombin epitope seemed to relieve the toxicity but did not greatly improve solubility. The protein could be expressed in Sf9 insect cells and a soluble isoform detected. However, using standard adherent culture methods, it was difficult to raise large numbers of these of cells in order to produce sufficient protein for purification. Future approaches might consider raising Sf9 insect cells in a spinner flask so that larger numbers of cells can be grown. Alternatively, it may be possible to express UNC-119 in a *Pichia* expression system to enhance yield.

Although a variety of purification methods are touted by companies and other researchers no single approach is best in all cases. While purification of HIS-6 tagged proteins over a nickel column produces respectable yields, the purity is not as high as might be desired. The Tandem Affinity Protocol (TAP) achieves higher purity with good yield but requires adding two fairly large epitopes to the amino end of the protein. This may have an undesirable effect on protein characteristics and it would be preferable to permit the cleavage of the entire TAP epitope by incorporating an intein or other cleavage site immediately downstream. In this work I describe the construction of a TAP-based cassette incorporating a large number of restriction sites that may be used as a general purification and epitope tag. In addition to TAP epitopes, I also added Myc, HIS-6 and FLAG epitopes. However, my experience has been that the placement of the FLAG epitope near the carboxyl end of the TAP tag is not optimal for immunohistochemistry and, in the future, this epitope should be placed near the amino end. Alternatively other epitopes that are quite specific but can be detected internally within a protein (such as the V5 epitope) might be considered as a replacement.

Using antibodies to detect the tissue-specific or subcellular localization of a protein is an excellent approach but requires dedicated effort to master difficult techniques. Using an epitope-tagged transgene to obviate the need to develop new antibodies should not be considered superior to GFP fusion proteins as both systems suffer from having to interpret expression patterns when an excess of the normal protein is present. This is likely to completely mask any localization that depends on stoichiometric co-localization with other factors and yield misleading data, especially intracellularly.

In addition, both co-immunoprecipitation and yeast two-hybrid methods for identifying protein-protein interactions assume a relatively stable, long-term relationship between proteins. Many interactions between cytosolic proteins may be highly transient and current methods may not easily detect them. For example, a kinase may bind a phosphorylation motif with high affinity only until the target residue is phosphorylated at which time the activated protein is released. Transient interactions of this nature may be detectable only if the interaction is stabilized, as is the case with activated human Arl2(Q70L) and PDE $\delta$ .

This work has discussed several molecules and mechanisms that may be important in axonogenesis but that have other deleterious effects when their function is disrupted. For instance, two lines of evidence suggest that exocytosis and/or endocytosis of extracellular guidance or neurotrophic cues and their intracellular adaptors or modulators may play an important role in axonogenesis. First, ectopic UNC-119 expressed in body wall muscles seems to be secreted and, thereby, to rescue the mutant neural phenotype. Second, UNC-119 seems to interact with LET-2, a collagen

component of the extracellular matrix over which axons elongate.

Unfortunately, with one exception, all *let-2* mutant alleles are embryonic lethal (either always or in a temperature-sensitive fashion) and the single non-ts allele has no phenotype by itself. Thus, any possible effect that mutations in LET-2 may have on nervous system structure are not easily observed as the animal dies of other problems before NS development. Testing the role of endocytosis in NS development encounters a similar problem. Though mutants in various components of the endocytic pathway have been isolated they are almost always lethal during embryogenesis. Some temperature-sensitive mutants have been discovered and these animals can be raised to adulthood to study the role of endocytosis in synaptic vesicle recycling. Unfortunately, raising these strains at the restrictive temperature during development results in embryos that die before or during NS development of problems unrelated to the NS.

A method to specifically reduce the function of a selected protein in a single tissue has recently been developed. RNA interference can generally be used to reduce levels of a selected protein but spreads easily to other tissues and does not work well in neurons in worms. Recently several mutant strains have been developed that circumvent these problems. For example, *rrf-3* mutant worms permit RNAi to reduce protein levels in the nervous system of the worm while *syd-1* mutants lack the mechanism to transport small, non-coding RNA fragments (such as found in RNAi) between cells and so the RNAi effect can be localized to one tissue (J. Smith, personal communication). By coinjecting two plasmids with the same promoter but with a selected gene in both forward and reverse orientations, it is possible to elicit RNAi knockdown of that gene. If these plasmids were injected into *syd-1;rrf-3* double mutants and a strong neural

promoter (such as the F25B3.3 promoter) were used then knockdown of a specific gene only within neurons should be achievable.

This method will allow us to investigate gene function in neurons, when those genes are intrinsic to many other processes in other tissues that cause embryonic death or other undesirable complicating phenotypes. With this technique we can disrupt such generic processes as exocytosis, endocytosis or adhesion in a tissue-specific manner and reveal neural phenotypes that might be hidden in a simple mutant. This approach will lead us closer to determining which role UNC-119 plays in the development of the *C. elegans* nervous system.